DIRECT QUANTITATIVE GROSS αβ-MEASUREMENTS OF ENVIRONMENTAL WATER CONTAMINATED WITH NUCLIDES FROM THE URANIUM, THORIUM AND ACTINIUM DECAY SERIES AND SEMI-QUALITATIVE IDENTIFICATION OF NUCLIDES CONCERNED

By

MACHEL MASHABA

A dissertation in partial fulfillment of the

requirements for the degree of

MASTER OF APPLIED RADIATION SCIENCE AND TECHNOLOGY

AT

NORTH WEST UNIVERSITY (Mafikeng campus)

SUPERVISOR: Prof. Dr Arnaud FAANHOF
South African Nuclear Energy Corporation Ltd. (Necsa)
Specialist Scientist: Research & Development

MENTOR: Mr. Deon KOTZE
South African Nuclear Energy Corporation Ltd. (Necsa)
Senior Scientist: RadioAnalysis

November 2011

DECLARATION

I declare that this research, direct quantitative gross αβ-measurements of environmental water contaminated with nuclides from uranium, thorium and actinium decay series and semi-qualitative identification of nuclides concerned is my own work, carried out in the RadioAnalysis Department at the South African Nuclear Energy Corporation (NECSA) in collaboration with the Centre of Applied Radiation Science and Technology (CARST) at the North West University (Mafikeng campus) between July 2009 and July 2011. It has not been submitted for any degree in any other university, and that all the sources of data I have used, have been indicated and fully acknowledged.

Full name: Machel Mashaba Date: November 2011

Signed: 

ACKNOWLEDGEMENT

I express my deepest appreciation to a number of individuals who contributed on the development and success of this project, without their support, this work could not have been completed.

First, I would like to thank my supervisor, Prof Dr Arnaud Faanhof, who offered me the opportunity to perform this research, guided and supported me throughout this work. Without his support, advice and encouragement, this work could not have been possible.

I would like to thank my mentor, Deon Kotze, whose doors were open 24 hours to help me from the conception to the completion of this project, without his support, I could not have managed.

Special thanks go to the Centre of Applied Radiation Science and Technology (CARST) at the North West University (Mafikeng Campus) for funding and giving me the opportunity to pursue my career in the nuclear industry and NECSA for giving the opportunity to do the necessary practical research.

Finally, I would like to express my gratitude to my family for the support and encouragement throughout this journey.

ABSTRACT

Naturally occurring radioactive materials (NORMs) in environmental samples are of crucial importance in the case of radiological impact studies in any environmental compartment. For this reason, valuable information is needed for the determination of NORMs in environmental samples and this requires accurate measurement techniques. This information can be obtained from liquid scintillation counter (LSC) by fast screening of contaminated water samples with NORMs. However, direct determination of these nuclides via LSC is far from straight forward since LSC can only quantitatively determine total α/β-activity. In addition, identification of α-β emitters with the LSC method requires an exact determination of the peak position or end-point energy. This requires energy calibration under various quenching conditions. The α-energy calibration is a correlation of α-energy and the channel peak position of the spectrum. The appearance of quenching in the sample affects not only counting efficiency but the α-β discrimination as well. LSC allows the measurement of both α- and β-activities and in some cases an indication can be obtained of the α-energy, although the resolution of α-spectra is much poorer than that attained by semi-conductors.

In this investigation we evaluated the potential of a low-background liquid scintillation system with advanced spectrometry capabilities, the Quantulus 1220^{TM}, to be used directly for the determination of the gross α- and β-activities and the identification of the most likely nuclides that contribute to the activity of NORM-nuclides in environmental water. Although element specific radiochemical separations followed by α-spectrometry are still the better option the method developed offers an attractive and cost-effective alternative.

Keywords

Liquid scintillation counter (LSC), Gross α and β activity measurements.

TABLE OF CONTENTS

CHAPTER 3

CHAPTER 4

CHAPTER 5

CHAPTER 6

CHAPTER 7

LIST OF FIGURES

LIST OF TABLES

LSC TERMINOLOGY

Chemi-luminescence:	Random single photon events which are generated as a result of the chemical interaction of the sample components. Except at high rates, most chemi-luminescence events are excluded by the coincidence circuit.
Cocktail:	The scintillation fluid. A mixture of three chemicals (solvent, emulsifier, and fluor) which produces light flashes when it absorbs the energy of particulate radioactive decay.
Counts per minute (cpm):	This is the number of light flashes or counts the LSC registers per minute.
Discriminator:	An electronic circuit which distinguishes signal pulses according to their pulse height. It is used to exclude noise or background radiation counts.
Disintegration per minute (dpm):	The sample's activity in units of nuclear decays per minute.
Efficiency:	The ratio, cpm/dpm, of measured counts per minute to the number of decays per minute, which occurred during the measurement time.
Emulsifier:	A chemical component of the liquid scintillation cocktail that absorbs the UV light emitted by the solvent and emits a flash of blue light.
Fluor:	Chemicals present in the liquid scintillation cocktail that convert the energy of the β decay to flashes of light.
Fluorescence:	The emission of light resulting from the absorption of incident radiation and persisting only as long as the stimulating radiation is continued.
Luminescence:	A general term applied to the emission of light by causes other than high temperature.
Measurement uncertainty:	Uncertainty of measurement is defined as a parameter, associated with the result of a measurement that characterizes the dispersion of values that could reasonably be attributed to the measurand. The uncertainty of a measured value is typically expressed as an estimated standard deviation, called a standard uncertainty.

The Photo-Multiplier Tube:	It is the device that detects and measures the blue light flashes from the fluor and converts them into electrical pulses.
Phosphor:	A luminescent substance or material capable of emitting light when stimulated by radiation.
Photo-luminescence:	Delayed and persistent emission of single photons of light following activation by radiation such as ultraviolet.
Pulse:	Electrical signal of the PMT; its size is proportional to the radiation energy absorbed by the cocktail.
Quench:	Anything which interferes with the conversion of decay energy emitted from the sample vial into blue light photons. This usually results in reduction in counting efficiency.
Secondary scintillator:	Material in the scintillation cocktail which absorbs the emitted light of the primary scintillator and remits it at a longer wavelength, nearer the maximum spectral sensitivity of the photomultiplier tubes. It is added to improve the counting efficiency of the sample.
Solvent:	A chemical component of the liquid scintillation cocktail that dissolves the sample, absorbs excitation energy and emits UV light which is absorbed by the fluors.
SQP(E):	The Quenching Index Parameter is a value that indicates the sample's level of quenching. Another parameter that describes the amount of quenching present is the transformed Spectral Index of External Standard (tSIE) or "H" number.
Radionuclide/Nuclide:	A radionuclide is an element or isotope that is radioactive as a result of the instability of the nucleus of its atom (e.g. uranium or radium).

SYMBOLS AND ABBREVIATIONS

α	Alpha
β	Beta
ε	Counting efficiency
γ	Gamma
CPM (cpm)	Counts per minute.
DPM (dpm)	Disintegration per minute.
IAEA	International Atomic Energy Agency.
keV	Kilo electron volts.
LSC	Liquid scintillation counting.
MeV	Million electron volts.
NECSA	South African Nuclear Energy Corporation Pty Ltd.
NORM	Naturally occurring radioactive material.
PMT	Photomultiplier tube.
SQP(E)	Spectral quench parameter of the external standard.
Th	Thorium
U	Uranium
WCA	Wonderfonteinspruit catchment area.

CHAPTER 1

INTRODUCTION, SIGNIFICANCE AND OBJECTIVES OF THE STUDY

1.1 Introduction

The presence of radioactivity in environmental water in South Africa is mainly caused by naturally occurring radioactive material (NORM). NORM is present in all water resources and the impact is normally of a chronic nature.[1] Natural environmental radioactivity results mainly from natural radionuclides, such as potassium-40 (^{40}K) and the nuclides from the uranium-238 (^{238}U), uranium-235 (^{235}U) and thorium-232 (^{232}Th) series and their decay products, which occur at trace levels in all ground formations. The radioactive nuclides of the three decay series decay either by emitting α or β particles, in some cases followed by γ radiation.

The subject of radioactivity has gained considerable public importance because of the Chernobyl accident. In the past, regulatory attention has been focused mostly on exposure arising from the mining and processing of uranium ores because such activities are part of the nuclear fuel cycle. More recently, attention has been broadened to include exposure from other industrial activities involving NORM.[2]

The concentration of radionuclides in water is extremely small,[3] hence the risk is generally regarded as negligible. However, higher concentrations may occur as a result of the intervention of humans in the environment (e.g. mining and mineral processing). Mining and mineral processing industries that are associated with NORM-bearing ore bodies have the potential to increase the risk of radiation exposure to the environment and humans, by concentrating NORM nuclides beyond normal background levels.

The long lasting mining related discharges of naturally occurring radionuclides from point and diffuse sources into the Wonderfonteinspruit catchment area (WCA), resulted in a complex pattern of radioactive contamination of the water and sediment bodies throughout the area.[4] As a consequence of the different sources of radionuclides (mine water and slime dams) a high temporal and spatial variability of the contamination levels can be expected due to their different geochemical and transport behavior in the environment and variations in the source term.

South Africa became the fourth largest producer of uranium worldwide based on the survey and production of uranium in the Witwatersrand, which was initiated by the Manhattan project.[5] The high geochemical mobility of some of the NORM nuclides in the environment allows them to move easily and to contaminate much of the environmental water.[6] Thus the presence of NORM nuclides in the WCA has been observed during studies of the Department of Water Affairs and Forestry and the National Nuclear Regulator (NNR).[4, 7]

Preliminary monitoring by the Institute for Water Quality Studies (IWQS) of the Department of Water Affairs and Forestry done in 1995/97, showed that activity concentrations of radioactive elements in surface and ground waters were elevated in the Wonderfonteinspruit during 1997.[7] Since then some further studies have been done.[4]

Detection and quantification of α and β emitting radionuclides are routine tasks in environmental monitoring in and around sites where nuclear activities are done.[8] However, liquid scintillation counting (LSC) is often the method of choice when high throughput screening for the presence of α-β activity is required. To be useful for screening analysis, gross α-β determinations require straightforward methods with minimal sample handling and rapid measurement applied to a wide range of samples.

LSC has been a very popular technique for the detection and quantitative measurement of radioactivity since the early 1950s.[9] LSC is an excellent method because α's are counted with nearly 100% counting efficiency with low backgrounds, even with severe quenching.[10]

Ultra low level liquid scintillation counting coupled to α-β discrimination allows rapid and simple determination of gross α and β activities. They can be measured simultaneously and differentiated between, using the Wallac Quantulus 1220 (Perkin Elmer) liquid scintillation detector that uses a pulse shape analysis circuit (PSA) to distinguish between α and β disintegrations, but optimization of the PSA has to be done before gross α and β measurements can be taken.[11]

1.2 Significance of the study

There are concerns that the NORM radioactivity content in environmental waters in general may cause a threat to people living around the catchment areas. There are many informal settlements within these catchment areas, giving rise to a possible consumption of untreated surface and ground water pumped into the catchment area to de-water the operational area of the various mines.

Uranium isotopes (^{238}U, ^{234}U, and ^{235}U) have a low radiotoxicity [12], but several radionuclides in the radioactive decay series starting from ^{238}U, ^{235}U, and ^{232}Th are highly radiotoxic. The most radiotoxic among them are ^{231}Pa, ^{227}Ac, ^{210}Pb, ^{210}Po, and ^{228}Ra and accordingly their presence in water would pose a health risk to humans requiring particular attention.

The analysis of NORM nuclides is labour intensive as radiochemical separation of uranium (U), thorium (Th), radium (Ra), lead (Pb), polonium (Po), and protactinium (Pa) are to be done and accordingly the analyses are expensive. On the other hand, detecting and quantifying α and β emitting radionuclides are routine tasks in environmental monitoring, but these techniques are not nuclide specific.

The research aimed to answer the identification and measurement of gross α and gross β particle activities in raw water from the WCA using the Quantulus ultra low level liquid scintillation

spectrometer and thereby potentially avoiding the necessity for further analysis. Special attention has been paid to the identification of radionuclides which significantly influenced the selection parameters of LSC.

1.3 Research objective

The main purpose of the research was to determine the NORMs in water from the WCA. Since there is great concern about radionuclides in the environment, it has become increasingly important to accurately quantify α and β emitters.

The research has achieved the following objective:

To use the Quantulus ultra low level liquid scintillation spectrometer directly on the raw water samples without extensive sample preparation to do quantitative α and β activity measurements as well as semi-qualitative identification of NORM nuclides.

1.4 Thesis outline

This dissertation is categorized into seven sections. It starts with an overview of the background of this study including the introduction, significance of the study and the research objective work in-terms of identification of NORMs in environmental water (Chapter 1). The next chapters are outlined as follows:

Chapter 2 entails the theoretical background of environmental water contaminated with NORMs including the concentration levels of radionuclides of the uranium, actinium and thorium chain series.

Chapter 3 describes different possible techniques for measuring environmental samples. Principles and applicability of each technique for different purposes are also mentioned.

Chapter 4 explains the principles of liquid scintillation counting (the technique used in this work), as well as cocktail integer descriptions.

Chapter 5 describes the methodology used. It gives an overview of the catchment area (Wonderfonteinspruit) and it also presents the results obtained from the calibration and gives some conclusions on selection of PSA levels.

Chapter 6 summarises the results obtained in counting raw water samples by a Quantulus ultra low level liquid scintillation counter.

Chapter 7 gives the final conclusions and recommendations for possible follow-up studies.

CHAPTER 2

THEORETICAL BACKGROUND OF ENVIRONMENTAL CONTAMINATED WATER

2.1 Natural Radioactivity in the Environment

Radioactivity in the environment can be categorized according to three types, namely those of anthropogenic (man-made), cosmogenic or extra-terrestrial, and primordial or terrestrial nature.

Anthropogenic radionuclides are man-made radionuclides, do not naturally belong in the environment and are found there because of human activities such as the testing of nuclear weapons or accidents in nuclear power plants. For instance, the cesium isotopes ^{137}Cs and ^{134}Cs that were released in the Chernobyl accident belong to this group of radionuclides. These isotopes are relatively short lived.

Cosmogenic radionuclides are radionuclides produced by nuclear reactions in the atmosphere and at the surface of the lithosphere by cosmic radiation. These include amongst others ^{7}Be, ^{14}C and ^{3}H.

Primordial radionuclides are radionuclides that have been present on earth since its formation. These radionuclides have substantially longer half-lives. In order to stay around for so long, they would seemingly have to be very long-lived. Many of the primordial radionuclides occur in decay chains, which are characterized by the fact that the decay of a radionuclide often leads to the formation of another radionuclide according to a certain decay pattern.[13]

2.2 Radioactivity in Water

Many scientists worldwide work in the field of natural radionuclides measurements in water by using LSC to determine mostly gross α-β activities in water. Andriambololona *et al.*[14] measured the activity of radium and its progenies in drinking water in Vinaninkarena, Antsirabe-Madagascar. The village of Vinaninkarena, Antsirabe-Madagascar is located in a natural high radioactive area, and the survey was conducted around an abandoned radium mine.

Lasheen *et al.*[15] simultaneously measured ^{226}Ra and ^{228}Ra in natural water by liquid scintillation in three different areas in Egypt. Water originating from the Eastern Nile delta area is characterized by low ^{226}Ra levels and high ^{228}Ra activity.

Palomo *et al.*[16] determined tritium activity level in the environmental water samples from different areas of Catalonia (Spain), using a distillation procedure before LSC. Different types of water, from rivers, rain, mineral bottled waters and tap waters, were analyzed. They found that tritium activity in the river was greater than the normative limit in Spain for waters intended for

human consumption. This can be caused by the nuclear power station of Asco, which is located on the banks of this river.

Kleinschmidt[17] analyzed gross α and β activity in water using liquid scintillation analysis by Australian laboratories. The aim of this work was to develop a method to provide rapid results, adequate sensitivity, minimum sample preparation and operator intervention for waters with widely varying chemical and physical properties. In this work, intercomparisons of various results were reported.

Happel *et al.*[18] determined gross α activity in drinking water using a highly specific resin and LSC. Gross α activities were determined using α-β discrimination LSC by direct measurement of the dried resin after extraction. A method for the determination of α emitting nuclides in drinking water was further developed and tested using intercomparisons of spiked drinking water samples.

Rusconi *et al.*[19] assessed radioactivity of drinking water by liquid scintillation counting (set up for high sensitivity and emergency procedures), both in normal and in emergency situations. They also evaluated the uncertainty in low-level LSC measurements of gross α and β activities in water samples.[20]

Vesterbacka[21] summarized the results of measurements of natural radioactivity in drinking water in Finland.

Zapata-Garcia *et al.*[22] established a method for the rapid measurement of gross α and β activities in sea water.

Hamzah *et al.*[23] used liquid scintillation counting to measure ^{226}Ra in water samples from Sungai Kelantan, Malaysia.

The Department of Water Affairs and Forestry (DWAF)[7] in South-Africa reported the radioactivity monitoring studies in the Mooi river (Wonderfonteinspruit area) with the aim of measuring the concentrations of a large range of radionuclides in the natural uranium and thorium decay chains in the Wonderfonteinspruit catchment area from the viewpoint of use as drinking water by local settlers and the consequent potential radiological impact.

2.3 Natural Sources of Radiation

2.3.1 Introduction

Natural radioactive substances are found in the atmosphere, but most of them are present in the lithosphere. On earth the most important sources are the ores of uranium and thorium, but potassium salts also contribute to natural radioactivity.

2.3.2 Uranium

Uranium (U) isotopes occur naturally within the two uranium decay series, with the parents ^{238}U and ^{235}U, which give rise to decay series that end in the stable isotopes lead-206 (^{206}Pb) and lead-207 (^{207}Pb) respectively, while uranium-234 (^{234}U) is part of the ^{238}U chain.[24] The half-lives of ^{238}U and ^{235}U are 4.47×10^9 and 7.13×10^8 years respectively. Due to their long half-life, these isotopes are still present in the environment.[3] ^{234}U is present, being the third progeny of the ^{238}U decay chain. Its natural abundance of 0.0055% is due solely to the ^{238}U decay chain.[3] More information on the uranium decay chains can be found in Tables 2.1 and 2.2.

Uranium is the heaviest naturally occurring radioactive element on earth, with a global background concentration in the earth's crust of approximately 2 to 4 mg/kg. [25] Uranium is partially soluble in water mainly due to its ability to form complexes with the carbonate ion, and is therefore rather mobile in the environment. Uranium occurs in natural waters in three oxidation states, uranium (IV) (e.g. U^{4+}), uranium (V), (e.g. UO_2^+) and uranium (VI) (e.g. uranyl ion UO_2^{2+}). In reducing surface waters, uranium occurs as U^{4+} and UO_2^+. Uranium (IV) has a strong tendency to precipitate (e.g. as uraninite, $UO_2(s)$) and to remain immobile, whereas UO_2^+ forms soluble, but relatively unstable, complexes. Uranium occurs in oxidizing surface waters as UO_2^{2+}, which forms stable, readily soluble, cationic, anionic or neutral complexes, which are highly mobile.[26]

All of the naturally occurring uranium isotopes are α emitters. The presence of uranium in environmental samples means that all of its progeny will be present to a varying extent based on solubility.[3] The ^{238}U decay chain has 14 progeny participants. This means that typical environmental samples containing ^{238}U will also contain some concentration of all of its progenies as well. The amount of each will depend on the sample's history, environmental conditions and the individual chemistry of each progeny and the parent.[3]

In previous studies, uranium was identified as a major concern of contamination in surface and groundwater in the Wonderfonteinspruit catchment area (WCA). Uranium originates mainly from mining activities in the catchment area which liberate radioactive heavy metals from the lithosphere and allow for its migration from the mining properties into the environment, polluting surface and ground water.[26]

About 100 000 tons of uranium is contained in tailing dams within the WCA. Apart from tailings, underground water in contact with uraniferous reefs constitutes another source of waterborne uranium pollution.[27] Fifty tons of uranium is discharged annually into the receiving water courses within the WCA.[25] The discharge of uranium polluted water together with the largely uncontrolled outflow of uraniferous seepage from tailing deposits are major sources of water pollution in the WCA.

2.3.3 Thorium

Thorium (Th) is naturally occurring as ^{232}Th, which gives rise to a decay series that ends in the stable isotope ^{208}Pb (Table 2.3), and has a half-life of 1.41×10^{10} years. Thorium has five additional naturally occurring radioisotopes (^{227}Th, ^{228}Th, ^{230}Th, ^{231}Th, and ^{234}Th, with half-lives of 18.7 days, 1.91 years, 7.54×10^4 years, 25.5 hours and 24.1 days, respectively) that result from the uranium and thorium decay chains.

Natural thorium can be found in several minerals. It is recovered commercially from the mineral monazite that contains 3 to 9% ThO_2 together with rare earth minerals. Thorium was discovered in 1828 by Berzelius who named it after Thor, the Scandinavian god of war. Thorium occurs in the 4+ oxidation state and is a highly insoluble, highly reactive particle and of low environmental mobility. The presence of thorium is often not discovered directly, but through the radioactive emissions of its progeny radium, actinium, polonium, bismuth, and lead.[3]

Table 2.1. ^{238}U Decay Series [24]

Nuclide	Half life	Major energies (MeV) and intensities (%)*	
		α	β
^{238}U	4.47×10^9 y	4.15 (21%) 4.2 (79%)	–
↓ ^{234}Th	24.1 d	–	0.04 (100%)
↓ ^{234}Pa	1.17 m	–	0.82 (98%)
↓ ^{234}U	2.46x105 y	4.72 (28%) 4.77 (71%)	–
↓ ^{230}Th	7.54x104 y	4.62 (23%) 4.69 (76%)	–
↓ ^{226}Ra	1600 y	4.60 (5.5%) 4.78 (94.5%)	–
↓ ^{222}Rn	3.82 d	5.49 (~100%)	
↓ ^{218}Po	3.11 m	6.00 (100%)	–
99.98% ↓ 0.02% ^{214}Pb	26.8 m	–	0.21 (49%)
^{218}At	1.6 s	6.65 (6%) 6.69 (89.9%)	
↓ ^{214}Bi	19.9 m	5.45(1%)	0.64(99%)
99.96% ↓ 0.04% ^{214}Po	164 μs	7.69 (100%)	–
^{210}Tl	1.3 m	–	1.18 (100%)
↓ ^{210}Pb	22.3 y	3.72 (0%)	0.004 (84%) 0.016 (16%)
↓ ^{210}Bi	5.01 d	–	0.39 (100%)
~100% ↓ ~.00001% ^{210}Po	138.3 d	5.30 (100%)	–
^{206}Tl	4.19 m	–	0.54 (100%)
↓ ^{206}Pb	Stable	–	–

* Intensities refer to percentage of disintegrations of the nuclide itself, not to the original parent of the series.

Table 2.2. ^{235}U Decay Series [24]

Nuclide	Half life	Major energies (MeV) and intensities (%)*	
		α	B
^{235}U	7.04×10^8 y	4.37 (17%) 4.4 (55%) 4.6 (5%)	–
↓ ^{231}Th	25.5 h	–	0.08 (37%)
↓ ^{231}Pa	3.28×10^4 y	5.03 (20%) 5.01 (25.4%) 4.95 (22.8%)	–
↓ ^{227}Ac	21.8 y	4.95 (0.66%) 4.94 (0.55%) 4.87 (0.09%)	–
98.8% ↓ 1.2% ^{227}Th	18.7 d	5.76 (20.4%) 6.04 (24.2%) 5.98 (23.5%)	–
^{223}Fr	21.8 m	–	0.35 (96%)
↓ ^{223}Ra	11.44 d	5.61 (25.7%) 5.72 (52.6%) 5.54 (9.2%)	–
↓ ^{219}Rn	3.96 s	6.43 (7%) 6.55 (12.9%) 6.82 (79.4%)	–
↓ ^{215}Po	1.83 ms	7.38 (100%)	–
↓ ^{211}Pb	36.1 m	–	0.45 (100%)
↓ ^{211}Bi	2.14 m	6.28 (16.2%) 6.62 (83.5%)	0.18 (0.28%)
0.32% ↓ 98.68% ^{211}Po	0.52 s	7.45 (98.9%)	–
^{207}Tl	4.77 m	–	0.5 (100%)
↓ ^{207}Pb	Stable	–	–

* Intensities refer to percentage of disintegrations of the nuclide itself, not to the original parent of the series.

Table 2.3. ^{232}Th Decay Series [24]

Nuclide	Half life	Major radiation energies (MeV) and intensities*	
		α	β
^{232}Th	1.41×10^{10} y	3.95 (21.7%) 4.01 (78.2%)	–
↓ ^{228}Ra	5.75 y	–	0.007 (100%)
↓ ^{228}Ac	6.15 h	–	0.38 (93%)
↓ ^{228}Th	1.91 y	5.34 (27.2%) 5.42 (72.2%)	–
↓ ^{224}Ra	3.66 d	5.45 (5.05%) 5.69 (94.9%)	–
↓ ^{220}Rn	55.6 s	6.29 (99.9%)	–
↓ ^{216}Po	0.145 s	6.78 (100%)	–
↓ ^{212}Pb	10.64 h	–	0.1 (100%)
↓ ^{212}Bi	60.6 m	6.09 (9.75%) 6.05 (25%)	0.77 (64%)
64.0% ↓ 36.0% ^{212}Po	304 ns	8.78 (100%)	–
^{206}Tl	4.1 m	–	0.54 (100%)
↓ ^{208}Pb	Stable	–	–

* Intensities refer to percentage of disintegrations of the nuclide itself, not to the original parent of the series.

2.4 Radioactive Decay

2.4.1 Introduction

Radioactive decay occurs when an unstable isotope transforms to a more stable isotope, generally by emitting a subatomic particle such as an α or β particle, while γ radiation is not a mode of radioactive decay. Uranium, thorium and actinium occur in three natural decay series, headed by uranium-238, thorium-232 and uranium-235 respectively. The parent radionuclides have a half-life much longer than that of any other radionuclide in the series. In nature, the radionuclides in these series are approximately in a state of secular equilibrium, in which the activities of all radionuclides within each series are nearly equal.

The secular equilibrium can be disturbed, for example, in the decay series of ^{238}U series, ^{226}Ra decays to the daughter ^{222}Rn by an α decay, and ^{222}Rn decays further to ^{218}Po and consequently to ^{214}Pb. Since ^{222}Rn is a gas, it might escape the matrix and thus disturb the secular equilibrium. The disturbance of secular equilibrium due to ^{220}Rn (^{232}Th series) or ^{219}Rn (^{235}U series) is less significant due to their short half-lives of 55.6 s and 3.96 s respectively, implying that ^{220}Rn or ^{219}Rn build-up will be negligible. The radionuclides of the ^{238}U, ^{232}Th and ^{235}U decay series are shown in Tables 2.1, 2.2 and 2.3 above.

There are several types of radiation associated with radioactivity each having different characteristics, but for the purpose of this research only α and β emitters were studied.

2.4.2 Decay modes

2.4.2.1 α decay

An α particle is equivalent to the nucleus of a helium atom, it consists of two protons and two neutrons. Many naturally occurring heavy nuclei, with atomic numbers ranging from Z = 92 to Z = 81, decay by α emission in which the parent nucleus loses both mass and charge (A, Z) [28]. The α type reaction can be represented as

$$^{A}_{Z}X \rightarrow ^{A-4}_{Z-2}Y + ^{4}_{2}\alpha + DE$$

where X represents a chemical symbol of the parent atom and Y that of the daughter. A is the atomic number and Z is the number of protons while DE is decay energy.

An α particle is the heaviest particle emitted during radioactive decay except for fission.[3] These particles have a high energy ranging between ~4 to 10 MeV (Tables 2.1, 2.2 and 2.3). If α emitting materials are taken into the body either by eating, drinking, or breathing, they can cause biological damage if exposed to internal tissue directly. Externally, they can be stopped completely by a sheet of paper or by the thin surface layer of skin. A large portion of each decay series (Tables 2.1, 2.2 and 2.3) emits α particles.

2.4.2.2 β decay

β decay is characterized by electrons with either a positive (positron) or negative (negatron) charge. In negative or negatron β particle (β^-) emission, a neutron, in the nucleus, is converted into a proton, electron, and an anti-neutrino. In this case the decaying radionuclide possesses an excess of neutrons or a neutron/proton imbalance. The reaction is symbolized by

$$^{1}_{0}n \rightarrow ^{1}_{1}p + ^{0}_{-1}\beta + \overline{\nu_e}$$

Although free electrons do not exist inside the nucleus, the β particle originates there and must pass the nuclear potential barrier to escape, and from the above equation it follows that when a

nucleus emits a β particle, it is increased in atomic number by one unit but retains the same mass number.[28] This leads to the equation

$$^{A}_{Z}X \rightarrow {}^{A}_{Z+1}Y + {}^{0}_{-1}\beta + \overline{\nu_e}$$

The product nucleus may be in an excited state, which leads to emission of one or more gamma-rays.

The β^+ particle emission is an example of the radioactive decay of a nuclide with proton excess or neutron deficiency. A proton is converted to a neutron and a positron (β^+) by

$$^{1}_{1}p \rightarrow {}^{1}_{0}n + {}^{0}_{1}\beta^{+} + \nu_e$$

and the transformation is now

$$^{A}_{Z}X \rightarrow {}^{A}_{Z-1}Y + {}^{0}_{1}\beta^{+} + \nu_e$$

Again, when the product nucleus is in an excited state, gamma-ray emission will follow.

β-Particles are smaller and have less energy and they penetrate more compared to α particles and can pass through about 1 cm of water.[1] They can therefore pass through the outer layer of the skin and strike the cells below. When taken into the body, they can also cause damage to the cells but less severe than α particles.

2.4.3 Decay Rates

The activity of a radioactive sample or a radioactive source is defined as its rate of decay, or in other words, it is described by its intensity or the number of nuclei decaying per unit time. During a series of radioactive decays, the original radioactive (parent) nucleus N_1 decays to a radioactive (daughter) nucleus until the end of the series, where a stable nucleus is formed (^{206}Pb in the case of the ^{238}U (Table 2.1) series, ^{207}Pb for ^{235}U (Table 2.2), and ^{208}Pb for ^{232}Th (Table 2.3), Activity is given by the fundamental law of radioactive decay:

$$\frac{dN}{dt} = -\lambda N \qquad (2.1)$$

Where $\frac{dN}{dt}$ is the disintegration rate, λ is the decay constant and the negative sign indicates that N, the number of radioactive atoms is decreasing with time (t). The solution of the integral Equation 2.1 is

$$N = N_0 e^{-\lambda t} \qquad (2.2)$$

Where N_0 being the number of radioactive nuclei present at time $t = 0$ and e is the base of the natural logarithm.

Radionuclide decay rates are usually expressed in terms of half-life ($t_{1/2}$) which is the time required for a given amount of radionuclide to lose half of its activity. The half-life ($t_{1/2}$) may be expressed as $t_{1/2} = \frac{\ln 2}{\lambda}$

or the decay constant can be defined as $\lambda = \frac{\ln 2}{t_{1/2}}$ (2.3)

The activity (A) of a radionuclide, defined by its disintegration rate can be represented by

$$A = \frac{dN}{dt} = -\lambda N \quad (2.4)$$

The unit of radioactivity is the Becquerel (Bq), named after the French physicist Henri Becquerel (1852-1908), one of the discoverers of radioactivity. The old unit being the Curie (Ci), named after Marie Curie (1852-1908) who discovered radium in 1898, whereby: 1 Ci = 3.7 x 10^{10} decays per second and 1 Bq = 1 decay per second.

The relationship between radionuclides as they decay (parents and daughters) to a stable nuclide can be written as Equation 2.5.

$$\text{nuclide 1} \xrightarrow{\lambda_1} \text{nuclide 2} \xrightarrow{\lambda_2} \text{nuclide 3} \quad (2.5)$$

The parent nuclide 1 decays to a daughter nuclide 2 with a decay constant λ_1 which in turn decays to a stable nuclide 3 with a decay constant λ_2. The decay rate of the daughter nuclide is dependent on its own decay rate as well as the rate at which it is formed by the parent and is expressed as:

$$\frac{dN_2}{dt} = -\frac{dN_1}{dt} - \lambda_2 N_2 = \lambda_1 N_1 - \lambda_2 N_2 \quad (2.6)$$

$\lambda_1 N_1$ is the rate of decay of the parent (forming the daughter) and $\lambda_2 N_2$ is the rate of decay of the daughter. The decay rate of nuclide 1, equation 2.6 may be transposed into the linear differential equation as follows:

$$\frac{dN_2}{dt} + \lambda_2 N_2 - \lambda_1 N_1^0 e^{-\lambda_1 t} = 0 \quad (2.7)$$

N_1^0 is the number of atoms of nuclide 1 at time $t = 0$. The solution of the linear differential equation 2.7 as a function of time is given as

$$N_2 = \frac{\lambda_1}{\lambda_2 - \lambda_1} N_1^0 \left(e^{-\lambda_1 t} - e^{-\lambda_2 t}\right) + N_2^0 e^{-\lambda_2 t} \tag{2.8}$$

Where N_2^0 is the number of atoms of nuclide 2 present at time $t = 0$. If nuclide 1 and 2 are separated quantitatively at $t = 0$, the situation becomes simpler and two fractions are obtained. In the fraction containing nuclide 2, this nuclide is not produced any more by decay of nuclide 1, and for the fraction containing nuclide 1 it follows that $N_2^0 = 0$

$$N_2 = \frac{\lambda_1}{\lambda_2 - \lambda_1} N_1^0 \left(e^{-\lambda_1 t} - e^{-\lambda_2 t}\right) = \frac{\lambda_1}{\lambda_2 - \lambda_1} N_1 \left(1 - e^{-(\lambda_2 - \lambda_1)t}\right) \tag{2.9}$$

From Equation 2.5, the radioactive equilibrium between parent nuclide and a daughter nuclide has been derived. For the last daughter (nuclide 3), the following equation is obtained:

$$N_3 = \lambda_1 \lambda_2 N_1^0 \frac{e^{-\lambda_1 t}}{(\lambda_2 - \lambda_1)(\lambda_3 - \lambda_1)} + \frac{e^{-\lambda_2 t}}{(\lambda_1 - \lambda_2)(\lambda_3 - \lambda_2)} + \frac{e^{-\lambda_3 t}}{(\lambda_2 - \lambda_3)(\lambda_1 - \lambda_3)} \tag{2.10}$$

If a chain of numerous nuclides such as $N_4, N_5 \ldots N_n$, is involved, Bateman [29] has given the solution for a chain of n-numbers with special assumption that at $t = 0$ the parent substance alone is present, that is, $N_2^0 = N_3^0 = \ldots . N_n^0 = 0$ The solution is given as

$$N_n = C_1 e^{-\lambda_1 t} + C_2 e^{-\lambda_2 t} + \ldots C_n e^{-\lambda_n t}, \text{ where} \tag{2.11}$$

$$C_1 = \frac{\lambda_1 \lambda_2 \ldots \lambda_{n-1}}{(\lambda_2 - \lambda_1)(\lambda_3 - \lambda_1) \ldots (\lambda_n - \lambda_1)} N_1^0, \text{ and}$$

$$C_2 = \frac{\lambda_1 \lambda_2 \ldots \lambda_{n-1}}{(\lambda_1 - \lambda_2)(\lambda_3 - \lambda_2) \ldots (\lambda_n - \lambda_2)} N_1^0, \text{ etc.}$$

The time necessary to reach radioactive equilibrium depends on the half-life of the daughter nuclide. In equilibrium, the ratio of the activities N_2/N_1 is constant. Radioactive equilibrium is not an equilibrium in the sense used in thermodynamics and chemical kinetics, because it is not reversible, and it generally does not represent a stationary state. Three cases of radioactive equilibrium can be distinguished:

Secular equilibrium (Figure 2.1a)

In secular equilibrium, the parent nuclide must be long-lived and the daughter nuclide must have a relatively short half-life $(t_{1/2}[1] >> t_{1/2}[2])$. Therefore, the expression of ingrowths (Equation 2.9) of daughter atoms with the parent becomes

$$N_2 = \frac{\lambda_1}{\lambda_2} N_1 \left(1 - e^{-\lambda_2 t}\right) \tag{2.12}$$

After $(t >> t_{1/2}[2])$ (in practice, after about 10 half-lives of nuclide 2), equilibrium is established and the activities of the parent nuclide and of all the nuclides emerging from it are the same: $A_1 = A_2$. Secular equilibrium can be used for the determination of a long-lived parent nuclide, if the activity of the daughter is easier to measure. Examples are the determinations of ^{210}Pb via the daughter ^{210}Bi, ^{228}Ra via ^{228}Ac, and ^{226}Ra via ^{222}Rn.

Transient equilibrium (Figure 2.1b)

In transient equilibrium, the parent nuclide must have a slightly longer half-life than its daughter, but almost the same half-life than that of the parent nuclide $(t_{1/2}[1] > t_{1/2}[2])$.[9] In transient equilibrium, the Bateman equation cannot be simplified by assuming the daughter's half-life is negligible compared to the parent's half-life. The ratio of daughter-to-parent activity is given by:

$$\frac{A_2}{A_1} = \frac{\lambda_2}{\lambda_2 - \lambda_1} \tag{2.13}$$

Accordingly, after attainment of equilibrium, the daughter activity is always higher than the parent activity.[30]

The state of no equilibrium (Figure 2.1c)

In this case, the daughter nuclide is longer lived than its parent nuclide $(t_{1/2}[1] < t_{1/2}[2])$. Therefore the parent nuclide of short half-life decays faster than the daughter nuclide leaving only the daughter nuclide to decays at its specific half-life. The ratio between the two changes continuously, until the parent nuclide has disappeared. No radioactive equilibrium is attained.

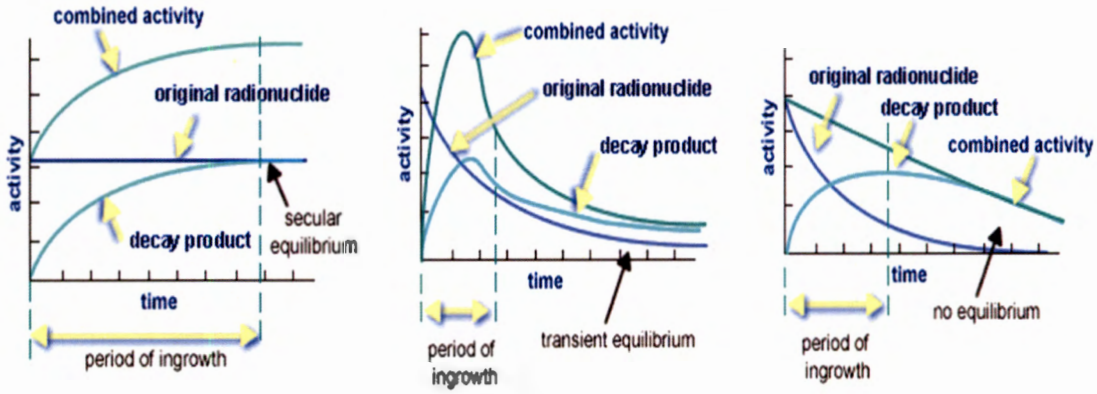

a) Secular equilibrium b) Transient equilibrium c) No equilibrium

Figure 2.1. Three cases of radioactive equilibrium.[31]

CHAPTER 3

TECHNIQUES FOR MEASURING ENVIRONMENTAL SAMPLES

3.1 Introduction

Analysis of natural radionuclides has become very important in environmental science particularly for the monitoring and identification of the activity concentration of radionuclides present in water, mainly because of health risks associated with water intended for human consumption. Yet, not many analytical techniques are available to measure radionuclides in environmental samples. The available techniques have different advantages and disadvantages and are frequently selected to suit the available resources and research objectives of a particular study. For example, if one is only interested in the total α and β activity, liquid scintillation and/or gas-flow proportional counting techniques can be used. If one wants to have more specific information to quantify the specific radionuclides one can use γ spectrometry in combination with neutron activation analysis and/or element specific chemical separations followed by α spectrometry. Some of the more common techniques that can be applied in radioactivity monitoring are described in this chapter.

3.2 Geiger-Müller Detectors

A Geiger-Müller detector is a gas-filled radiation detector. It consists of two components, a Geiger-Müller tube (the detector in which the ionized particles are produced) and an electronic amplifier (which activates a device that counts the current particles).

The detector requires only a moderately stable voltage, a simple amplifier and a ratemeter to construct a useful instrument. Figure 3.1 is a schematic representation of the device. Common forms include:

The Geiger tube (A). A cylindrical tube containing a tubular cathode and an axial wire anode. As a side window detector, the tube is enclosed within a metal shield which has a shutter. The shield protects the tube and provides a means to discriminate between penetrating and non-penetrating radiations.

The end window Geiger tube (B). A cylindrical thin metal body forms the cathode which is sealed at one end by a thin window. α, β and photon radiations are detected through the window but with poor detection efficiencies.[32]

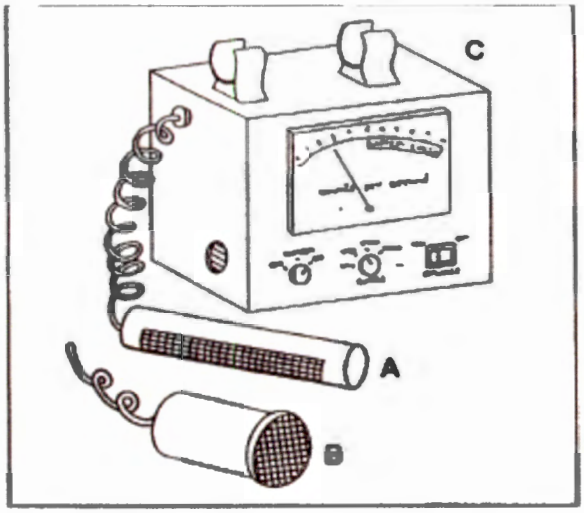

Figure 3.1. Schematic representation of a Geiger-Müller counter (with different tubes) and a ratemeter.[32]

Geiger-Müller counters are the most commonly commercially used instruments to measure dose rate. The pulsed output of Geiger counters is often made to form an audible indication of the detected count rate. The Geiger counter has a high sensitivity but is very dependent upon the energy of photon radiations.

They are used to determine if radiation is present, rather than what the radionuclide's identity is, or how much radioactivity is present. They come in a wide variety of shapes and sizes.

3.3 Semiconductor Detectors

A semiconductor detector is a device that uses a semiconductor, usually silicon or germanium to detect photons. The most commonly used semiconductor material is High Purity Germanium (HPGe). These detectors use the electronic carriers (electron-ion and electron-hole pairs) created by absorption of γ ray photons in the germanium, causing a flow of electric current through the semiconductor and produce an output voltage pulse of an amplitude proportional to the energy of the incident gamma photon.

Figure 3.2 is the cross sectional diagram of a germanium detector with a Dewar to cool the germanium to the temperature of liquid nitrogen.

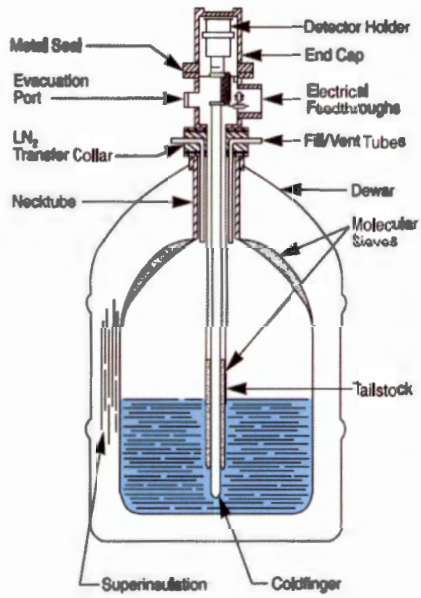

Figure 3.2. A typical germanium detector, cryostat and liquid nitrogen reservoir (Dewar).[33, 63]

3.4 Alpha Spectrometry

α spectrometry is applicable for determining the activity of any α-emitting radionuclide. An α-particle spectrometry system typically consists of a solid-state detector in a vacuum chamber, a high voltage detector bias supply, a charge-sensitive preamplifier, an amplifier, an analogue-to-digital converter and a digital memory storage device. α Spectrometry systems normally are operated to cover the energy range between 3 and 10 MeV.

The system includes the personal computer (PC) software program, which allows data processing and instrument control (Figure 3.3). The element of interest is chemically separated from other elements and deposited in a very thin layer by electrodeposition or by co-precipitation, and then placed to open lid (front view) of alpha spectrometry to be counted. Information specific of each identified element are provided by the computer software. The activity of the nuclide of interest is measured by the number of counts in the appropriate energy region, taking the detection efficiency into consideration.

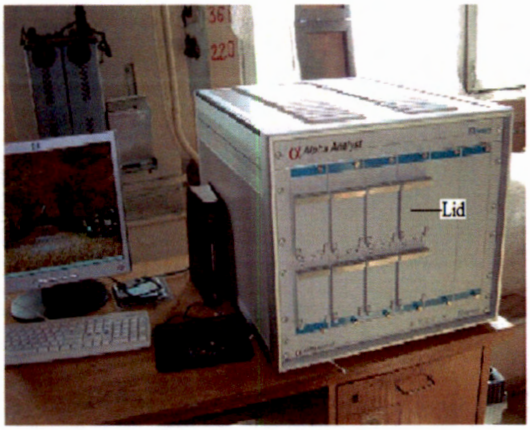

Figure 3.3. α spectrometry [34]

3.5 Gas Flow Proportional Counters

The gas flow proportional counter is often used for the simultaneous detection of α-β particles in the same sample. It is constructed of stainless steel and high conductivity copper or aluminum. The components of a gas proportional α-β counter consist mainly of a detector, an amplifier, a bias voltage supply, a pulse selector and a scaler. A gas flow detector consists of a tube with a high conductivity copper body, anode wire, a thin Mylar window positioned between the sample and the detector to shield the detector from external contamination and gas inlet and outlet ports. α and β particles penetrate the window and ionize the gas. The thin wire anode is stretched crosswise inside the counting volume to improve the collection of electrical charge.[35]

The measurements of α and β activities by a gas flow proportional counter is done in two channels. These channels are set to detect mainly α's in one channel and β's in the other channel, which obviously will cause some interference from α's in the β channel and vice-versa. It has the major advantage of high detection efficiency but the disadvantage is that it lacks the feasibility to discriminate between the energy of the particles and thus characterize the α or β particles according to their energies.

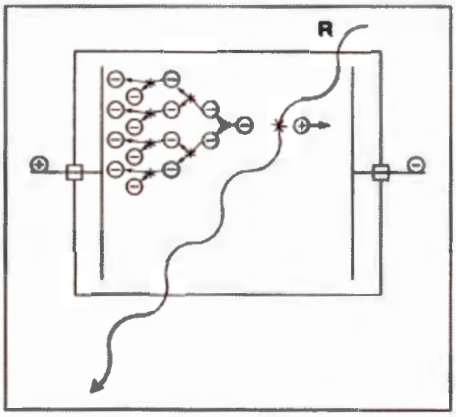

Figure 3.4. Schematic of a gas flow proportional counter.[32]

3.6 Liquid Scintillation Counters

The liquid scintillation counting (LSC) method is applicable to any α and/or β emitting nuclide. It is most applicable to the measurement of low-energy αβ emitters. The principle of LSC is based on a homogeneous distribution of the radioactive substance in a scintillation cocktail. An aliquot of a sample is added to a liquid scintillation "cocktail" which is coupled to photomultiplier tubes. The α and β particles transfer energy to the scintillator resulting in the production of light photons which strike a photomultiplier tube, converting the light photons to electrical pulses which are counted. The intensity of light produced in the scintillation cocktail is directly proportional to the energy of the particle. The flash of light is simultaneously detected by two photomultiplier tubes, giving rise to an electronic pulse whose amplitude is linearly related to the energy of the particle. The spectrometer is adjusted to establish a channel or "window" for the pulse energy appropriate to the nuclide of interest. The activity of the nuclide of interest is measured by the counting rate in the appropriate energy channel. The principles of this LSC device will be discussed fully in chapter 4 as this technique was used in this study.

CHAPTER 4

LIQUID SCINTILLATION COUNTING (LSC)

4.1 Introduction

The LSC technique is one of the most frequently used techniques for quantitative analysis of radionuclides. It measures both α and β particles simultaneously due to the fact that their pulses can be identified using pulse shape analysis (PSA). Weak γ, x-ray and Auger electron emitters can also be measured.[9]

The radioactive samples are usually mixed with the liquid scintillation solution (cocktail) and measured. Due to the close contact of the radionuclide to the detector medium high efficiencies can be achieved, so that even nuclides with low energy β radiation, such as tritium and ^{241}Pu, can be measured with high efficiencies.

The counting efficiency is nearly 100% for α emitters. Due to its high efficiencies for α as well as β emitters and accordingly the low detection limits, and the wide range of measurement flexibility, our work has focused on this technique.

4.2 The Liquid Scintillation Process

LSC is a method used for quantifying the activity of radioactive samples based in a liquid medium. The liquid medium consists of solvents and organic scintillators that convert the energy absorbed by charged particles into light that is detectable by PMTs. In the late 1930s, the German Professor, Kallmann discovered that certain organic materials fluoresced under ultraviolet light. He also revealed that aromatic solvents which contain dissolved solutes were efficient scintillation sources when subjected to nuclear radiation [36] and from here on the LSC detection method was further developed.

In liquid scintillation counting, the radioactive sample is mixed with a cocktail (scintillator solution). The principle is based on a homogeneous distribution of the radioactive substance in a scintillation cocktail, which consist of a solvent and scintillator (fluor); the solvent absorbs most of the energy of the particle and the decay energy is transferred to the scintillator (fluor) molecules and then photons of visible light are emitted.

These photons are detected by photo multiplier tubes (PMTs). The scintillation process and light that is produced are different for the α and β decay processes. About one photon of light is produced per keV of decay energy for α particles while for β particles, 10 photons of light are

produced per keV.[9] α emitters are generally in the energy range of 4 to 10 MeV, but appear in the liquid scintillation spectra at about 100 to 600 keV because of their reduced photon yield, as compared to β particles. The schematic principle of the liquid scintillation process in a scintillation cocktail is shown in Figure 4.1.

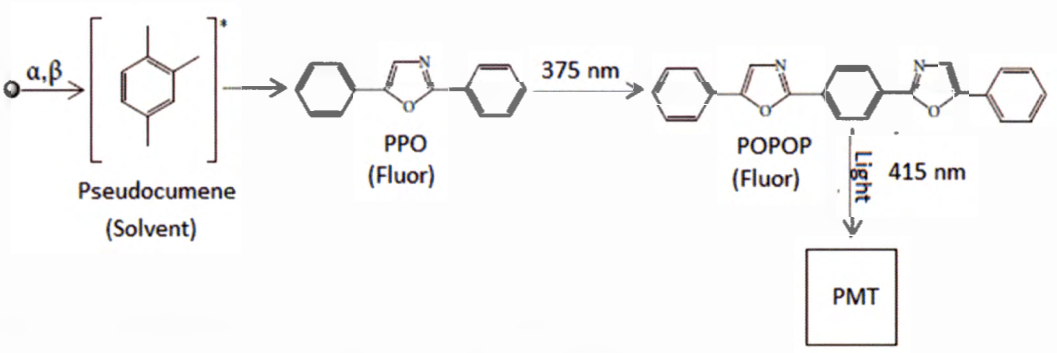

Figure 4.1. Principle of liquid scintillation counting

Liquid scintillation detectors have a poor energy resolution, which leads to broad pulses.[37] This is due to a relatively large amount of energy required to produce a single photon at the PMT photocathode and, to a lesser extent, because of the inefficient light production by α particles relative to β's, (Table. 4.1).

Table 4.1. Relative scintillation yield for different types of ionizing particles.[36]

Type of particle	Fraction of particle energy converted to photons compared to electrons
Electrons (>80 keV)	1.0
Protons (1-10 MeV)	0.20-0.50
α's (4-6 MeV)	0.08-0.12

The α pulse is about 35 to 40 ns longer than a pulse produced by β particles. α Particles can therefore be distinguished from most other nuclear decay radiations with the liquid scintillation analyzer because of the slower pulse decay time. The counting efficiency is approximately 100% for almost all α decays, whereas the counting efficiency for β emissions depends on the β decay energy. For most β decays with energies higher than 100 keV, the counting efficiency is about 90 to 100%, but for low energy β decays, it is in the range of 10 to 60%.[9]

4.3 Scintillation Solution

A scintillation solution (cocktail) is the medium that holds the sample during the analysis process. The LSC cocktail is both fundamental to and necessary for analysis. To appreciate the significance of a correct cocktail selection, it is useful to explain some fundamental concepts about the components of LSC cocktails. It is composed of solvents (or a solvent) and solutes (or solute). The solvent acts as a medium for absorbing energy of the nuclear radiation and for dissolving the sample. The solute acts as an efficient source of photons after absorbing the energy from the excited solvent molecules. The base for the scintillation cocktail is an aromatic solvent. Aromatic solvents are the best solvents due to the high density of electrons associated with these solvents. When they react with β particles, a large amount of fluorescence can be produced.

Solvents are classified as either primary or secondary (Table 4.2 and 4.3), depending on the relative amounts and their function in the scintillation processes. The primary solvent is the initial energy absorber and produces the initial excited molecules while the secondary solvent act as an intermediary in the energy transfer process, which increases the efficiency of the energy migration from the initial primary solvent excited molecules to the emitting solute molecules.

Table 4.2. Properties of a few primary scintillators.[30, 36, 38]

Scintillator	Structure	Peak fluo-rescence (nm)	Decay Time (ns)
2,5-Diphenyloxazole (PPO)	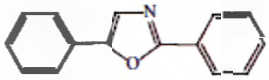	375	1.4
p-Terphenyl		342	1.0
Butylphenylbiphenyl-oxadiazole (Butyl-PBD)	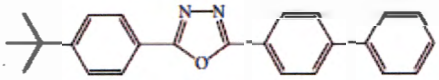	385	1.0
Naphthalene	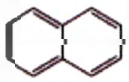	334	96.0

The photomultiplier tubes are not sensitive to the fluorescence wavelength of the aromatic solvents. A fluor (or scintillator) is often used to capture the solvent energy and emit light at a wavelength more easily detected. Earlier photomultiplier tubes were not sensitive in the region of fluorescence emission of the primary scintillators, but a secondary scintillator (wavelength shifter) was introduced to solve this problem. Common secondary scintillators are bis-MSB and POPOP (Table 4.3).

Table 4.3. Some commonly used secondary scintillators[30, 36, 38]

Compound	Structure	Average wavelength (nm)
Diphenyloxazolylbenzene (POPOP)	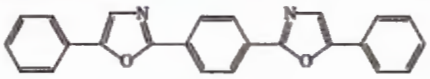	415
1,4-Bis(2-methystryryl)benzene (bis-MSB)	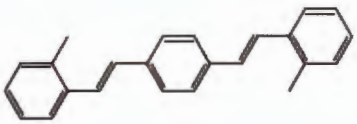	425
2-(1-Naphthyl)-5-phenyloxanole (α-NPO)	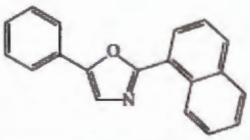	400

Previously, highly toxic solvents, such as toluene, dioxane, xylene, or 1,2,4-trimethylbenzene (pseudocumene) were commonly used. However, the common solvents used today, for example phenyl-xylylethane (PXE) and di-isopropylnaphthalene (DIPN) (Table 4.4), are safer, low toxicity solvents possessing higher flash points (the temperature at which a particular organic compound gives off sufficient vapour at which the application of an ignition source causes the vapors of a specimen to ignite).

Dioxane has a very low yield. The addition of naphthalene and its derivates, such as DIPN, will in general raise the scintillation yield, because they possess properties of a primary scintillator (i.e. they emit light with wavelengths < 400 nm). Naphthenic solvents have poor scintillation properties but the addition of a secondary solvent boosts the counting efficiency of the solvent. Together, naphthalene and dioxane as the primary solvent acts as such an intermediary in the energy transfer processes in solutions.

4.4 Surfactants

The majority of radioactive species is present in an aqueous form and are therefore not miscible in aromatic solvents. As such, the presence of surfactants in the cocktail enables water or aqueous samples to come into intimate contact with the aromatic solvent forming a stable micro-emulsion. The application of a nonionic/anionic surfactant combination, whatever the solvent is, shows that the sample load capacity is relatively independent of temperature and this enables a high quench resistance.[39]

Table 4.4. Some commonly used solvents in LSC[30, 36, 38]

Solvent	Structure	Relative scintillation yield	Flash point (°C)
Toluene	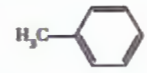	100	4
Dioxane	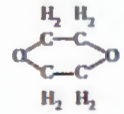	65	11
p-Xylene		110	25
1,2,4-Trimethylbenzene (Pseudocumene)	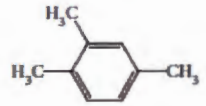	112	50
Phenyl-xylylethane (PXE)	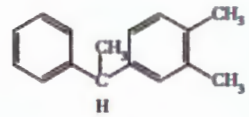	110	150
Di-Isopropylnaphthalene (DIPN)	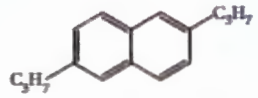	112	150

The introduction of combined surfactants results in higher sample load capacities for water, enabling a stable micro emulsion to be formed when aqueous samples are present. Surfactants are also necessary for ensuring stable conditions over the whole counting period. Examples of surfactants used in scintillation cocktails are alkyl phenol ethoxylates (nonionic), succinates (anionic), carboxylates (anionic) and sulphonates (anionic).[39]

4.5 LSC Counting Vials

The purpose of a counting vial is to hold the sample and the scintillation solution. The vial should be transparent to the light produced in the liquid scintillation system, since the common scintillator solutes emit photons of energy corresponding to wavelengths between 300 and 500 nm.[36] The most common types of counting vial materials are summarized in Table 4.5, each of which has certain advantages for specific needs.

Table 4.5. Different types of scintillation counting vials.[36]

Type	Main advantage	Main disadvantage	
Glass (borosilicate)	Low cost	High background absorption in near UV	
Low K glass	Reduced background from ^{40}K	Absorption in near UV, expensive	
Quartz	Increased transmission in the UV region	Expensive	
Plastic (polyethylene)	Low background, low cost, higher efficiency	Some solvent loss	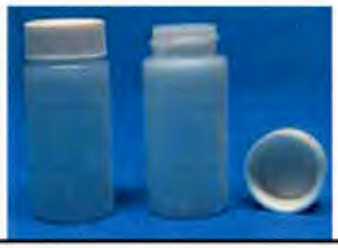
Nylon	Low background	Cost, solvent loss	
Teflon	Low background, can be re-used, high efficiency	Cost, has to be machined	

The advantage of plastic vials, that is polyethylene, nylon, and Teflon, is that they give higher counting efficiencies. This higher efficiency may be the result of several factors, among which are increased transmission of light and reduction of light trapped in the vial walls.

4.6 Interferences in Liquid Scintillation Counting

4.6.1 Introduction

The most common interferences found in liquid scintillation analysis are background radiation, quench, and multiple radionuclides in the same sample. Among all these common interferences, only background radiation and quench were given special attention in this research for elimination or means of correcting for any errors that these may generate.

4.6.2 Background radiation

Background is defined as counts arising from sources external to the sample, for example cosmic or environmental radiation, and instrument noise. There are many sources of background events in liquid scintillation counting. The sources are those produced in the scintillation solution and those which result from events that have no connection with the scintillation solution. Table 4.6 summarizes many of the common background sources.

Another important impact to the background in liquid scintillation counting is the luminescence effect. Luminescence refers to the emission of light photons as a consequence of energy absorption. As interference in liquid scintillation counting, luminescence can occur in sample-scintillation solution (cocktail) mixtures. There are two types of luminescence: photoluminescence and chemiluminescence.

Photoluminescence results from the exposure of the sample-scintillation cocktail mixture to ultraviolet light. This effect can occur in the solution as well as in the vial. The photoluminescence is normally a single photon and it decays mostly within minutes.

Chemiluminescence results from chemical reactions in the scintillator solution, mostly reactions with oxygen or hydrogen peroxide impurities.

Luminescence can be detected by the photomultiplier and could lead to high count rates in the low energy part of the β spectrum. The luminescence spectrum occurs at the very low level part of the pulse height spectrum in the range of 0 to 6 keV.

In addition, the vial materials may also contribute to the background radiation. Most used vials consist of glass (low-potassium borosilicate or quartz) or polyethylene (PE). The background count rate for PE vials is lower than for glass vials, because of the lower content of ^{40}K and ^{232}Th, along with its daughters, in the polymer material compared to glass.

4.6.3 Quench

In liquid scintillation counting, in order to quantify radioactive events as activities, the LSC counts the number of flashes of light in a given time, to provide a count rate (cpm). The count rate depends on the nuclear decay events converted to light flashes that are detected. As a consequence of the complex processes involved in the energy transfer in the liquid scintillation detector, various disruptions in the energy transfer can occur which lead to the reduction of the counting efficiency. Anything that reduces the counting efficiency of the scintillation process is called quenching.

Quenching is the most common interference in LSC.[40] When the sample is quenched more and more, the maximum observed pulse height is reduced further and the cpm collected under the pulse height spectrum is reduced. Strong quenching can shift the majority of pulses below the threshold of detection. Below the threshold of the detection energy, particles do not generate enough photons to be detected. The overall conclusion is that, as the quench of the sample is increased, the spectrum peaks are shifted to lower pulse heights, and also the cpm varies according to the level of quench in the sample due to the pulse height spectral shifting from higher to lower magnitudes caused by quenching.

Two types of quenching may be encountered in liquid scintillation counting:

Chemical quenching is due to the presence of materials in the scintillation solution that interfere with the processes leading to the production of light resulting in fewer photons per quanta of particle energy and a reduction in counting efficiency.[9]

Colour quenching results in a reduction of the scintillation intensity (as seen by the photomultiplier tubes) because of the absorption of the fluor scintillation by coloured materials present in the cocktail. It occurs when colour is visible in the sample that is being counted.[9]

Table 4.6. Sources of background in liquid scintillation counting.[36]

Source	Contributors
Liquid scintillator materials	Natural radioactivity in the liquid scintillator cocktails(^{3}H, ^{14}C).
	Chemiluminescence and phosphorescence of certain solvents enhanced by the presence of the solutes.
Sample	Natural radioactivity in the sample which may be the same or different from the nuclide to be assayed.
	Chemiluminescence and phosphorescence produced by the sample or impurities in the sample.
	Contamination with the same or other radioactive material.
Vial	Natural radioactive compounds in the counting vial walls or cap. (^{40}K, ^{232}Th)
	Cosmic-ray-induced background-Cerenkov and secondary electrons and γ rays.
	Light flashes in the sample vial produce chemiluminescence and phosphorescence.
	Static charge buildup during movement in the sample changer.
Photo multiplier tube (PMT)	Natural radioactivity in materials which make up the PMT (^{40}K, ^{232}Th and its daughters, uranium).
	Interaction of cosmic radiation with PMT window which produce Cerenkov radiation, secondary electrons and γ rays.
	Photomultiplier cross talk from discharge of static electricity.
Other radioactive sources	Radioactive sources such as γ rays in the surroundings of the liquid scintillation counter.

4.6.4 Quench correction

There are several methods that have been used to correct quenching and those that are available depend on the instrument manufacturer. These methods allows analyzers to relate and convert the count rate (cpm-counts per minute) to the actual number of nuclear decays or disintegration rate (dpm-disintegrations per minute) of a sample.[9] For the Wallac 1220 Quantuls ultra low level liquid scintillation counter, the quenching index of this instrument is determined by using a Spectral Quench Parameter (External), abbreviated as SQP(E). The SQP(E) is measured with ^{226}Ra or ^{152}Eu as external standard sources to study the quench in a sample by placing it close to the sample and this external standard produces the Compton electron spectrum in the scintillation cocktail. The SQP(E) is therefore defined as the endpoint or uppermost channel of the Compton electron spectrum which is obtained from the subtraction of two Compton electron spectra. An MCA with 1024 logarithmic channels is used to determine the position of 99th percentile of the endpoint of the external standard spectrum to define SQP(E).[36]

The advantage of this quench index are that it provides a fast, easy and nondestructive evaluation of the quench. For analysis of an unknown activity sample by LSC, its SQP(E) value is determined by the instrument and its counting efficiency is then determined from the calibration graph of the counting efficiency versus the SQP(E) value. [36] Figure 4.2 is the external standard spectrum of the ^{226}Ra source used in this work, measured with a Wallac Quantulus1220™. The determined SQP-value was 830.54 for this measurement.

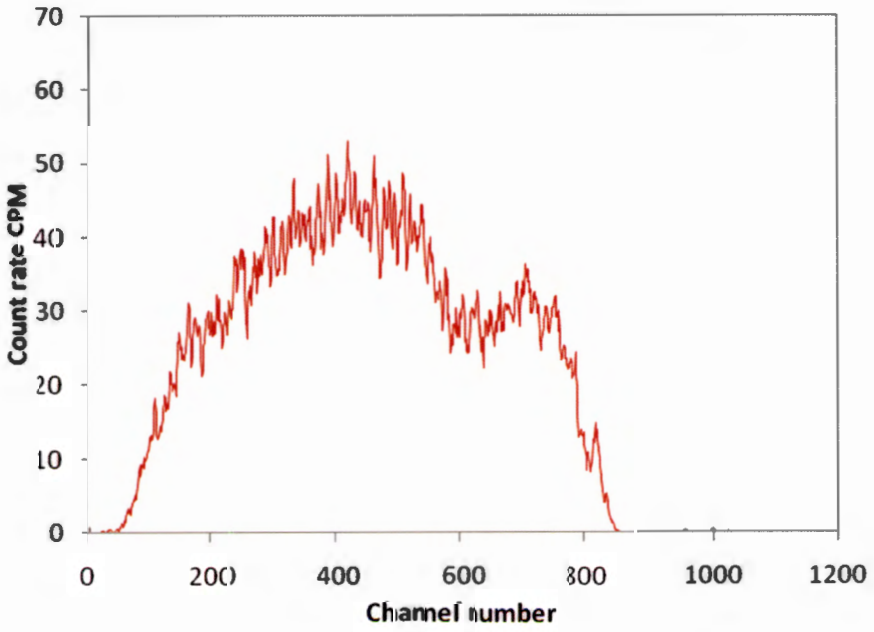

Figure 4.2. The external standard spectrum of ^{226}Ra standard solution, measured with a Wallac Quantulus 1220.

4.7 Pulse Shape Analysis

4.7.1 Introduction

Environmental studies involving the determination of NORMS in raw water require measuring mixtures of α and β emitters. The usual method for counting low level α and β radioactivity is to use LSC, coupled to α-β discrimination, to allow rapid and simple determination of gross α and β activities. The fact that the α particle scintillation yield is low compared to that of an electron (Table. 4.1) makes it difficult to separate α and β decay solely on the basis of the decay energy, in spite of the fact that α particles have much higher energies than β particles.

An α particle in a liquid scintillation solution will on average produce the same number of photons per MeV of energy as an electron which has about one-tenth of its energy, that is a 5 MeV α particle and a 0.5 MeV electron will produce the same number of photons emitted from the same liquid scintillation.[36] Furthermore, it is possible to measure simultaneously both α and β emitting radionuclides by using a Wallac Quantulus 1220™ (Perkin Elmer) liquid scintillation detector that uses a pulse shape analysis circuit (PSA) to distinguish between α and β disintegrations.

Pulse Shape Analysis (PSA) refers to the ability to separate α and β into their respective spectra in a mixed sample[41] by comparing the area of the pulse tail after 50 ns from the start with its total area.[42] Pulse shape discrimination is accomplished using a software adjustable parameter which varies between 1 and 256.[42]

The benefit of using PSA is that it allows very low α background, as most of the background pulses are short and fall in the β spectrum. Therefore a small α background leads to excellent sensitivity. PSA can also detect natural decay series at far better sensitivity by α counting than by measuring total α-β signals.[41]

4.7.2 Discrimination device

The pulse shape analysis uses special pulse decay time discrimination electronics to differentiate α pulses from β pulses basically on the basis of the time it takes for the pulse to decay in a liquid scintillator. It is performed by comparing the ratio of the area of the tail of a pulse, (see also 4.7.1). This value is compared to a previously set numeric parameter (PSA level) and with the help of this comparison it is possible to decide whether a pulse originates from α decay, or from β decay.

The liquid scintillation counter, which is equipped with pulse shape discrimination (PSD) for α-β analysis, is therefore equipped with two Multi-channel analyzers (MCAs). The MCAs counts and sorts the pulses into their different channels because of their amplitudes. All the pulse events originating from scintillation photon emissions with a decay time longer than the PSD setting are sent to the α-MCA and those events which have a shorter lifetime are sent to the β-MCA. This is

based on the fact that pulses are made up of two components, the prompt and the delayed component, and these components occur in different proportions in α and β pulses with the result that α pulses are longer than β pulses. The difference in the duration of α and β pulses is illustrated in Figure 4.3

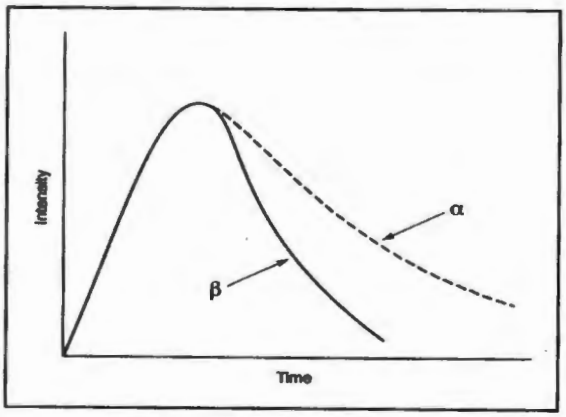

Figure 4.3. Characteristic light pulse shapes of α and β pulses in a liquid scintillator.[9, 43]

In addition, it is necessary to find the optimum PSA setting to get the best separation of α and β radionuclide activities from mixtures into separate MCAs. Different settings of the PSA level assign the pulse into either a long (α-like) or a short (β-like) category. Thus, different PSA settings allow pulses to be categorized according to their length or shape. Typically, increasing the PSA setting will direct more pulses toward the long or α category.[43] At the optimum PSD setting there is a minimum spill of α counts into the β spectrum and β counts into the α spectrum. The determination of the spill-over requires two samples; one pure α and one pure β sample. For the most accurate results, the samples should have the same chemical properties, volume, and geometry as the unknown samples to be counted.

Better α-β discrimination can be achieved by using a cocktail based on di-isopropylnaphthalene or adding a few percent naphthalene to the scintillation cocktail, which generally increases the pulse decay time.[44]

4.8 Description of the Liquid Scintillation Counting System (LSC)

4.8.1 Physical layout of LSC.

Figure 4.4 shows the system setup. The system includes the personal computer (PC) software program, Quantulus 1220™, which allows complete data processing and instrument control. It offers a number of parameter groups or protocols constrained by the hard disk size of the computer and also provides live display of selected spectra on the computer screen.

Figure 4.4. The Wallac Quantulus 1220™ (PerkinElmer Life and Analytical Sciences) frontal view with open lid, showing the auto sampler trays

4.8.2 System electronic description

4.8.2.1 Introduction

The block diagram of the electronic liquid scintillation counting system is shown schematically in Figure 4.5. Three basic components are found in this part of the LSC, namely, detectors, a counting circuit, and a sorting circuit. The system consists of a sample detector chamber that encloses a matched pair of photomultiplier tubes, a counting circuit that involves coincidence unit, sum amplifier and A/D converter while the sorting circuit involves multi channel analyzers (MCAs).

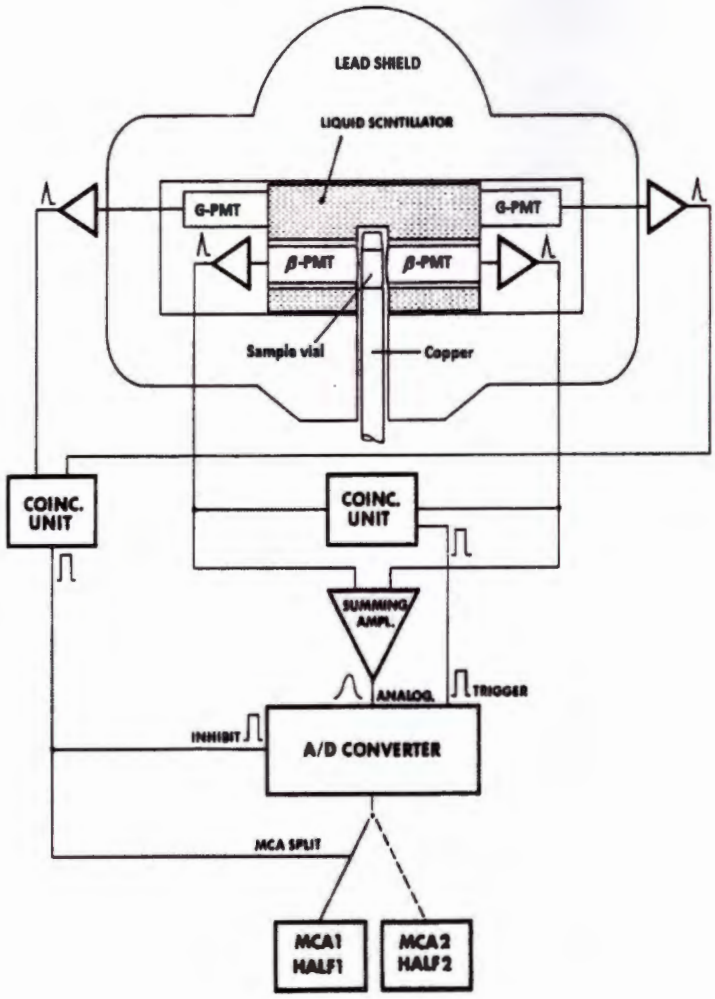

Figure 4.5. Schematic diagram illustrating the components of an LSC used to acquire data. [45]

4.8.2.2 Detector shielding

The scintillation detector well is located inside the lead shield. Samples are automatically lowered into the detector well. The detector assembly consists of two PMTs, operated in a coincidence counting mode. The shielding assembly consists of a sample chamber enclosed with lead to reduce external radiation.

Detectors are used as specialized devices to detect the resultant unwanted counted radiations like γ rays emitted from the irradiation process. The instrument is a low background system which uses unique detector shielding, consisting of a passive and an active shield to achieve low backgrounds.

With both passive and active shielding, the Quantulus employs a universal background reduction system which is optimized according to the application of the instrument. Its background reduction allows very long counting times of ultra low activity samples and does not affect the sample count rates.

Passive shielding

The passive shield consists of the following three layers:

The first layer consist of a lead shield (630 kg), asymmetrically placed around the detector, with a maximum thickness of 20 cm above the measuring position. The lead shield will absorb high energy cosmic radiation (mostly coming from above) and gradually transform it to low energy radiation, which will not disturb the LSC measurements. This shield can also reduce the soft cosmic muon components of the background.[9]

Low energy (thermal) neutrons and X-rays produced in the lead shield by fluorescence reactions are absorbed by cadmium in the second layer.

The third layer is made of copper, to shield any X-ray fluorescence produced in the cadmium.

Active shielding

The active shield consists of a tank, filled with a mineral oil based scintillator solution. The guard detector is an external detector that surrounds the area between the PMTs and the sample. Two photomultiplier tubes (G-PMT) circuited in coincidence, are used to detect scintillations in the tank while β-PMT, also circuited in coincidence, surrounds the sample. The active shield is used to detect ionizing radiation moving through, by the photomultiplier tubes of the guard detector. The pulse in the guard detector activates a logical signal. If this signal is coincident with a pulse in the β-PMT it can be used to inhibit the analogue to digital conversion of the pulse. The active guard performance and the intensity are monitored during counting by the MCAs.

4.8.2.3 Photo multiplier tube (PMT)

The PMTs are mounted around and view the scintillating solution contained in a vial. Pre-amplifiers mounted along with PMTs process the electrical pulses representing radioactive decay events from both the PMTs.

4.8.2.4 Counting circuit

The signals from the PMTs are fed into the coincidence circuit. The purpose of the coincidence unit is to reduce the background signal caused by PMT noise. The coincident pulses from the

output of the PMTs are summed, and the output obtained is proportional to the total intensity of the scintillation. The scintillation process, resulting from energy dissipation and photon production, results in an analog pulse rising to its maximum amplitude and falling to zero. The amplitude of the analog pulse is converted to a digital value. The conversion is achieved by an analog-to-digital converter (ADC), and the digital value, which represents the α-β particle energy in a range of 0 to 2000 keV, is sorted by the spectrum analyzer. The spectrum analyzer accumulates counts representing the complete energy spectrum of the radionuclide in the memory slot of the MCA.

4.8.2.5 Multi channel analyzer

The operation of the multi channel analyzer (MCA) is based on the principle of converting an analog signal, which is basically the pulse amplitude into an equivalent digital number usually referred to as a channel. After this is done, the digital events will be stored appropriately in the memory to be displayed on the monitor. The Quantulus incorporates two dual programmable MCAs, each having two sections, and thus enables two simultaneous measurements of four spectra, each with 1024 channel resolution. The pulse amplifiers yield a linear pulse height spectrum. The analogue to digital conversion is logarithmic (Figure 4.6). One of the MCAs is used to register the sample decay events (MCA 1) and the other for the guard detectors that measure the interfering background (MCA 2). MCA 11 contains pure sample β events and MCA 12 contains pure sample α events. The guard pulses, which are coincident with the sample coincidence pulses, are directed to MCA 22 as active guard pulses. The anticoincident guard pulses with sample or inactive guard pulses remain in MCA21. The windows based software (Quantulus) provides on-line display of energy spectra, total counts, and elapsed time of the sample along with set parameters displayed. All pulses counted in MCAs are not only counted but analyzed in terms of their number and height, therefore, the liquid scintillation counter (LSC) is now more often referred to as the liquid scintillation analyzer (LSA).

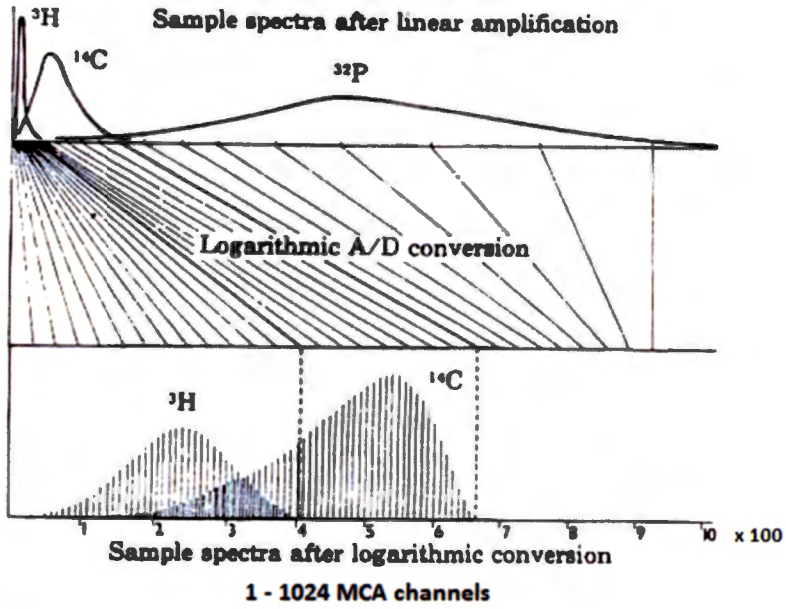

Figure 4.6. Logarithmic AD conversion of the linear amplification.[45]

4.9 Sample Preparation

The technique of LSC involves minimal sample preparation since the sample containing radioactivity is placed into a scintillation vial and a scintillation cocktail is added.

4.10 Sample Handling

The counting vial is placed into one of three trays located beneath the shield, and counting data (tray position number 1-60, sample identification, counting requirements, etc.) entered into a computer. Counting vials are automatically lowered into the detector well.

4.11 Advantages and Limitations of LSC

The wide popularity of LSC is a consequence of numerous advantages which are mainly:

High counting efficiencies. The α particles are detected at a very high counting efficiency of about 100% even with high degrees of quench in the scintillation cocktail.

Low backgrounds. An LSC device is designed with two detectors with PMTs, which use conventional coincidence counting and additional lead shielding to reduce the background.

Multi-sample capability. An LSC device has the basic advantage of high sample throughput. It has holding trays containing up to sixty slots for samples.

Minimal sample preparation. The water sample is normally directly dissolved in the scintillation liquid and counted.

Simultaneous α-β counting. With separation of each other using pulse shape analysis.

High precision, accuracy and sensitivity.

Although there are several advantages to α-β particle counting with the liquid scintillation method, this technique also has drawbacks. For example, calibration difficulties due to factors affecting the performance of the instrument such as quenching, vials and cocktail/sample ratio. Of these, quenching is the one which has been specifically studied in this research.

4.12 Applications of Liquid Scintillation Counting (LSC)

Low level LSC is commonly used for the following applications:

Measurement of naturally occurring radionuclides (NORM)

This is routinely measured at natural environmental levels in a wide range of sample matrices including water, soil, sediment, air, and rock samples. These can provide information about the concentrations of radionuclides, mainly Ra, U, Th, ^{231}Pa, which can have an impact on health related issues.[46, 47, 48, 49]

Monitoring the environment for radionuclide releases associated with nuclear fuel cycle activities

LSC can be used to assess the quantities and composition of radionuclides generated from nuclear power plants to resolve practical problems of radioactive waste management at present and in the future. This can be applied for the analysis of the following radionuclides: ^{3}H, ^{90}Sr, ^{14}C, ^{99}Tc, ^{129}I, ^{241}Pu, etc.[50, 51]

Studying the rates of process in the environment

This is mainly based upon radionuclides of natural origins and thus includes mainly ^{14}C dating, and ground water movement and dating using ^{3}H. Evaluating ^{3}H and ^{14}C measurements and seasonal variations of isotopes provide insight into the age structure of ground waters.[52, 53, 54] In addition, marine sediment mixing, productivity and particle flux can also be studied using ^{234}Th and ^{210}Po. These radioisotopes can be used for tracing and understanding the currents, mixing of water, the behavior of particles and organisms, and the exchange of gas between the atmosphere and the sea.[55]

4.13 Sensitivity of LSC

Sensitivity is the smallest amount of a particular element that can be detected in a specific sample of interest. LSC systems use an organic phosphor compound as the primary detector. This organic phosphor is dissolved in an appropriate solvent that achieves a uniform dispersion (this combination is commonly referred to as the cocktail). The α-β particles interact with the solvent and primary phosphor to produce photons. The use of this solvents results in pulse shapes that are sufficiently different so that they produce optimum separation of α from β events. The sensitivities for LSC to obtain meaningful results depend upon the parameters settings, cocktail choice, counting time, and detector efficiency.

4.14 Accuracy of LSC

Accuracy is defined as the closeness of the agreement between the result of a measurement and a true value. The qualitative (identification of elements) accuracy may be affected by factors such as background counts, quench spectra being assigned to erroneous radionuclides due to instrumental drift of the spectrometer from calibration conditions, under-estimation of interfering nuclear reactions, and γ ray spectrum interferences. For accurate results, the standards for calibration must be as nearly identical as possible to the unknown samples in their chemistry, volume, vial type and so on. The instrument setup also must be optimized or adjusted accurately to fit parameters for gross α and β measurements.

CHAPTER 5

EXPERIMENTAL PROCEDURE

5.1 Sampling Area – Wonderfonteinspruit

5.1.1 Wonderfonteinspruit

The Wonderfonteinspruit catchment area (WCA) is situated on the far west Rand with the upper section in the Gauteng Province and the lower part of the catchment area in the North-West Province. The area is shown in Figure 5.1 and 5.2. The eastern part of the Mooi River is also in the WCA. Most of the catchment area is underlain by dolomite whose compartments are dewatered by gold mines. Although the research does not include sampling, it is important to know the area where the samples were collected.

The water body has its origin in the Krugersdorp area and flows through the Tudor dam and the attenuation dam past Kagiso, Azaadville, and Randfontein into the Donaldson dam near Bekkersdal. It is then deviated into a pipeline (1 m diameter) at the Donaldson dam, which carries the water over the dolomitic groundwater compartments, dewatered due to gold mining activities, until a discharge point near Carltonville. From Carltonville, the river runs south-west passing Oberholzer, Khutsong, and Welverdiend, joining with the Gerhardminnerbron and flowing together south into the Boskop dam and further to Potchefstroom. The catchment dams forming part of the system include Harry's dam, Padda dam, Coetzee dam, and Visser dam, as well as the large Boskop and Potchefstroom dams between Carltonville and Potchefstroom.

The region has several large active gold mines which discharge fissure and process water into the aquatic environment. The upper section of the catchment area also has numerous diffuse sources from old and abandoned mine workings and mine deposits. Various pathway mechanisms whereby contaminants spread from their sources and enhance the concentrations of the NORM and other pollutants can be identified. Mine tailings and processed water eventually end up in the river system by erosion processes, for example water-soil erosion. The land surrounding these catchment areas is used mainly for mining. Drainage of acidic mine waters may be found to contribute, especially from abandoned mines.[25]

The Wonderfonteinspruit and its tributaries pass through the districts of Potchefstroom, Oberholzer, Westonaria, and Randfontein. A few expanding communities are found along the catchment area, for example Kagiso, Mohlakeng, Toekomsrus, Rietvallei, and Bekkersdal. These settlements, as well as the developments along the catchment area add to the discharge of pollution (e.g. sewage) into the surrounding water.[25]

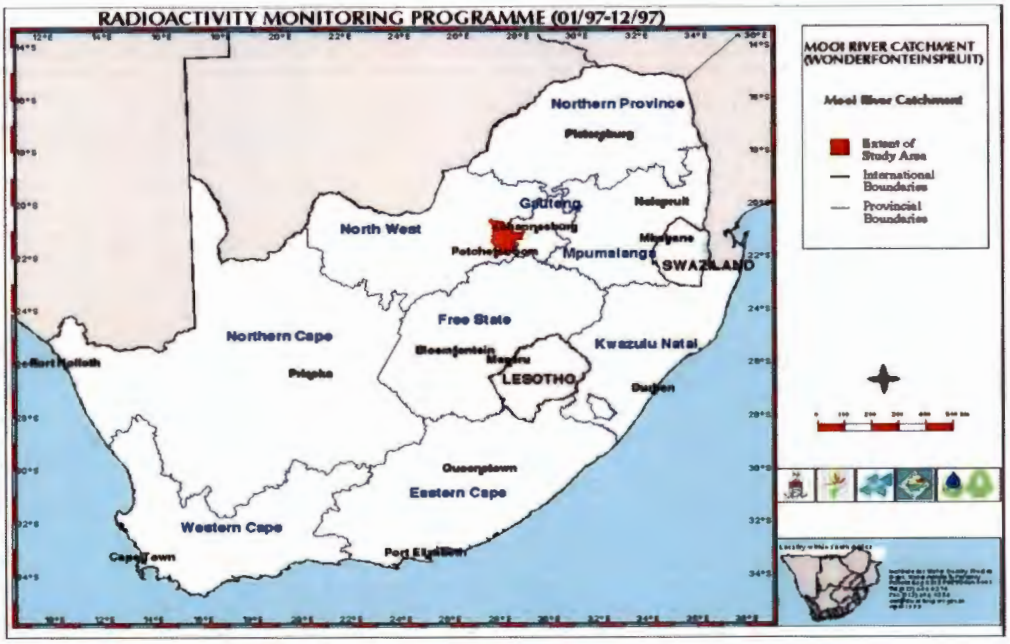

Figure 5.1. Locality of the Mooi River catchment area, including the Wonderfonteinspruit.[25]

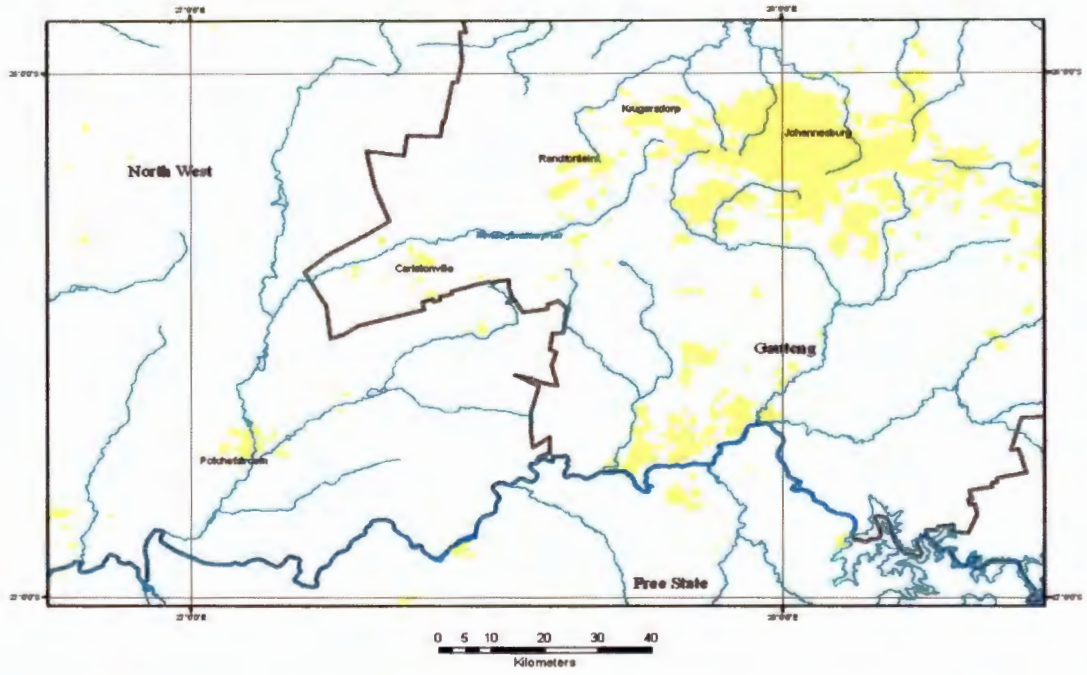

Figure 5.2. Locality plan of the Wonderfonteinspruit and surrounding area.[25]

Commercial farming is not extensively practiced in the area, but the farming activity that is encountered is mostly meant for local consumption. The development of settlements around the catchment area also plays a role in the overall impact on the environment and the water quality. People living along the catchment area may be using this contaminated water for drinking and agriculture, increasing the uptake of the NORM radioactive nuclides.[27]

The WCA has been identified in a number of studies as the site of significant radioactive and other pollution, generally attributed to the mining and processing of uraniferous gold ores in the area.[25] The Far West Rand was the first goldfield in South Africa where large-scale uranium production was established.

The mining Reefs around the catchment area include carbon leader, Middlevlei Reef, white Reef, Monarch Reef, Elsburg Reef, Composite Reef, Ventersdorp Contact Reef, and the black Reef.[25] The mined Reefs contain not only gold, but also high concentrations of uranium (up to 5.8%).[25]

Mining related activities continue to release naturally occurring radionuclides from point and diffuse sources into the WCA resulting in a pattern of radioactive contamination of water bodies and sediments and soils throughout the area.[27] The difference in sources of radionuclides (mine waters and slime dams), their different geochemical and transporting behavior in the environment, and variations in the source extension (intermittent mine water discharges, infrequent seepage water emission, and sporadic erosion from slime dams after heavy rainfalls) are contributing contamination factors.

Research done in the catchment area reported that approximately up to 70% of chemical contamination observed in the mine water discharged into the environment was from the pyritic oxidation processes in underground stopes.[24]

The red areas in Figure 5.3 indicate elevated concentrations of radioactive materials in the wetlands of the WCA.[25] These high radioactivity levels occur mainly due to the surrounding mining activities.

Preliminary monitoring by the Institute for Water Quality Studies (IWQS) of the Department of Water Affairs and Forestry done in 1995-97, showed that activity concentrations of radioactive elements in surface and ground waters were elevated in the Wonderfonteinspruit.[56] Since then regular monitoring studies have been done.[25]

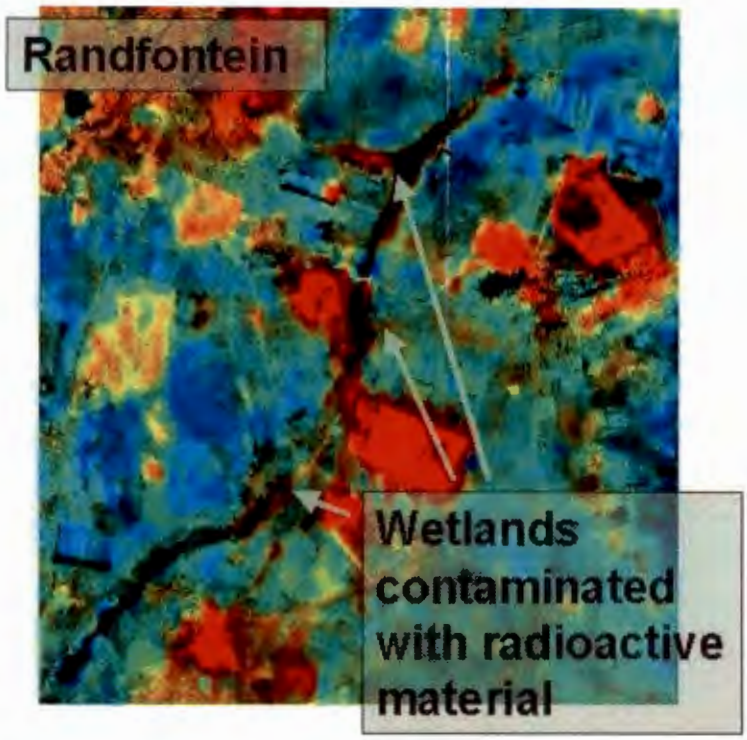

Figure 5.3. Radiometric image of the Wonderfonteinspruit catchment area.[25]

5.2 PSA Calibration

5.2.1 Introduction

Liquid scintillation counting (LSC) performed with the Quantulus 1220 counts pulses produced by α and β radiation. In doing so, it discriminates α-events from β-events in the sample based on the duration of the pulses they produce in a scintillation liquid. The discrimination of α and β pulses is based on the well known difference between the delay component of their decay.[37] The discrimination of the pulse decay is done by a special electronic device called a pulse shape analyzer (PSA) to categorize the pulses as either α events or β events and stores the events proportionally in separate channels of a multichannel analyzer (MCA).

For the most accurate results, PSA must be optimized. With the purpose of finding the optimal PSA setting, two reference standards simulating the activity concentration values of real samples for α particles emitted by naturally occurring radionuclides were measured at different PSA values. α emitting ^{241}Am was used as a reference standard simulating the activity concentration values of real samples for α particles emitted by naturally occurring radionuclides while ^{90}Sr/^{90}Y was used as a β reference standard simulating gross β activity.

Table 5.1. Emission energies for α and β emitting radionuclides used for calibration of gross α and β measurements

Radionuclide	Alpha energy (MeV)	Beta energy (MeV)
^{241}Am	5.49 (85%), 5.44 (13%)	–
^{90}Sr	–	0.546 (100%)
^{90}Y	–	2.281 (100%)

5.2.2 Quench effect

It is a known fact that counting efficiencies and the optimized settings are affected by the degree of quenching in the sample. The effect of quenching was also studied for getting an idea on the PSA setting. The quenching was monitored by the sample quenching parameter (SQP(E)).

Quenching has many effects on α/β separation:

1. with increased quenching the α spillover to the β channel increases, whereas the β spillover to the α channel decreases [57, 58,59]
2. the optimum PSA is influenced by a chemical quencher [60, 61], and
3. the α background increases and β background decreases with increasing quenching when samples are measured at their optimum PSAs.

Furthermore, the β spillover is influenced by β particle energy; the effect is more significant for higher energy β emitters [59,60,61]. Consequently, the exact efficiency, spillover, and background corrections for real samples with variable quenching are rather complicated. [59,62] These references indicate that the PSA level should be optimized according to each sample quench level using the same energy β emitter and same quenching agents as in real samples. The composition of the standard and real samples should be as similar as possible.

Figure 5.4 shows the effect of quenching on the spectrum of the α-emitters. The spectrum shifts to a lower channel with increasing quench. An increase in quench level indicates a count rate and efficiency reduction for α emitters.

The effect of quenching on the PSA was studied. It was found that significant differences in percentage spillover can occur when samples with different quenching parameters are counted at the same PSA settings. Therefore the quench effect was further experimented using test samples.

Seven test samples were first measured at arbitrary PSA level of 100. It was observed that two of the test samples were highly quenched (^{232}U tracer and ^{229}Th tracer solutions). Consequently, calibrations with different PSA levels were done to check if quench levels do change with different PSA settings. It was observed that the quench level is consistent at any PSA level. Although the quench level stayed consistent, the α-β count rates changed dramatically because of different PSA levels.

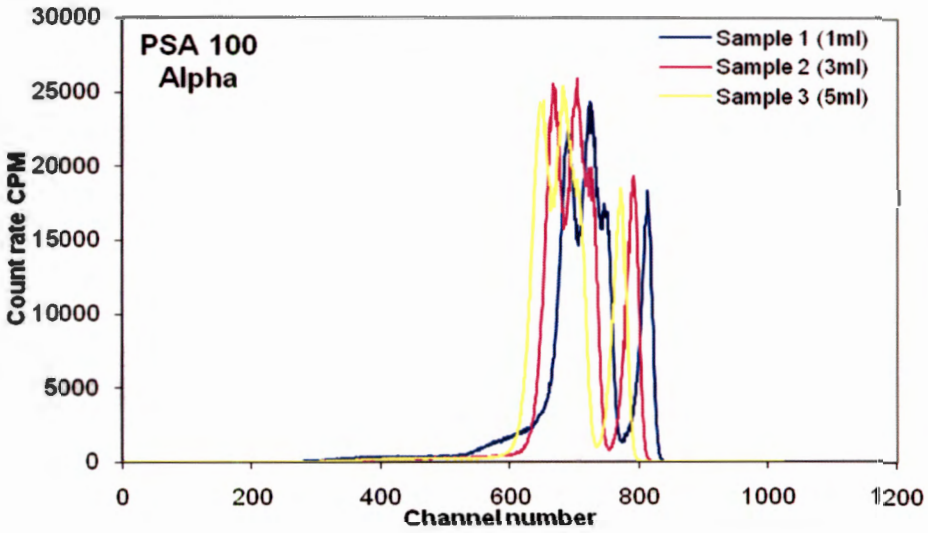

Figure 5.4. The α spectra of ^{226}Ra (+ progeny) samples measured at a constant PSA level of 100. Sample 1 is least quenched and sample 3 is most quenched.

Figure 5.5a shows the effect of quench, increase of the α spillover to the β channel, on ^{232}U tracer solution (SQP(E) = 740.88) measured at an arbitrary PSA level of 100. The α spectra (red line) in Figure 5.5a shows that there are no α's in the spectra, but ^{232}U has many α's (including its progeny). The spectra indicate that large quenching "transfers" the α count rate into to the β channel, increasing β count rates and accordingly the visibly large spillover.

Figure 5.5b shows the spectrum of ^{238}U test solution (SQP(E) = 795.34) measured at an arbitrary PSA level of 100. The α spectra (red line) in Figure 5.5b shows that there are α's in the spectra, but with large α spillover into the β channel. Therefore the PSA for test samples must also be calibrated.

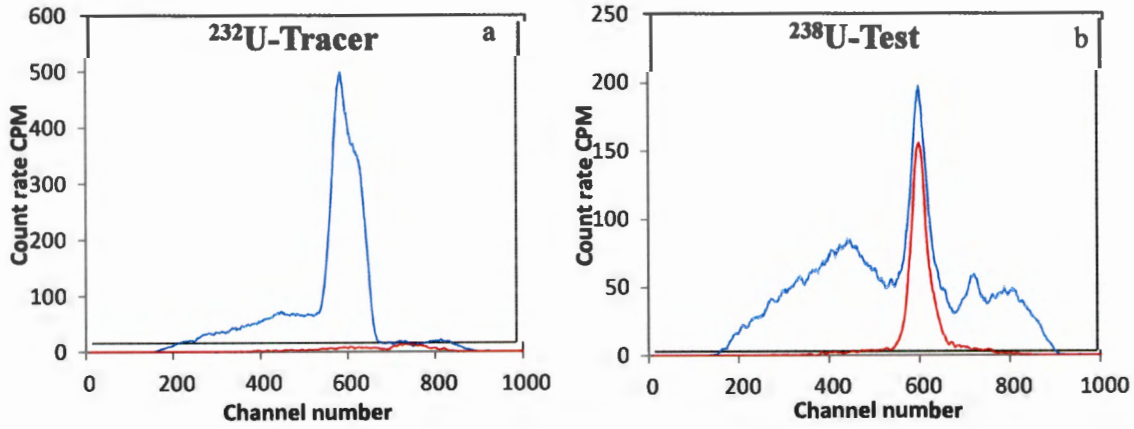

Figure 5.5. Effect of quenching on the spillover at PSA 100.

The dependence of the quench level on the PSA level was further experimented with ^{226}Ra standard solution quenched to different degrees and then measured at various PSA levels. The α and β spectra given in Figure 5.6 affirm the same effects as observed in Figure 5.4 and Figure 5.5

The α spillover to the β channel is very small at low quenching. However, it can already be observed that at higher PSA settings the α's start to spill over to the β channel. At increased quenching (Sample 2) the increased effect of spill over depending on the PSA setting can be clearly seen.

Sample 1: **SQP(E) = 862 ± 2**

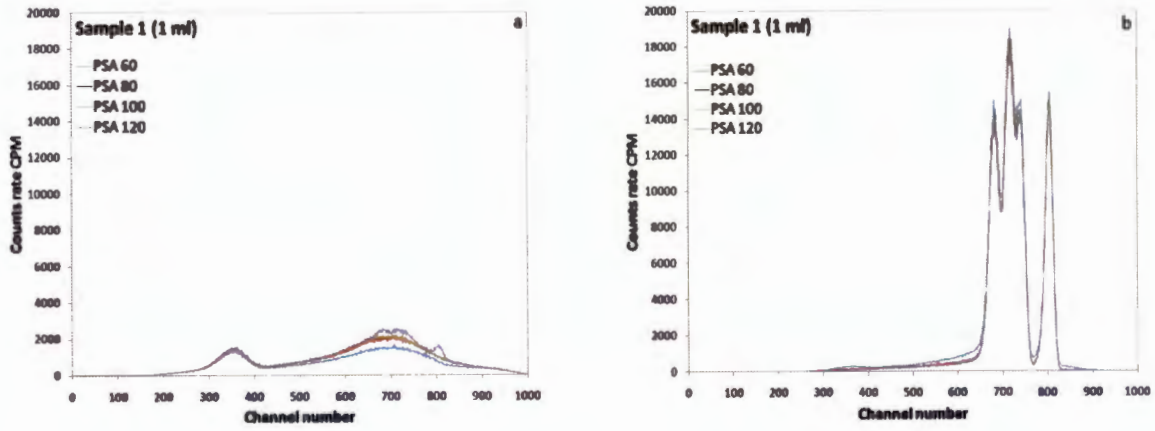

Sample 2: **SQP(E) = 825 ± 10**

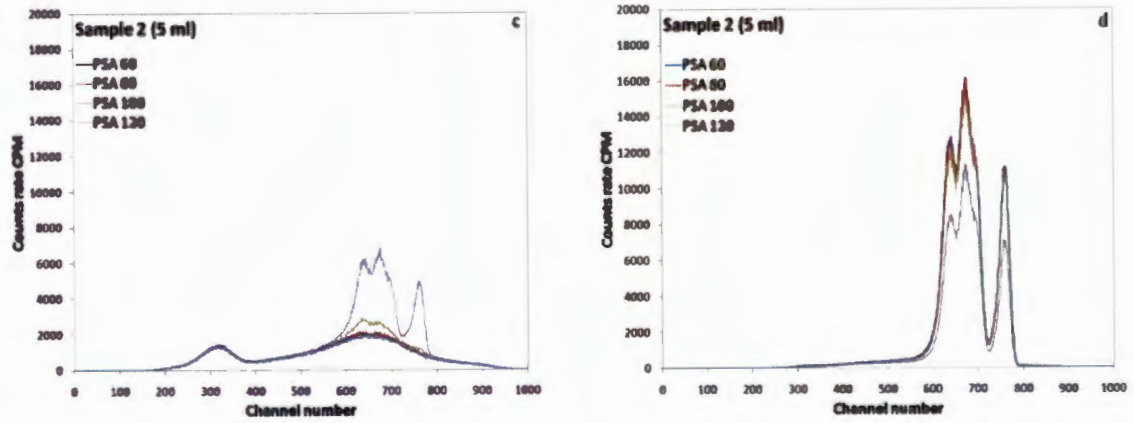

Figure 5.6. The β and α spectra of two ^{226}Ra samples with different quenching measured at four different PSA levels.

5.2.3 Procedure for optimum PSA calibration

The following procedure for the determination of the optimum PSA setting was applied:

- 10 minutes counting of quenched standards and on the basis of these results;
- Counting of quenched standards at various PSA levels.
- Construction of a PSA calibration curve (changeover values used).
- Determination of spillover of α's into the β channel, vice versa, and α/β detection efficiency.

The aim of the PSA calibration was to minimize spillover. Table 5.2 presents the α and β spillovers for samples quenched to different levels and obtained by different PSA settings. The total count rates in both channels were very consistent at different PSA levels while the count rates in the β channel and α channel vary at different PSA levels depending on the amount of α/β spillovers. ^{241}Am was used to get α spillover and ^{90}Sr for β spillover. The count rates for both α and β standards solutions depend on the activity concentration used for the individual standards. Different quench levels were obtained by preparing standards with different volumes of distilled water (hence the milliliters indicated). The quench levels used in this study vary in the SQP(E)-range of 740 to 820 as environmental water samples used in this study fall within this range.

In Table 5.2 it is easy to see that at a given PSA setting the β spillover decreases and α spillover increases when the quenching is enhanced (decrease of α count rates and increase of β count rates). On the other hand, it is also obvious that quenching affects more drastically the α spillover than to β spillover when quenching increases (see also figure 5.6). The highlighted changeover values graphically represented in Figure 5.7 were used to construct a PSA calibration curve. The changeover values were assumed to be at the start of the spillover (or minimum spillover) of α's into the β channel. The dependence of optimal PSA settings on the quenching parameter SQP(E) is presented in Figure 5.7, and can be mathematically presented, through linear regression, by,

$$Y = 0.690x - 485.2 \quad r^2 = 0.95 \tag{5.1}$$

where:

Y = the optimum PSA setting

x = the measured quench value/parameter (SQP(E))

This relationship makes it possible to find the optimum PSA setting once the quench value has been determined of each individual environmental sample (from an arbitrary PSA level). This, however, makes routine monitoring more labour intensive and requires highly skilled personnel to do the analytical work. Furthermore, as environmental samples will differ in composition of α/β-activities and -energies it will be difficult to match the parameter settings for environmental samples to laboratory conditions obtained from ^{241}Am and ^{90}Sr standards.

Table 5.2. α and β spillover for quenched standards at different PSA settings. The values corresponding to optimized PSA settings are denoted using bold characters.

PSA	0 ml		2 ml		5 ml		7ml	
	α spillover	β spillover	α spillover	β spillover	α spillover	β spillover	α spillover	β spillover
30	0.00007	0.95951	0.00010	0.78426	0.00014	0.71249	0.00021	0.68979
40	0.00008	0.93051	0.00022	0.57384	0.00025	0.45515	0.00032	0.45061
50	0.00007	0.88665	0.00042	0.26639	0.00041	0.18309	0.00037	0.17624
55	0.00007	0.84015	0.00049	0.16931	0.00039	0.12045	0.00042	0.12270
60	0.00015	0.76395	0.00044	0.09533	0.00040	0.07370	**0.00039**	**0.07278**
65	0.00022	0.64888	0.00050	0.07182	0.00052	0.05960	0.00065	0.06096
70	0.00022	0.50795	0.00055	0.04105	**0.00049**	**0.03307**	0.00075	0.03630
75	0.00037	0.37124	0.00059	0.03954	0.00084	0.03488	0.00115	0.03838
80	0.00038	0.24262	**0.00057**	**0.02132**	0.00125	0.02028	0.00191	0.02199
90	0.00045	0.09625	0.00142	0.01382	0.00637	0.01531	0.00804	0.01646
100	0.00053	0.04085	0.00690	0.00910	0.02776	0.00956	0.03072	0.01142
110	0.00063	0.02050	0.03386	0.00817	0.08439	0.00772	0.08653	0.00932
120	**0.00058**	**0.01051**	0.10532	0.00583	0.19382	0.00705	0.18419	0.00689
130	0.00164	0.00739	0.23713	0.00499	0.33846	0.00462	0.31381	0.00679

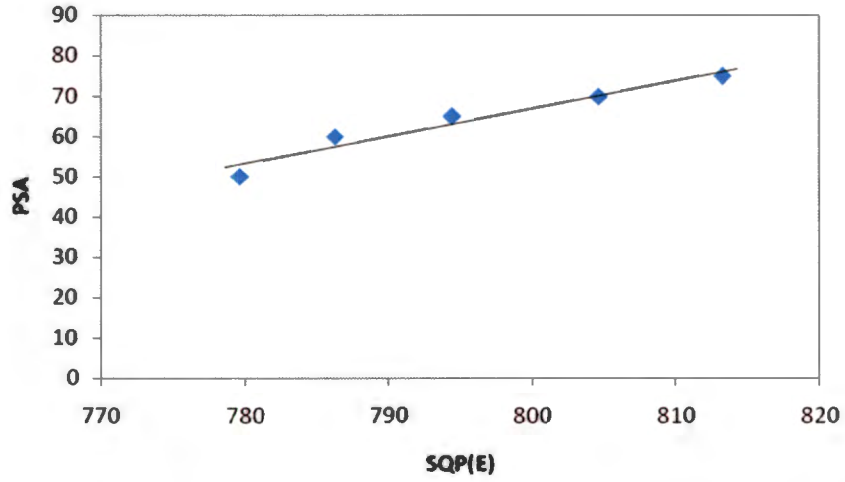

Figure 5.7. Relation between quenching parameter (SQP(E)) and optimized PSA setting.

The relation between spillover, quench parameter and PSA values is shown in Figures 5.8 and 5.9. It is clearly seen in Figure 5.8 that, an increase in PSA level increases the α spillover, at high quench values, and from Figure 5.9 that the lower the PSA level for low quenched parameters,

the higher the β spillover. Therefore from both Figures, 5.8 and 5.9, it can be concluded that low PSA settings are suitable for higher quench values while for lower quench values, higher PSA settings are acceptable to minimize spillover.

The following expressions were used to calculate the spillovers (X). It is important to note that the spillover differs according to PSA settings.

$$X_{\alpha} = \frac{MCA\ 11}{MCA\ 12 + MCA\ 11} \tag{5.2}$$

$$X_{\beta} = \frac{MCA\ 12}{MCA\ 12 + MCA\ 11} \tag{5.3}$$

Where, X_{α} is the fraction of counts observed in the β channel (MCA 11) with respect to the counts observed in α and β channel (MCA 12 + MCA 11) when a pure α emitter is measured; the β spillover (X_{β}) is the fraction of counts observed in the α channel (MCA 12) with respect to the counts observed in α and β channels (MCA 12 + MCA 11) when a pure β emitter is measured.

MCA 11 contains pure sample β events while MCA 12 contains pure sample α events.

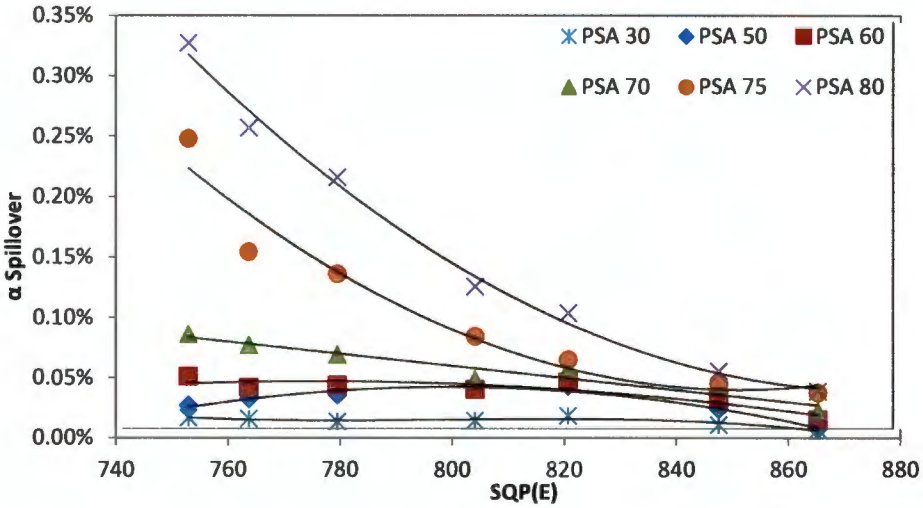

Figure 5.8. α Spillover as a function of quenching for different PSA values. ^{241}Am activity was 2.415 ± 0.013 kBq/g.

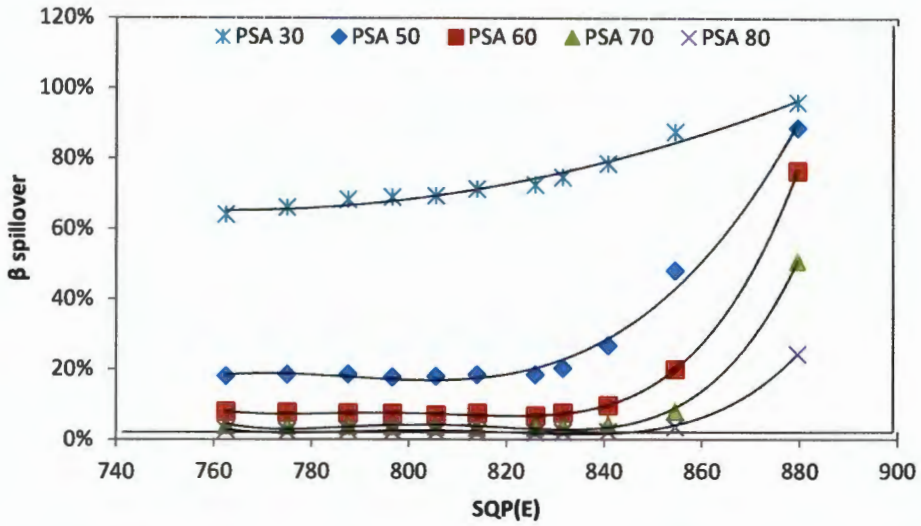

Figure 5.9. β Spillover as a function of quenching for different PSA values. ^{90}Sr activity was 2.415 ± 0.013 kBq/g.

5.2.4 Detection Efficiency

Quantification of quench levels with respect to detection of (ε_α and ε_β) and spillover efficiencies of α and β radiation is accomplished by constructing quench curves using a set of quenched standards. It was assumed that the total efficiency determination, chemical, color quench and efficiency detection are all accounted for using an internal standard method. The efficiency tracing curves generated from standards of ^{241}Am and ^{90}Sr at optimized PSA settings are shown in Figures 5.10 and 5.11.

The α detection efficiency (ε_α) was evaluated by measuring ^{241}Am standard solutions and β detection efficiency (ε_β) was evaluated by measuring ^{90}Sr standard solutions through the following equations,

$$\varepsilon_\alpha = \frac{MCA12_{G\alpha} - MCA12_{B\alpha}}{A_\alpha \cdot T} \tag{5.4}$$

$$\varepsilon_\beta = \frac{MCA11_{G\beta} - MCA11_{B\beta}}{A_\beta \cdot T} \tag{5.5}$$

where:

MCA $12_{G\alpha}$ and *MCA* $11_{G\beta}$ are the number of gross counts per minute recorded in the α and in β channel, respectively, when measuring the standard vials.

MCA $12_{B\alpha}$ and *MCA* $11_{B\beta}$ are the number of background counts per minute recorded in the α and in β channel, respectively, when measuring the blank vial.

A_α and A_β are the α and β activities (Bq).

T is the corrected measuring time (s) (60).

The α particle counting efficiency remains at 100% up to very high quench levels, provided the PSA is set accordingly. [45] Figure 5.10 indicates that the α efficiency is close to 100% irrespective of the quench level or PSA setting, while Figure 5.11 indicates that high PSA levels are required for less quenched samples.

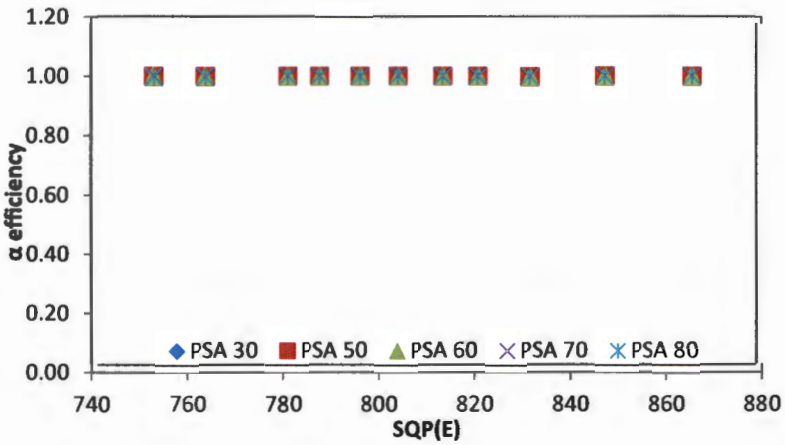

Figure 5.10. Dependence of α detection efficiency on optimized PSAs setting with various quench level, based on ^{241}Am standards.

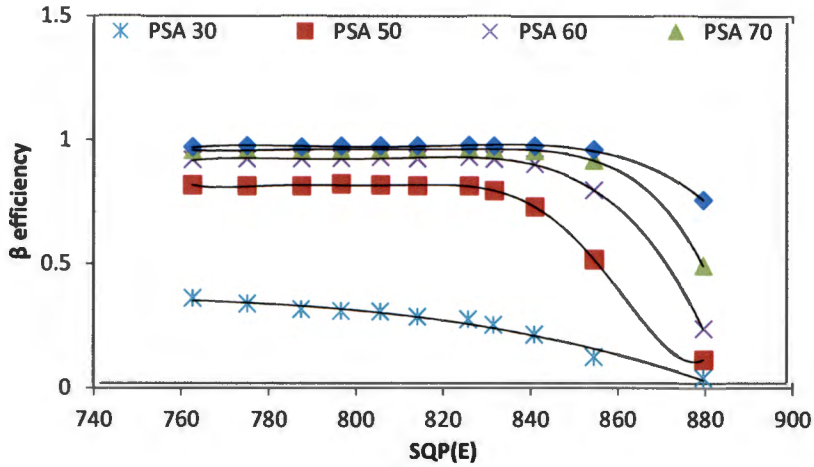

Figure 5.11. Dependence of β detection efficiency on optimized PSAs setting with various quench level, based on ^{90}Sr standards.

5.2.5 Summary of PSA calibration

The main conclusions observed in this chapter are the following:

- The minimum spillover observed for high quenched standards was at lower PSA parameters and low quenched standards at higher PSA parameters as expected.
- At arbitrary PSA 100 setting, the spillover of α into the β channel increases when the quench level increases.
- If the PSA parameter was correctly set, the variations in quenching produces little change in spillovers.

The following might also affect the results of the environmental sample measurements,

1. incorrect PSA setting,
2. sample volume,
3. counting time,
4. radionuclide energy, and
5. quench (especially high quench values make calibration difficult).

5.3 Energy Calibration

5.3.1 Introduction

To identify α-β emitters with spectrometric methods an energy calibration is necessary to ensure the proper conversion of channel numbers into the equivalent energy of a nuclide in a sample. However, the determination of equivalent energy is hampered by the poor resolution of the energies in the spectra. Therefore prior to acquisition of data, energy calibration under various quenching conditions has to be performed as part of the nuclide identification procedure.

Theoretically [8], one can use either a linear or quadratic calibration relation between the peak position (channel number) and the energy of the particle of interest,

$$E = A \times C + B \qquad \text{(Linear)} \qquad (5.6)$$

or

$$E = A \times C^2 + B \times C + D \qquad \text{(Quadratic)} \qquad (5.7)$$

Where:

E the energy in MeV.

A, B, D constants.

C the channel position (number).

A two point of energy calibration is normally acceptable for many occasions from a general measurement point of view.

In this study a somewhat different approach was used, because the energy-to-channel number calibration also appeared to be quenching dependent.

5.3.2 Alpha-energies to be expected theoretically from NORM nuclides

Taking into consideration that different elements have different mobility in aquatic systems and that short-lived progeny are in equilibrium with their relative long-lived parents we can first evaluate what we may expect from an energy point of view. Taking the relevant data from Nuchart (Canberra Industries) we can look at the following theoretical cases:

1. Water contaminated with Uranium
   Due to the presence of ^{238}U, ^{235}U and ^{234}U the following α energies and relative intensities can be expected (Table 5.3).

Table 5.3. Expected α energies and relative intensities for uranium

Nuclide	Half-life	keV	Intensity (%)
U-235	7.038E+08 yrs	3973.1	4.8E-05
U-238	4.468E+09 yrs	4038	7.8E-02
U-235	7.038E+08 yrs	4074.3	9.6E-04
U-235	7.038E+08 yrs	4150	4.3E-02
U-238	4.468E+09 yrs	4151	2.1E+01
U-238	4.468E+09 yrs	4198	7.9E+01
U-235	7.038E+08 yrs	4214.7	2.7E-01
U-235	7.038E+08 yrs	4217.1	8.2E-04
U-235	7.038E+08 yrs	4219	4.3E-02
U-235	7.038E+08 yrs	4271	1.9E-02
U-235	7.038E+08 yrs	4276.9	1.6E-03
U-235	7.038E+08 yrs	4284.6	4.8E-03
U-235	7.038E+08 yrs	4299.7	4.3E-04
U-235	7.038E+08 yrs	4323	2.1E-01
U-235	7.038E+08 yrs	4325.8	1.0E-02
U-235	7.038E+08 yrs	4359.6	1.1E-02
U-235	7.038E+08 yrs	4366.1	8.1E-01
U-235	7.038E+08 yrs	4378.6	7.7E-03
U-235	7.038E+08 yrs	4397.8	2.6E+00
U-235	7.038E+08 yrs	4414	1.0E-01
U-235	7.038E+08 yrs	4435	3.3E-02
U-235	7.038E+08 yrs	4502	8.1E-02
U-235	7.038E+08 yrs	4556	2.0E-01
U-235	7.038E+08 yrs	4596.4	2.4E-01
U-234	245500 yrs	4603.5	2.0E-01
U-234	245500 yrs	4722.4	2.8E+01
U-234	245500 yrs	4774.6	7.1E+01

This can graphically be represented by,

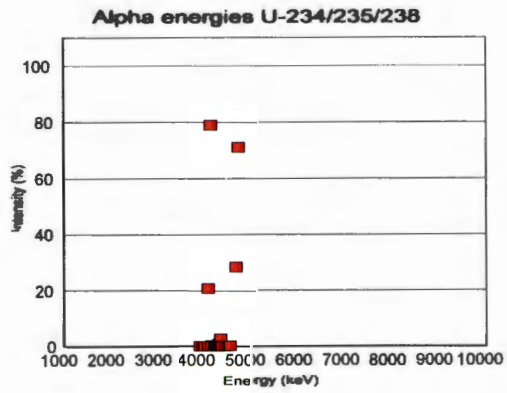

Figure 5.12. Graphic representation of α energies and relative intensities for natural uranium.

Taking into consideration that ^{234}U in environmental water can be enriched substantially, the energy peak on the right side can be much higher.

2. Water contaminated with Radium
Due to the presence of ^{226}Ra, which can be assumed to be in equilibrium with its short-lived progeny by the time the sample will be processed at the laboratory, the following α energies and relative intensities can be expected (Table 5.4).

Table 5.4. Expected α energies and relative intensities for ^{226}Ra and short-lived progeny.

Nuclide	Half-life	keV	Intensity (%)
Ra-226	1600 yrs	4601	5.6E+00
Ra-226	1600 yrs	4784.3	9.4E+01
Po-210	138.376 days	5304.33	1.0E+02
Rn-222	3.8235 days	5489.5	1.0E+02
Po-218	3.11 min	6002.35	1.0E+02
Po-214	164.3 µsec	6902.1	1.0E-02
Po-214	164.3 µsec	7686.82	1.0E+02

This can graphically be represented by,

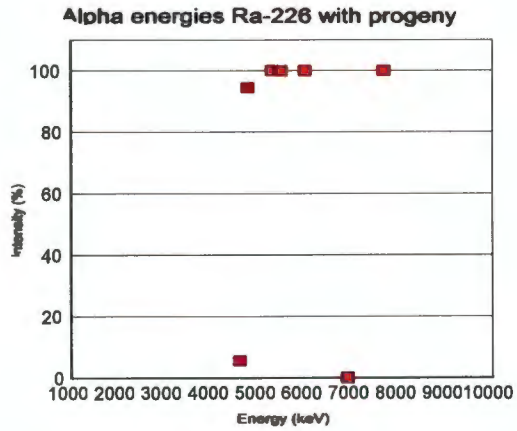

Figure 5.13. Graphic representation of α energies and relative intensities for ^{226}Ra and short-lived progeny.

The potential contribution from ^{223}Ra from the ^{235}U-series is not taken onto consideration as the expected contribution will be about 5%. ^{228}Ra from the ^{232}Th-series and its short-lived daughter are both β emitters, while ^{224}Ra from the same series has a relatively short half-life of 11.4 days and accordingly is not expected to be available in the aquatic system in large amounts.

3. Water contaminated with Thorium

Although thorium has a low mobility in the aquatic environment one might obtain a water sample from a specific ore processing plant. If this sample came from a uranium rich environment one may have ^{230}Th and to a lesser extent ^{227}Th (again at around 5% coming from the ^{235}U-series) the following α energies and relative intensities can be expected (Table 5.5).

Table 5.5. Expected α energies and relative intensities for ^{230}Th

Nuclide	Half-life	keV	Intensity (%)
Th-230	75380 yrs	4371.8	0.00097
	75380 yrs	4438.4	0.03
	75380 yrs	4479.8	0.12
	75380 yrs	4620.5	23.4
	75380 yrs	4687	76.3

This can graphically be represented by,

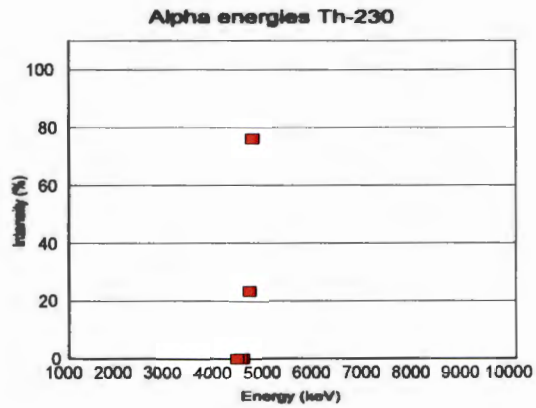

Figure 5.14. Graphic representation of α energies and relative intensities for ^{230}Th

If this sample came from a thorium rich environment one may have ^{232}Th and ^{228}Th with progeny having the following α energies and relative intensities can be expected (Table 5.6).

Table 5.6. Expected α energies and relative intensities from a Thorium rich environment.

Nuclide		Half-life	keV	Intensity (%)
Th-232		1.405E+10 yrs	3811.1	0.069
Th-232		1.405E+10 yrs	3947.2	21.7
Th-232		1.405E+10 yrs	4012.3	78.2
Ra-224		3.66 days	5034.11	0.003
Ra-224		3.66 days	5051.39	0.0081
Th-228		1.912 yrs	5137.83	0.038
Ra-224		3.66 days	5161.14	0.007
Th-228		1.912 yrs	5176.71	0.227
Th-228		1.912 yrs	5210.89	0.42
Th-228		1.912 yrs	5340.36	27.2
Bi-212	35.94%	60.55 min	5345.16	0.0004
Th-228		1.912 yrs	5423.15	72.2
Ra-224		3.66 days	5448.6	5.05
Bi-212	35.94%	60.55 min	5480.55	0.005
Bi-212	35.94%	60.55 min	5606.29	0.43
Bi-212	35.94%	60.55 min	5625.4	0.059
Ra-224		3.66 days	5685.37	94.92
Rn-220		55.6 sec	5748.24	0.114
Bi-212	35.94%	60.55 min	5767.97	0.64
Po-216		.145 sec	5988.2	0.0019
Bi-212	35.94%	60.55 min	6050.78	25.13
Bi-212	35.94%	60.55 min	6089.88	9.75
Rn-220		55.6 sec	6288.08	99.886
Po-216		.145 sec	6778.3	99.9981
Po-212	64.06%	.299 µsec	8784.86	64.06

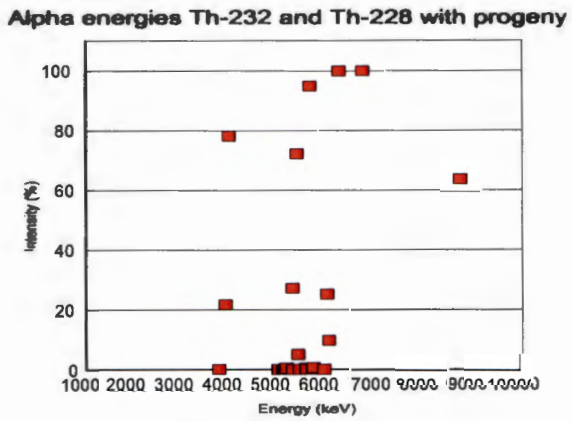

Figure 5.15. Graphic representation of α energies and relative intensities for Thorium from a Thorium rich environment.

4. Water contaminated with Polonium

As polonium has a fair mobility in the aquatic environment one might expect ^{210}Po from the ^{238}U-series to show. ^{214}Po, ^{218}Po (daughters of ^{226}Ra), ^{211}Po (from the ^{235}U-series), ^{212}Po and ^{216}Po (both from the ^{232}Th series) are too short-lived to make a contribution at the time of measurement in the laboratory. Accordingly, the following α energies and relative intensities can be expected (Table 5.7).

Table 5.7. Expected α energies and relative intensities for ^{210}Po.

Nuclide	Half-life	keV	Intensity (%)
Po-210	138.376 days	5304.33	100

This can graphically be represented by,

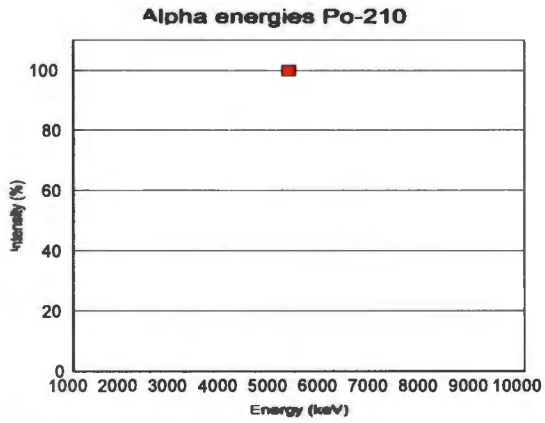

Figure 5.16. Graphic representation of α energies and relative intensities for ^{210}Po

5. Water contaminated with Protactinium

Here one might expect ^{231}Pa from the ^{235}U-series to show. ^{234m}Pa (from the ^{238}U-series) is β-active only. Accordingly, the following α energies and relative intensities can be expected (Table 5.8).

Table 5.8. Expected α energies and relative intensities for ^{231}Pa

Nuclide	Half-life	keV	Intensity (%)
Pa-231	32760 yrs	4410	0.001
	32760 yrs	4508	0.003
	32760 yrs	4566	0.008
	32760 yrs	4599	0.015
	32760 yrs	4632	0.1
	32760 yrs	4643	0.1
	32760 yrs	4681	1.5
	32760 yrs	4713	1
	32760 yrs	4736	8.4
	32760 yrs	4795	0.04
	32760 yrs	4853	1.4
	32760 yrs	4900	0.002
	32760 yrs	4934	3
	32760 yrs	4951.3	22.8
	32760 yrs	4975	0.4
	32760 yrs	4986	1.4
	32760 yrs	5013.8	25.4
	32760 yrs	5028.4	20
	32760 yrs	5032	2.5
	32760 yrs	5058.6	11

This can graphically be represented by,

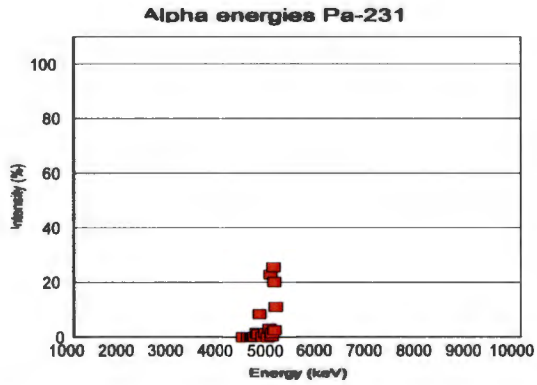

Figure 5.17. Graphic representation of α energies and relative intensities for ^{231}Pa

6. Water contaminated with Actinium

Here one might expect ^{227}Ac from the ^{235}U-series to show together with its short-lived progeny. ^{228}Ac (from the ^{232}Th-series) is β-active and too short-lived to make a contribution at the time of measurement in the laboratory. Accordingly, the following α energies and relative intensities can be expected (only 25 most intensive energies), (Table 5.9).

Table 5.9. Expected α energies and relative intensities for ^{227}Ac

Nuclide		Half-life	keV	Intensity (%)
Po-215			7400	1.0E+02
Bi-211	99.7%	2.14 min	6622.9	8.4E+01
Rn-219		3.96 sec	6819.1	7.9E+01
Ra-223		11.435 days	5716.2	5.3E+01
Ra-223		11.435 days	5606.7	2.6E+01
Th-227		18.72 days	6038.01	2.4E+01
Th-227		18.72 days	5977.72	2.4E+01
Th-227		18.72 days	5756.87	2.0E+01
Bi-211	99.7%	2.14 min	6278.2	1.6E+01
Rn-219		3.96 sec	6552.6	1.3E+01
Ra-223		11.435 days	5539.8	9.2E+00
Ra-223		11.435 days	5747	9.2E+00
Th-227		18.72 days	5708.8	8.3E+00
Rn-219		3.96 sec	6425	7.5E+00
Th-227		18.72 days	5713.2	4.9E+00
Th-227		18.72 days	5700.8	3.6E+00
Th-227		18.72 days	5959.7	3.0E+00
Th-227		18.72 days	6008.8	2.9E+00
Th-227		18.72 days	5866.45	2.4E+00
Ra-223		11.435 days	5433.6	2.3E+00
Th-227		18.72 days	5668	2.1E+00
Th-227		18.72 days	5693	1.5E+00
Th-227		18.72 days	5807.5	1.3E+00
Ra-223		11.435 days	5871.3	1.0E+00
Ra-223		11.435 days	5501.6	1.0E+00

This can graphically be represented by,

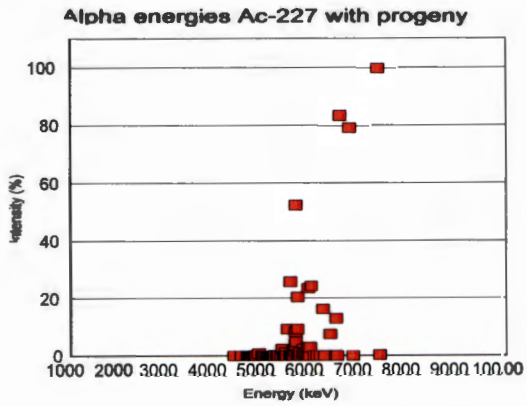

Figure 5.18. Graphic representation of α energies and relative intensities for ^{227}Ac

5.3.3 Alpha-spectra to be used for NORM nuclides

The theoretical data in the previous paragraph are obviously influenced by peak broadening, which will also depend on the quenching of individual samples. An example was already given in chapter 5.2.2 for an α-spectrum of ^{226}Ra in equilibrium with its progeny. According to the theoretical data the following main energies are expected (see Table 5.10) (^{210}Po is not expected to have grown-in substantially over the 22 year half-life of ^{210}Pb),

Table 5.10. Expected energies of ^{226}Ra in equilibrium with its progeny

Nuclide	Half-life	keV	Intensity (%)
Ra-226	1600 yrs	4784.3	9.4E+01
Rn-222	3.8235 days	5489.5	1.0E+02
Po-218	3.11 min	6002.35	1.0E+02
Po-214	164.3 μsec	7686.82	1.0E+02

However, it can be clearly seen that due to the peak-broadening a substantial peak-overlap can be expected, although the four peaks can still be identified. But it is also clear that quenching causes the peaks to shift. Accordingly, a quench dependent energy-to-channel number calibration has to be done to allow the identification of α-energies in environmental samples.

5.3.4 Quench dependent energy-to-channel number calibration for NORM nuclides

For this 11 samples were prepared from the available ^{226}Ra standard reference solution ACS/DC/48/02 (Annexure 5 refers). All samples were spiked with a small amount (100 μℓ) of the ^{226}Ra standard solution. To simulate various degrees of quenching distilled water was used in 1-mℓ fractions between 0 and 10 mℓ and the volumes were adjusted to 20 mℓ with scintillation liquid. The samples were counted for 5 hours to ensure good statistics. For each of the samples the peak positions of the four peaks were determined as well as the quench parameter. The spectra obtained are shown in Annexure 4. The following data were gathered from these spectra (Table 5.11),

Table 5.11. Samples prepared from ^{226}Ra standard reference solution.

		Po-214	Po-218	Rn-222	Ra-226
	Energy (MeV)	7.687	6.002	5.49	4.774
ml	Quench parameter	Channel number	Channel number	Channel number	Channel number
10	779.11	707	643	622	593
9	787.40	722	652	635	604
8	806.02	734	666	647	615
7	817.00	746	673	661	627
6	820.73	756	690	668	634
5	828.96	762	696	675	639
4	834.95	772	704	685	649
3	848.98	781	715	695	660
2	862.28	793	728	706	671
1	867.89	807	743	719	685
0	890.57	837	772	748	714

Graphically represented by,

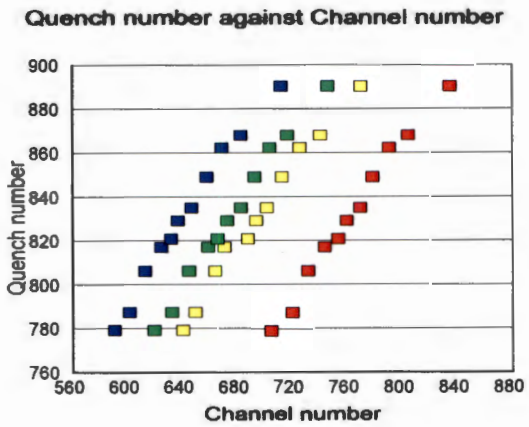

Figure 5.19. Graphic representation of samples prepared from ^{226}Ra standard reference solution.

For each of the eleven quench parameters a linear regression was done against the four energies, according to

$$E_\alpha = Ch \cdot A_i + B_i \quad (5.8)$$

where E_α = Energy of the alpha particle (MeV)
Ch = Channel number of the respective peak in the spectrum
A_i = Quench parameter dependent coefficient, and
B_i = Quench parameter dependent constant

This resulted in the following coefficients and constants in table 5.12, together with their respective uncertainties. Accordingly, it can be seen that the typical uncertainty in the energy calculation is between 2% and 5%, which will give us on a sample containing uranium an uncertainty of 100-200 keV.

Table 5.12. Results from a linear regression of the eleven quench parameters

Quench Parameter	A_i	Uncertainty in A_i	Bi	Uncertainty in B_i
779.11	0.025013	0.000510	-10.00472	0.04379
787.40	0.024914	0.000495	-10.16792	0.04267
806.02	0.024689	0.000526	-10.52628	0.04575
817.00	0.024554	0.000579	-10.73234	0.05060
820.73	0.024509	0.000601	-10.80146	0.05262
828.96	0.024407	0.000655	-10.95239	0.05759
834.95	0.024333	0.000698	-11.06089	0.06157
848.98	0.024158	0.000808	-11.31057	0.07168
862.28	0.023992	0.000917	-11.54156	0.08194
867.89	0.023922	0.000964	-11.63735	0.08638
890.57	0.023635	0.001156	-12.01478	0.10475

Thereafter, linear regression was applied to the values of the Quench Parameter against the Coefficient and Constant respectively, according to,

$$A_i = QP \cdot X + Y \quad (5.9)$$

where A_i = Quench parameter dependent coefficient,
QP = Quench parameter – SQP(E)-value for the specific sample,
X = Quench parameter dependent coefficient, and
Y = Quench parameter dependent constant.

and

$$Bi = QP \,.\, R + S \qquad (5.10)$$

where B_i = Quench parameter dependent constant,
QP = Quench parameter – SQP(E)-value for the specific sample,
R = Quench parameter dependent coefficient, and
S = Quench parameter dependent constant.

This gave the following results given in Table 5.13a and 5.13b,

Table 5.13a. Results of Quench Parameter against the Coefficient A_i

A_i	Regression Output:	
Y		3.4649E-02
Std Err of Y		4.0848E-06
R Squared		9.9992E-01
No. of Observations		11
Degrees of Freedom		9
X	-1.2360E-05	
Std Err of X	3.7685E-08	

Table 5.13b. Results of Quench Parameter against the Constant B_i

B_i	Regression Output:	
S		4.0525E+00
Std Err of S		1.9766E-02
R Squared		9.9909E-01
No. of Observations		11
Degrees of Freedom		9
R	-1.8081E-02	
Std Err of R	1.8235E-04	

This thus resulted in the following channel number -to- energy conversion Quench Parameter equation,

$$\text{Energy (MeV)} = \text{Channel Number} \,.\, \{[SQP(E)] \,.\, X + Y\} + \{[\, SQP(E)] \,.\, R + S\} \qquad (5.11)$$

Verification of equation (5.11) on the 11 samples prepared from the ^{226}Ra standard reference solution resulted in table 5.14a and 5.14b,

Table 5.14a. Results from verifying the equation from the ^{226}Ra standard reference solution

		Po-214			Po-218	
Energy (MeV)		7.687			6.002	
Quench parameter	Channel number	Energy (MeV)	% Deviation	Channel number	Energy (MeV)	% Deviation
779.11	707.2	7.661	-0.34%	638.7	5.947	-0.92%
787.40	716.5	7.668	-0.25%	648.2	5.968	-0.57%
806.02	737.1	7.677	-0.13%	669.5	6.007	0.09%
817.00	749.3	7.678	-0.12%	682.1	6.026	0.40%
820.73	753.5	7.677	-0.12%	686.3	6.032	0.50%
828.96	762.6	7.675	-0.16%	695.7	6.043	0.68%
834.95	769.3	7.672	-0.19%	702.6	6.049	0.79%
848.98	784.9	7.662	-0.33%	718.6	6.061	0.99%
862.28	799.6	7.647	-0.53%	733.8	6.067	1.09%
867.89	805.9	7.639	-0.63%	740.2	6.069	1.11%
890.57	831.1	7.599	-1.15%	766.2	6.064	1.03%
Averages		7.659	-0.36%		6.030	0.47%

Table 5.14b. Results from verifying the equation from the ^{226}Ra standard reference solution

		Rn-222			Ra-226	
Energy (MeV)		5.490			4.774	
Quench parameter	Channel number	Energy (MeV)	% Deviation	Channel number	Energy (MeV)	% Deviation
779.11	621.5	5.515	0.46%	590.0	4.728	-0.95%
787.40	630.5	5.526	0.66%	598.7	4.734	-0.83%
806.02	650.8	5.545	1.01%	618.2	4.741	-0.69%
817.00	662.7	5.552	1.13%	629.7	4.741	-0.70%
820.73	666.8	5.553	1.15%	633.6	4.740	-0.71%
828.96	675.8	5.555	1.19%	642.2	4.737	-0.78%
834.95	682.3	5.556	1.20%	648.5	4.734	-0.85%
848.98	697.6	5.553	1.14%	663.2	4.722	-1.08%
862.28	712.0	5.545	1.00%	677.1	4.707	-1.41%
867.89	718.2	5.540	0.92%	683.0	4.699	-1.57%
890.57	742.8	5.513	0.42%	706.7	4.659	-2.42%
Averages		5.541	0.93%		4.722	-1.09%

The relevance of the equation to other standard solutions was checked on the following reference solutions available; ^{238}U, ^{226}Ra, ^{210}Pb (^{210}Po), ^{209}Po, ^{229}Th, ^{232}Th and ^{232}U. The results obtained are shown in Table 5.15.

Table 5.15. Results from verifying equation (5.11) on other standard reference solutions.

Expected Energy (MeV)	Test solutions	Nuclides	Quench parameter	Channel number	Calculated Energy (MeV)	% Deviation
4.188	U-238	U-238	799.1	597	4.212	0.57%
4.756		U-234	799.1	623	4.827	1.49%
4.774	Ra-226	Ra-226	805.0	633	4.903	2.70%
5.490		Rn-222	805.0	659	5.517	0.50%
6.002		Po-218	805.0	684	6.108	1.76%
7.687		Po-214	805.0	758	7.856	2.20%
4.883	Po-209		801.3	633	5.003	2.46%
5.304	Pb-210	Po-210	800.96	652	5.439	2.54%
3.998	Th-232	Th-232	799.5	588	3.997	-0.02%
5.400		Th-228	799.5	648	5.416	0.30%
5.673		Ra-224	799.5	666	5.842	2.97%
6.288		Rn-220	799.5	682	6.220	-1.08%
6.778		Po-216	799.5	710	6.882	1.53%
8.785		Po-212	799.5	799	8.987	2.30%
5.302	U-232	U-232	754.8	599	5.462	3.01%
5.400		Th-228	754.8	599	5.462	1.14%
5.673		Ra-224	754.8	605	5.605	-1.20%
6.288		Rn-220	754.8	630	6.201	-1.38%
6.778		Po-216	754.8	639	6.416	-5.34%
8.785		Po-212	754.8	725	8.467	-3.61%

These results seem to be in reasonable agreement taking the relatively poor resolution of the α spectra into consideration. Annexure 1 refers to the spectra obtained. However, one can also see that some of the expected nuclides are not "seen" in the spectra. This will be further discussed in section 6.2.

5.3.5 Beta-energies to be expected theoretically from NORM nuclides

The gross β activity in water is normally caused by ^{210}Pb and ^{228}Ra. If the sample is not prepared and measured immediately, and if any ^{238}U, ^{226}Ra or ^{210}Pb exists in water, extra counts will be observed due to the ingrowths of their short lived daughters. Although one can already observe from Figures 5.5.b and 5.6 that there is very poor resolution of the β energies in LSC we still want to explore what to expect theoretically from possible dominant nuclides in the environmental water samples.

Accordingly, taking the relevant data from Nuchart (Canberra Industries) we can also look at the following theoretical cases:

1. Water contaminated with Uranium
   Due to the presence of ^{238}U, ^{235}U and ^{234}U the following β energies and relative intensities can be expected, and are graphically represented by Figure 5.20.

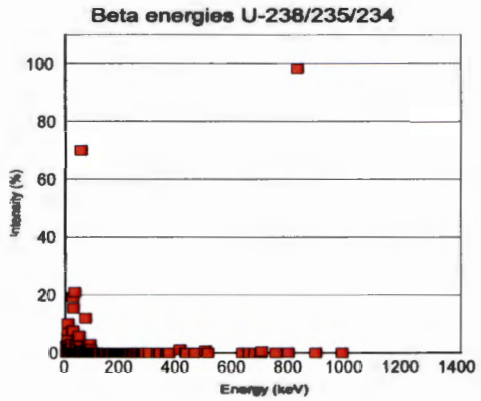

Figure 5.20. Graphic representation of β energies and relative intensities for natural uranium.

Accordingly, one can expect a low and high energy region as confirmed by Figure 5.5.b (omitting the α spillover in the β channel).

2. Water contaminated with ^{226}Ra with the respective short-lived progeny can graphically be represented by Figure 5.21, which indicates a low and medium energy region, which is confirmed in Figure 5.6 (omitting the α spillover in the β channel).

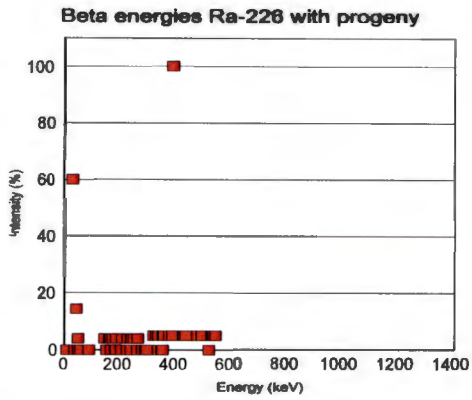

Figure 5.21. Graphic representation of β energies and relative intensities for ^{226}Ra

3. Water contaminated with Actinium-227 and progeny can graphically be represented by Figure 5.22, indicating a low and medium energy region.

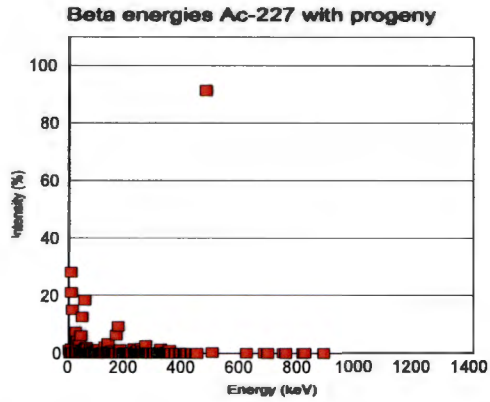

Figure 5.22. Graphic representation of β energies and relative intensities for ^{227}Ac

4. Water contaminated with ^{210}Pb and progeny can graphically be represented by Figure 5.23, indicating a low and medium energy region.

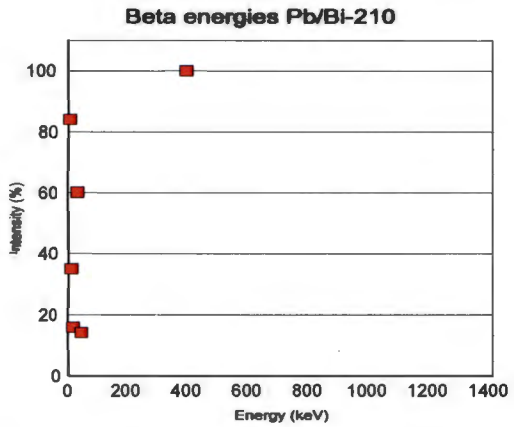

Figure 5.23. Graphic representation of β energies and relative intensities for ^{210}Pb and progeny

5. Water contaminated with ^{228}Ra and short-lived progeny can graphically be represented by Figure 5.24, indicating a low and medium energy region.

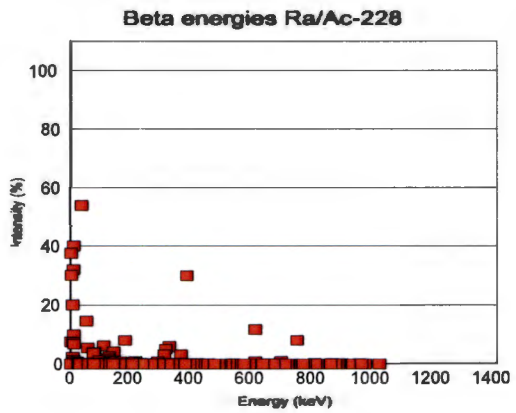

Figure 5.24. Graphic representation of β energies and relative intensities for ^{228}Ra and short-lived progeny

6. Water contaminated with ^{228}Th and progeny can graphically be represented by Figure 5.25, indicating a low and high energy region.

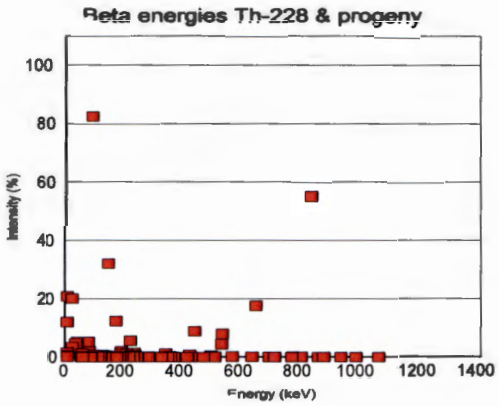

Figure 5.25. Graphic representation of β energies and relative intensities for ^{228}Th and progeny

5.3.6 Interpretation of Alpha- and Beta-spectra to be expected from NORM nuclides

According to the evaluations made in 5.3.4 and 5.3.5 one needs both the α and β spectra to make a useful evaluation of the most likely contaminants in the environmental samples. This will obviously only be a semi-qualitative indication and should be followed by nuclide specific determinations if the anticipated nuclide concentration would lead to potential radiological exposure above accepted limits if the water is assumed to be the only source of drinking water for communities surrounding the catchment area.

5.4 Measurement and Evaluation

5.4.1 Gross α and β determination method

Samples were prepared by taking a 5 ml portion of the environmental water samples (pipette) and transferring them to a polyethylene counting vial and thereafter 15 ml of the Ultima Gold AB cocktail was added and the sample was vigorously shaken. This cocktail is based on the di-isopropylnaphthalene solvent and consequently possesses outstanding α/β discrimination properties (see also 4.3). In addition, background samples were prepared the same way using distilled water. Different amounts (between 1 and 10 ml) of distilled water and Ultima Gold AB were prepared to obtain quench parameters (SQP(E)) for typical values obtained for natural samples. After 1 minute counting the SQP(E) parameters of all samples were obtained. Most of the LSC background counts were composed of short pulses and thus fall into the β spectrum while the α background is very small.

5.4.2 Counting procedure for environmental samples

The following procedure for determination of gross α β activity was applied:

- 1 minute counting of the environmental samples to test the resulting quenching:
  - Arbitrary optimal PSA setting
  - Calculation of the SQP(E) value for the individual samples

- Thereafter 300 minutes counting at an optimal PSA setting based on the SQP(E) value obtained for the samples from the first measurement (at arbitrary PSA level setting).

The results of the measurements are shown in Annexure 2, where the blue and red lines present the spectral data of the cpm (counts per minute) in the β and α channels respectively.

Finally, the gross activity concentrations (A_α and A_β) were calculated. According to literature, there are a number of options for gross α β activity calculations from the raw counts obtained. In this research two options were used. The first option quantified the α β activities without using spillover corrections. The activities are given by

$$A_\alpha = \frac{(MCA12_{G\alpha} - MCA12_{B\alpha})}{V \cdot T \cdot} \tag{5.12}$$

$$A_\beta = \frac{(MCA11_{G\beta} - MCA11_{B\beta})}{V \cdot T \cdot} \tag{5.13}$$

The second option used takes the spillover effect into account, and the expressions now become as follows:

$$A_\alpha = \frac{(MCA12_{G\alpha} - MCA12_{B\alpha})(1 - X_\beta) - (MCA11_{G\beta} - MCA11_{B\beta})X_\beta}{(1 - X_\alpha - X_\beta) \cdot \varepsilon_\alpha \cdot V \cdot T \cdot} \tag{5.14}$$

$$A_\beta = \frac{(MCA11_{G\beta} - MCA11_{B\beta})(1 - X_\alpha) - (MCA12_{G\alpha} - MCA12_{B\alpha})X_\alpha}{(1 - X_\alpha - X_\beta) \cdot \varepsilon_\beta \cdot V \cdot T \cdot} \tag{5.15}$$

where:

MCA $12_{G\alpha}$ and *MCA* $11_{G\beta}$ are the number of gross counts per minute recorded in the α and in β window, respectively, for the sample vial.

MCA $12_{B\alpha}$ and *MCA* $11_{B\beta}$ are the number of background counts per minute recorded in the α and in β window, respectively, for the blank vial.

A_α and A_β are the α and β activities (Bq/ℓ) of the sample respectively.

X_α and X_β are the α and β spillover respectively.

ε_α and ε_β are the α and β detection efficiency respectively.

V is the amount of sample analyzed (ℓ).

T is the corrected measuring time from minutes to seconds (60).

5.5 Validation for gross α - β measurements

To validate the results two independent methods were used,

- Gas flow proportional counting of 50 mℓ of the samples evaporated on stainless steel discs and counted for 300 minutes each, and
- Element specific separations (U, Ra, Pb/Po, Th) followed by α-spectrometry, from which the gross α and β activities were calculated assuming radioactive equilibrium between short-lived progeny and their long-lived parents.

Results from both analyses were obtained from routine techniques available within the Radioanalytical laboratories of Necsa.

5.6 Summary of calibration

A preliminary method is developed to measure NORM in water using the Wallac 1220™ Quantulus LSC. The method as presented in this project can still be further developed, tested and optimized as there were other features/parameters like "guard on-off" and "low-high coincidence" that were not studied yet. These parameters may further improve the accuracy of LSC.

The correct setting of the measurement parameters deserves special attention since a large number of radionuclides are involved in NORM analysis. The optimization of these parameters is necessary for the fast and accurate gross α-β screening method of NORM by LSC.

CHAPTER 6

RESULTS AND DISCUSSION

6.1 Gross α and β activities identification using LSC

6.1.1 Data obtained for nuclide reference standards

The measured gross α and β activities using LSC obtained with and without quench and spill-over corrections are presented in Table 6.1. It can be observed that the calculations including α-β spillovers corrections, as discussed in 5.4.2, did not change the results significantly, indicating a good optimization of the PSA settings to minimize spillovers. It can also be verified by spectra of highly quenched samples, RA_10750X022 and RA_10281X022, that have extremely high α-β activities, with less β spillovers into α channel vice-versa. These samples are further discussed in section 6.3.

Table 6.2 presents the information from the calculated activities obtained from nuclide specific analysis of the samples by element specific separations followed by α spectrometry and assumption of radioactive equilibrium between short-lived progeny and their respective long-lived parents. Details of these assumptions are shown in Annexure 3.

The gas flow proportional counter data are presented in Table 6.3.

In Table 6.4 the calculated and measured (by LSC) α-β ratios are presented. It can be seen that the activity of α's and β's is in reasonable good agreement between LSC and calculated values. There are some noticeable differences that will be discussed in 6.3.

Comparison of the gas flow proportional counter data with either the calculated data or the LSC data show that there is a substantial discrepancy between the data. This was already noted in previous studies [1] and is currently under investigation as part of another MSc-study.

6.2 Semi-qualitative nuclide identification from the spectral data of reference standards using LSC

Annexure 1 refers to the reference solutions available at the laboratory at the time of the research. The following nuclides should have been expected to be observed taking the age of the reference solutions into consideration

^{238}U (Reference date of certification: 15 January 2004, 12:00 GMT)

As this is most likely a depleted uranium solution one expects only the ^{238}U α-peak at 4.188 MeV in equilibrium with its daughters ^{234}Th and ^{234m}Pa, which are β active having the main β energies at 27-53 keV and 813-821 keV respectively. Some indication should be taken into consideration that ^{234}U may be present (at around 4.760 MeV), while no indication of ^{235}U (at around 4.390 MeV) is expected. Looking at the first graph in Annexure 1 this is confirmed by having one major α-peak and the associated low and high β energies from ^{234}Th and ^{234m}Pa. It also can be seen that there is some spill-over from α's into the β channel and from the β's into the α channel.

^{232}Th (Reference date of certification: 21 May 2002, 12:00 GMT)

As the reference date of this standard is May 2002 one can expect around 75% ingrowths of ^{232}Th daughters ^{228}Ra (half-life 5.75 years) and ^{228}Th with their relatively short-lived progeny. Accordingly we can expect a substantial contribution of the daughters. From the spectrum in Annexure 1 it can be seen that the following nuclides are present: ^{232}Th, ^{228}Ra, ^{228}Ac, ^{228}Th, ^{224}Ra, ^{212}Pb, ^{212}Bi and ^{208}Tl. The absence of ^{220}Rn cannot be readily explained while the absence of ^{216}Po and ^{212}Po can be explained by their ultra short half-lives preventing the system to detect the α's being in "busy" mode to process a former event from their respective parents. The β spectrum requires some imagination to allocate the various β's generated in the process. It also can be seen that there is virtually no spill-over from α's into the β channel and some spill-over from the β's into the α channel, especially from the higher energy β's of ^{212}Bi.

^{210}Pb (Reference date of certification: 01 January 2006, 12:00 GMT)

From this standard we can expect regarding the age of the standard that ^{210}Pb will be in equilibrium with its daughters ^{210}Bi an ^{210}Po, and accordingly showing β energies at around 10 keV and 390 keV from ^{210}Pb and ^{210}Bi respectively, as well as an α energy at 5.304 MeV from ^{210}Po. It also can be seen that there is a small spill-over from α's into the β channel and some spill-over from the β's into the α channel, especially from the lower energy β's of ^{210}Pb.

^{226}Ra (Reference date of certification: 04 March 2003, 12:00 GMT)

Two measurements were done for this sample to show the influence of the ingrowths of ^{222}Rn and its daughters with time. The first measurement was done shortly after preparing the sample showing that radon was lost while the still present ^{214}Pb/^{214}Bi parent-pair still produced some ^{214}Po. The second measurement was done after about 3 weeks now showing the full ingrowths of

all short-lived progeny. Furthermore, regarding the age of the standard we may expect that some (around 25%) ^{210}Pb (half-life 22.3 years) will have been formed in equilibrium with its daughters ^{210}Bi and ^{210}Po, of which the first two can be observed in both spectra, while the ^{210}Po peak causes the shoulder between the ^{226}Ra and ^{222}Rn peaks as can be best observed from the second spectrum.

^{209}Po (Reference date of certification: 01 August 2008, 12:00 GMT)

From this standard we expect one major α at around 4.884 MeV (99%) as well as a minor one around 4.662 MeV (1%) from ^{209}Po to be present in the sample, which can explain the low-energy tail in the α spectrum.

^{232}U (Reference date of certification: 01 July 2002, 12:00 GMT)

Here one expects ^{232}U with a fair amount (about 98.6%) of ^{228}Th in equilibrium with its short-lived daughters. However, it is observed that ^{220}Rn and its short-lived α-active daughters are absent, while the somewhat longer-lived β-active daughters ^{212}Pb and ^{212}Bi are present. ^{220}Rn could have escaped during sample preparation although its short half-life of around 1 minute does not explain its absence from the spectrum, which was also observed for the ^{232}Th standard. This has to be looked at in more detail in a follow-up study. The β spectrum requires some imagination to allocate the various β's generated in the process. It also can be seen that there is some spill-over from α's into the β channel and from the β's into the α channel, especially from the higher energy β's of ^{212}Bi.

^{229}Th (Reference date of certification: 01 January 1997, 12:00 GMT)

From this standard we expect ^{229}Th to be in equilibrium with all its daughters. The fact that ^{225}Ac (10 days half-life) and short-lived daughter ^{221}Fr are not in equilibrium can possibly be explained by adsorption of actinium to the wall of the container of the ^{229}Th standard. Furthermore the absence of the ultra short-lived daughters ^{217}At and ^{213}Po may again be explained by the dead-time of detection system being busy processing the signals of their respective parents and accordingly "missing" the signals of the daughters. Also here there is some spill-over from α's into the β channel and from the β's into the α channel.

6.3 Semi-qualitative nuclide identification from the spectral data from environmental samples using LSC

The gross α and β spectra of the Quantulus from 25 environmental water samples are presented in Annexure 2. In Table 6.4 it was already shown that there is a fair agreement between the data obtained from LSC and those obtained from nuclide specific analysis. Without going into the detail of every individual sample the following remarks are to be made.

1. In general it can be seen that the gross α activity of the samples can be attributed to ^{234}U and ^{238}U with a minor contribution from ^{226}Ra and its short-lived progeny. However, as indicated in 6.2 one has to be aware of the potential loss of ^{222}Rn and accordingly can not quantify its content on the ^{214}Po signal unless one aged the prepared sample for about 3 weeks to allow reinstating the activity equilibrium between ^{226}Ra and its daughters.

2. The relatively "free-standing" peak of ^{214}Po, however, makes it possible to calculate the contribution of ^{226}Ra and its daughters to the total activity and accordingly one can correct the total α activity to obtain better data for the uranium concentration.

3. The relative concentrations of ^{238}U and ^{234}U can be estimated from the height of their respective peaks.

4. In the less active samples the contribution of ^{40}K will influence the β-activity measured through LSC and care should be taken not to attribute this to some NORM nuclides like ^{228}Ra or ^{210}Pb. An example can be seen in sample RA_10479X009, RJ_2010-0408X004 and RA_11160X0001.

5. Sample RA_10199X001 is a typical example where the gross α and β activities cannot be attributed to the uranium content of the sample. Very useful information can thus be obtained from the spectrum showing that ^{210}Pb and its progeny is the major activity in the water sample.

6. For sample RA_11160X001 it can be seen that here there is a contribution from both ^{210}Pb and its progeny as well as ^{40}K, making it again possible to distinguish between other nuclides and accordingly wrongly attributing the activity to uranium again.

7. Samples RA_10750X022 and RA_10281X022 are the other extreme where the activity of uranium is so high that the spectra are so distorted that no real information can be reliably obtained. These samples should be diluted with distilled water and measured again.

Table 6.1. Gross α-β activities for environmental samples by LSC.

	Activity with spillover correction (Bq/ℓ)				Activity without spillover correction (Bq/ℓ)			
Water sample *	Gross α	α unc	Gross β	β unc	Gross α	α unc	Gross β	β unc
RA_10187_X003	9.46	0.23	8.69	0.09	9.77	0.23	8.15	0.08
RA_10417_X002	6.40	0.17	7.51	0.08	6.70	0.18	7.02	0.07
RA_10548_X002	11.5	0.26	12.9	0.13	12.1	0.26	12.0	0.12
RA_10479_X009	2.18	0.08	2.88	0.03	2.31	0.08	2.67	0.03
RA_10187_X007	12.9	0.28	13.2	0.13	13.5	0.28	12.2	0.12
RA_10187_X008	4.07	0.13	5.47	0.06	4.29	0.13	5.12	0.05
RJ_2010-0405X004	0.84	0.04	2.27	0.02	0.94	0.04	2.10	0.02
RA_10497_X007	13.7	0.29	12.5	0.13	14.2	0.29	11.6	0.12
RA_10187_X002	7.59	0.19	7.90	0.08	7.87	0.20	7.42	0.08
RJ_2010-0304X013	6.50	0.18	9.98	0.10	6.83	0.18	9.44	0.10
RA_10717_X008	14.1	0.29	11.4	0.12	14.5	0.30	10.7	0.11
RA_10548_X003	12.3	0.27	12.2	0.12	12.8	0.27	11.4	0.12
RA_10199_X001	3.42	0.11	14.5	0.14	3.93	0.12	13.7	0.14
RA_11160_X001	1.06	0.04	1.53	0.02	1.13	0.04	1.42	0.02
RA_10717_X015	15.8	0.32	13.8	0.14	16.3	0.32	12.9	0.13
RJ_2010-0304X015	7.37	0.19	9.59	0.10	7.71	0.19	9.03	0.09
RA_10548_X005	13.5	0.29	14.2	0.14	14.1	0.29	13.3	0.13
RA_10417_X001	9.82	0.23	4.95	0.05	9.96	0.23	4.39	0.05
RA_11221_X003	44.8	0.60	33.4	0.30	46.1	0.61	29.3	0.26
RJ_2009-0693X001	13.08	0.28	7.44	0.08	13.3	0.28	6.56	0.07
RA_10548_X004	14.5	0.30	11.7	0.12	15.0	0.30	10.2	0.10
RA_10354_X006	54.1	0.67	44.0	0.37	55.9	0.68	38.5	0.33
RA_11221_X002	38.4	0.37	54.1	0.56	46.4	0.45	37.0	0.38
RA_10281_X022	5242	6.92	1172	3.94	5383	7.47	814	2.71
RA_10750_X022	9638	5.43	7414	21.95	11404	10.9	1252	3.55

- The sample identification codes are laboratory reference numbers of samples analysed from batches delivered to the laboratories for nuclide specific analysis.
- unc = Uncertainty at 1 sigma

Table 6.2. Calculated gross α-β activities from nuclide specific analysis results.

	Calculated values (Bq/ℓ)			
Water sample	Gross α	α unc	Gross β	β unc
RA_10187_X003	7.46	0.07	7.01	0.06
RA_10417_X002	6.14	0.06	5.96	0.06
RA_10548_X002	10.77	0.11	10.79	0.12
RA_10479 _X009	2.19	0.07	1.97	0.05
RA_10187_X007	12.42	0.14	12.10	0.14
RA_10187_X008	3.56	0.07	3.56	0.07
RJ_2010-0405X004	1.02	0.04	0.68	0.03
RA_10497_X007	14.03	0.10	11.74	0.09
RA_10187_X002	6.99	0.06	7.23	0.06
RJ_2010-0304X013	6.05	0.14	6.12	0.12
RA_10717_X008	12.90	0.08	11.26	0.08
RA_10548_X003	11.06	0.12	10.97	0.12
RA_10199_X001	3.56	0.05	3.35	0.04
RA_11160_X001	0.30	0.02	0.20	0.01
RA_10717_X015	14.17	0.09	13.87	0.09
RJ_2010-0304X015	6.64	0.09	6.59	0.07
RA_10548_X005	13.27	0.09	13.34	0.09
RA_10417_X001	7.28	0.08	6.51	0.07
RA_11221_X003	34.38	0.29	33.25	0.28
RJ_2009-0693X001	8.55	0.08	6.95	0.08
RA_10548_X004	12.41	0.09	12.67	0.09
RA_10354_X006	41.22	0.30	37.05	0.29
RA_11221_X002	32.36	0.30	30.79	0.28
RA_10281_X022	344.46	2.84	181.46	2.02
RA_10750_X022	528.30	4.25	11.30	3.01

- unc = Uncertainty at 1 sigma

Table 6.3. Comparison of results with Gas flow proportional counter activities.

Measured with Gas flow proportional counter (Bq/ℓ)				
Water sample	Gross α	α unc	Gross β	β unc
RA_10187_X003	3.99	0.32	5.41	0.29
RA_10417_X002	3.75	0.15	0.38	1.24
RA_10548_X002	6.69	0.51	4.73	0.59
RA_10479_X010	1.37	0.26	1.21	0.24
RA_10187_X007	5.62	0.41	6.25	0.33
RA_10187_X008	2.15	0.16	2.30	0.17
RJ_2010-0405X004	0.56	0.32	1.50	0.20
RA_10497_X007	6.26	0.50	3.76	0.29
RA_10187_X002	3.03	0.22	3.63	0.22
RJ_2010-0304X013	NA		NA	
RA_10717_X008	10.98	0.80	5.14	0.39
RA_10548_X003	5.81	0.45	4.81	0.59
RA_10199_X001	0.99	0.60	1.19	0.16
RA_11160_X001	0.23	0.06	0.38	0.10
RA_10717_X015	8.47	0.65	6.49	0.42
RJ_2010-0304X015	NA		NA	
RA_10548_X005	3.39	0.43	5.58	0.57
RA_10417_X001	3.77	0.16	0.37	1.57
RA_11221_X003	NA		NA	
RJ_2009-0693X001	7.03	0.73	3.21	0.57
RA_10548_X004	5.40	0.42	3.39	0.56
RA_10354_X006	33.14	2.90	39.79	2.90
RA_11221_X002	NA		NA	
RA_10281_X022	NA		NA	
RA_10750_X022	NA		NA	

- NA = No data available
- unc = Uncertainty at 1 sigma

Table 6.4. Activity ratios of calculated data from nuclide specific analysis over the gross α-β activity results obtained by LSC.

Ratio	Activity with spillover correction				Activity without spillover correction			
Water sample	Gross α	α unc	Gross β	β unc	Gross α	α unc	Gross β	β unc
RA_10187_X003	0.79	0.03	0.81	0.01	0.76	0.03	0.86	0.01
RA_10417_X002	0.96	0.03	0.79	0.01	0.92	0.03	0.85	0.01
RA_10548_X002	0.93	0.02	0.83	0.01	0.89	0.02	0.90	0.01
RA_10479_X009	1.01	0.05	0.68	0.03	0.95	0.05	0.74	0.03
RA_10187_X007	0.96	0.02	0.92	0.01	0.92	0.02	0.99	0.02
RA_10187_X008	0.87	0.04	0.65	0.02	0.83	0.04	0.70	0.02
RJ_2010-0405X004	1.21	0.06	0.30	0.05	1.09	0.05	0.32	0.05
RA_10497_X007	1.02	0.02	0.94	0.01	0.99	0.02	1.01	0.01
RA_10187_X002	0.92	0.03	0.92	0.01	0.89	0.03	0.97	0.01
RJ_2010-0304X013	0.93	0.04	0.61	0.02	0.89	0.04	0.65	0.02
RA_10717_X008	0.92	0.02	0.99	0.01	0.89	0.02	1.05	0.01
RA_10548_X003	0.90	0.02	0.90	0.01	0.86	0.02	0.97	0.01
RA_10199_X001	1.04	0.04	0.23	0.01	0.91	0.03	0.24	0.02
RA_11160_X001	0.28	0.07	0.13	0.07	0.26	0.07	0.14	0.07
RA_10717_X015	0.89	0.02	1.01	0.01	0.87	0.02	1.07	0.01
RJ_2010-0304X015	0.90	0.03	0.69	0.01	0.86	0.03	0.73	0.01
RA_10548_X005	0.98	0.02	0.94	0.01	0.94	0.02	1.00	0.01
RA_10417_X001	0.74	0.03	1.32	0.01	0.73	0.03	1.48	0.01
RA_11221_X003	0.77	0.02	1.00	0.01	0.74	0.02	1.14	0.01
RJ_2009-0693X001	0.65	0.02	0.93	0.01	0.64	0.02	1.06	0.02
RA_10548_X004	0.86	0.02	1.09	0.01	0.83	0.02	1.24	0.01
RA_10354_X006	0.76	0.01	0.84	0.01	0.74	0.01	0.96	0.01
RA_11221_X002	0.84	0.01	0.57	0.01	0.70	0.01	0.83	0.01
RA_10281_X022	0.07	0.01	0.15	0.01	0.06	0.01	0.22	0.01
RA_10750_X022	0.05	0.01	0.00	0.27	0.05	0.01	0.01	0.27

- unc = Uncertainty at 1 sigma

CHAPTER 7

CONCLUSIONS

This study indicates the measurement of the gross α-β activity in environmental water samples and the identification of nuclides concerned is a great tool to obtain semi-quantitative and – qualitative information for environmental monitoring of water sources in and around mining areas where uranium is one of the major contributors to NORM-nuclide contamination.

It also gives the analyst a powerful tool to avoid wrong assumptions in attributing the activity of the environmental samples taken in routine monitoring programmes to uranium only. LSC using the Quantulus has proven to be an adequate, versatile and accurate technique for investigating water samples for NORM contamination. With the application of special software for spectrum analysis, this technique may be the most convenient technique for analyzing radionuclides in general in liquid samples. Gross α-β-activities can be measured with quick and simple procedures.

This method also avoids costly nuclide specific analysis methods and according is very suitable for routine monitoring of water sources.

The following to be evaluated is whether the sensitivity is adequate for proper dose evaluations of the potential use of the water sources by people living in and around the catchment areas. It should be kept in mind that this technique only uses 10 mℓ of the original sample. If required, substantial pre-concentration can be obtained by commercially available high element selective resins. This, however, should be the subject of a follow-up study resulting from the work done in this dissertation.

REFERENCES

1. South Africa. Department of water affairs and forestry (DWAF). 2002. Radioactivity dose calculation and water quality evaluation guideline for domestic water use. http://www.dwaf.gov.za/iwqs/radioact/DWAFGuideline/temp.htm Date of access: 15-04-2010

2. Faanhof, A. 2008. Theme 2: Environmental Radioanalysis module. NUCI 687-TH-02. Mafikeng: North-west University.

3. U.S Environmental Protection Agency. 2006. Inventory of radiological methodologies for sites with radioactive materials. (EPA 402-R-06-007).

4. National Nuclear Regulator (NNR). 2007. Radiological Impacts of the mining activities to the public in the Wonderfonteinspruit catchment area. (Technical Report. TR-RRD-07-00006).

5. Coetzee, H., Wade, P., Venter, J. 2007. Risk assessment of contaminated sediments downstream of Witwatersrand gold mining operations. Environmental geosciences.

6. Otton, K.J., 1994. Natural radioactivity in the environment. U.S. Geological Survey. http://energy.usgs.gov/factsheets/Radioactivity/radioact.html Date of access: 15-04-2010

7. South Africa. Institute for Water Quality Studies (IWQS). 1999. Report on the radioactivity monitoring programme in the Mooi River (Wonderfonteinspruit) catchment. (N/C200/00/RPQ/2399).

8. Packard Instrument Company. The Effect of Quench on Quantitating α Radionuclides by liquid Scintillation Counting. Application Note.

9. L'Annunziata, M.F. 2003. Handbook of Radioactivity Analysis. 2nd Edition. San Diego, CA: Academic Press.

10. Borai, E.H., Lasheen, Y.F., Seliman, A.F and Abo-Al, M.M. 2007. Assessment of Quench Indicating Parameters (QIP) of an Alternative Scintillation Cocktail Mixture by Low Level Liquid Scintillation Counting. *World Journal of Chemistry*, 2(1): 1 - 9

11. Palomo, M., Villa, M., Pefialver, A., Aguilar, C., Borrull, F., Bruach, J.M ., Casacuberta, N and Masque, P. 2008. 63-Optimization and Study of Parameters Affecting Liquid Scintillation Counting for Gross α and β Activities in Water Samples.

12. Ahmed, K.N. 2004. Natural Radioactivity of Ground and Drinking Water in Some Areas of Upper Egypt. *Turkish journal of engineering environmental science*, 28: 345-354.

13. Lidman, F. 2005. Isotopic disequilibrium for assessment of radionuclide transport in peat lands. Uranium-Thorium Series Nuclides in a Core from Klarebacksmossen, Oskarshamn, Sweden. Examensarbete 20p. UPTEC W05 019

14. Adriambololona, R., Rabesiranana, N., Rasolonirina, M. and Rakotonga, H. 2004. Radon progenies as a source of gross α - β activities in drinking water in Vinaninkarena, Antsirabe-Madagascar. (In HEP-MAD' 04 International conference, Antannarivo, Madagascar).

15. Lasheen, F.Y., Seliman, F.A and Abdel-Rassoul, A.A. 2007. Simultaneous measure of ^{226}Ra and ^{228}Ra in natural water by liquid scintillation counting. *Journal of Environmental Radioactivity,* 95: 86-97.

16. Palomo, M., Peñalver, A., Aguilar, C. and Borrull, F. 2007. Tritium activity levels in environmental water samples from different origins. *Applied Radiation and Isotopes*, 65: 1048-1056.

17. Kleinschmidt, I.R. 2004. Gross α and β activity analysis in water - a routine laboratory method using liquid scintillation analysis. *Applied Radiation and Isotopes,* 61: 333-338.

18. Happel, S., Letessier, P., Ensinger, W., Eikenberg, J.H., Thakkar, A.H. and Horwitz, E.P. 2004. Gross α determination in drinking water using a highly specific resin and LSC. *Applied Radiation and Isotopes*, 61: 339-344.

19. Rusconi, R., Azzellino, A., Bellinzoma, S., Forte, M., Gallini, R. and Sgorbati, G. 2004. Assessment of drinking water radioactivity content by liquid scintillation counting: Set up of high sensitivity and emergency procedures. *Anal Bional Chem*, 379(2): 247-253.

20. Rusconi, R., Forte, M., Caresna, M., Bellinzona, S., Cazzaniga, M.T. and Sgorbati, G. 2006. The evaluation of uncertainty in low-level LSC measurements of water samples. *Applied Radiation and Isotopes*, 64: 1124-1129.

21. Vesterbacka, P. 2007. Natural radioactivity in drinking water in Finland. *Boreal Environment Research*, 12: 11-16.

22. Zapata-Garcia, D., Llaurado, M. and Rauret, G. 2009. Establishment of a method for the rapid measurement of gross α and gross β activities in sea water. *Applied Radiation and Isotopes*, 67: 978-981.

23. Zikovsky, L. 2006. α radioactivity in drinking water in Quebec, Canada. *Journal of Environmental Radioactivity,* 88: 306-309.

24. International Atomic Energy Agency (IAEA). 2003. Guidelines for radio-element mapping using gamma ray spectrometry data. (IAEA-TECDOC-1363).

25. Deissmann, G. and Barthel, R. 2007. Impact of gold mining on levels of naturally occurring radionuclides in aquatic ecosystems of the Witwatersrand Basin, South Africa. Goldschmidt Conference Abstracts. BS Associates (Pty) Ltd, Bedfordview, South Africa.

26. Coetzee, H., Winde, F., Wade, P.W. 2006. An assessment of source, pathways, mechanisms and risks of current and future pollution of water and sediments in gold-mining areas of the Wonderfonteinspruit catchment. South Africa Water Research Commission. (WRC Report No.1214/06).

27. Winde, F. 2010. Uranium pollution of the Wonderfonteinspruit, 1997-2008. Part 1: Uranium toxicity, regional background and mining-related sources of uranium pollution. *Water SA*, 36 (3)

28. Ralph, E.L. and Howard L. A. 1955. Nuclear Radiation Physics. 2nd Edition. London: Sir Isaac Pitman & Sons, Ltd.

29. Friedlander, G and Kennedy, J.W. 1960. Nuclear and Radiochemistry. New York. John Wiley & Sons, Inc.

30. Johansson, L.Y. 1976. Determination of Pb-210 and Po-210 in aqueous environmental samples. MSc Dissertation. Von der Naturwissenschaftlichen Fakultat der Gottfried Wilhelm Leibniz Universitat Hannover zur Erlangung des Grades. Frandefors, Schweden. www.zsr.uni-hannover.de/arbeiten/drjohans.pdf Date of access: 19-10-2010

31. US Environmental Protection Agency. 2009. Radioactive Equilibrium. http://www.epa.gov/radiation/understand/equilibrium.html Date of access: 19-10-2010

32. International Atomic Energy Agency (IAEA), 2004. Practical radiation technical manual. Workplace monitoring for radiation and contamination. (IAEA-PRTM-1 (Rev1)).

33. Gilmore G.R. 2008. Practical gamma-ray spectrometry. 2nd edition. Warrington, UK. John Wiley & Sons. Ltd.

34. Canberra, http://www.jmu.ruenindex.phpcid=63.jpg Date of access: 15-09-2011

35. Faanhof A. 2008. Theme 4: Measurement of radioactivity. Part 1: Gross αβ-counting. NUCI 687-TH-04. Mafikeng: North-West University.

36. Horrocks, D.L. 1974. Application of liquid scintillation. New York and London. Academic Press, Inc.

37. Knoll, G. F. 1999. Radiation, detection and measurement. 3rd Edition. Hoboken, NJ: John Wiley & Sons, Inc.

38. Environmental measurement laboratory (EML). 1996. Calibration of a liquid scintillation counter for α, β and Cerenkov counting. U.S. Department of energy. New York 10014-4811

39. Wiel, J.T and Hegge, T. 1992. Advances in scintillation cocktails. Liquid scintillation counting and organic scintillators. pp. 51-59. www.lsc-international.org/conf/pfiles/lsc1989_051.pdf

40. Kessler, MJ. 1989. Liquid Scintillation Analysis Science and technology. Packard Instrument. Rev. G. Publication No.169-3052

41. Davies, J. 2006. The Ultra Low Level Liquid Scintillation Spectrometer. 1220 Quantulus. http://www.npl.co.uk/upload/pdf/20060124_lsuf_davies_1.pdf Date of access: 19-10-2010

42. Sanchez-Cabeza, J.A and Pujol, L. 1998. Simultaneous determination of radium and uranium activities in natural water samples using liquid scintillation counting. 123: 399-403.

43. Gruber, V. 2009. Radiation Exposure by Natural Radionuclides in Drinking Water in Upper Austria. A Radioanalytical and Evaluation in an International Context. DISSERTATION zur Erlangung des askademischen Grades. UNIVERSITAT FUR BODENKULTUR WIEN. http://www.google.co.za/url?q=https://zidapps.boku.ac.at/abstracts/download.php%3Fdataset_id%3D7123%26property_id%3D107&sa=U&ei=R16hTuTSCYew8gO-wJnmBQ&ved=0CA4QFjAA&usg=AFQjCNE2ytc4YXec_lS4mZACTg3A5SZmgQ Date of access: 15-04-2011

44. Rodriguez Barquero, L and Grau Carles, A. 1998. The influence of the primary solute on α / β discrimination. In: *Appl. Radiat. Isot.* 49: 1065-1068.

45. Wallac 1220 Quantulus™ manual. Ultra Low Level Liquid Scintillation Spectrometer Internal software version 1.D. PerkinElmer

46. Sato, K., Hashimoto, T., Noguchi, M., Nitta, W., Higuchi, H., Nishikawa, N and Sanada, T. 2000. A simple method for determination of ^{226}Ra in environmental samples by applying α-β coincidence liquid scintillation counting. *Journal of Environmental Radioactivity*, 48: 247-256.

47. Saarinen, L and Suksi, J. 1993. Determination of Uranium Series Radionuclide ^{231}Pa Using Liquid Scintillation Counting. In ref. Liquid Scintillation Spectrometry 1992, Proceedings of the International Conference on Advances in LSC, LSC 92, Vienna, Austria, September 14-18, 1992. Edited by Noakes, J.E. Schönhofer, F. and Polach, H.A. *Radiocarbon*. 209-215.

48. Chalupnik, S., Lebecka, J., Mielnikow, A. and Michalik, B. 1996. Determining radium in water: Comparison of methods. In Liquid Scintillation Spectrometry 1994, Edited by Cook, G.T. Harkness, D.D. MacKenzie, A.B. Miller, B.F. and Scott, E.M. *Radiocarbon.* 103-109.

49. Van derLoeff, M.R., Sarin, M.M., Baskaran, M., Benitez-Nelson, C., Buesseler, K.O., Charette, M., Dai, M., Gustafsson, Ő., Masque, P., Morris, P.J., Orlandini, K., Baena, A.R., Savoye, N., Schmidt, S., Turnewitsch, R., Voge, I and Waples J.T. 2006. A review of present technologies and methodological advances in analyzing ^{234}Th in aquatic systems. *Marine chemistry*, 100: 190-212.

50. Gudelis, A., Luksiene, B., Druteikiene, R.,Gvozdaite, R and Kubareviciene, V. 2006. Application of LSC for the determination of some radionuclides in waste matrices from the Ignalina. In Liquid Scintillation Spectrometry 2005. Advances in LSC. 343-353.

51. Povenic, P.P., Baxter, M.S., Gastaud, J., Liong Wee Kwong, L and Oregioni, B. 1996. Low level liquid scintillation spectrometry of soft β emitters. In Liquid Scintillation Spectrometry 1994, Edited by Cook, G. T., Harkness, D. D., MacKenzie, A. B., Miller, B. F. and Scott, E. M. *Radiocarbon.* 149-155.

52. Rank, D. 1993. Environmental tritium in hydrology: Present state. In Liquid Scintillation Spectrometry 1992. Edited by Noakes, E., Schonhofer, F. and A. Polach, H. *Radiocarbon.* 327-334.

53. Brown, L., Cook, G.T., Mackenzie, A.B and Thomson, J. 2001. Radiocarbon age profiles and size dependency of mixing in Northeast Atlantic sediments. *Radiocarbon*, 43: 929-937.

54. Aleissa, K.A., Islam, M.S and Alshammari, H. 2006. Measuring of ^{210}Po and ^{210}Pb in groundwater using an α Liquid scintillation counter. In Liquid Scintillation Spectrometry 2005. Advances in LSC. Edited by Chalupnik, S., Schönhofer, F. and Noakes, J. 197-209.

55. KawaKami, H. 2009. Scavenging of ^{210}Po and ^{234}Th by particulate organic carbon in the surface layer of the Northwestern North Pacific Ocean. *Far East Journal of Ocean Research.* 2: 67-82.

56. Institute for Water Quality Studies (IWQS); 1999. Report on the Radioactive Monitoring Programme in the Mooi River (Wonderfonteinspruit) Catchment. Department of Water Affairs and Forestry.

57. Sanchez-Cabeza JA, Pujol LI, Merino J, León L, Molero J, Vidal-Quardias A, Schell WR, Mitchell PI. 1993. Optimization and calibration of a low-background liquid scintillation counter for simultaneous determination of α and β emitters in aqueous samples. In: Noakes, JE, Schönhofer F, Polach HA, editors. *Liquid Scintillation Spectrometry 1992.* Tucson: *Radiocarbon.* 43–50.

58. Pates JM, Cook GT, MacKenzie AB, Passo Jr CJ. 1996b. Quenching and its effect on α/β separation liquid scintillation spectrometry. In: Cook GT, Harkness DD, MacKenzie AB, Miller BF, Scott EM, editors. *Liquid Scintillation Spectrometry 1994*. Tucson: *Radiocarbon*. 75–85.
59. Warwick PE, Croudace IW. 2002. Measurement of gross α and β activities in acid leachates using α β discriminating liquid scintillation counting. In: Möbius S, Noakes J, Schönhofer F, editors. *LSC 2001, Advances in Liquid Scintillation Spectrometry*. Tucson: *Radiocarbon*. 75–82.
60. Pates JM, Cook GT, MacKenzie AB, Passo Jr CJ. 1998. Implications of β energy and quench level for α/ β liquid scintillation spectrometry calibration. *Analyst* 123:2201–7.
61. Villa M, Manjón G, García-Leon M. 2003. Study of colour quenching effects in the calibration of liquid scintillation counters: the case of ^{210}Pb. *Nuclear Instruments and Methods in Physics Research A* 496:413–24.
62. Salonen L. 2006. α spillover depends on α energy: a new finding in α/β liquid scintillation spectrometry. LSC 2005, Advances in *Liquid Scintillation Spectrometry*. Edited by Stanislaw Chalupnik, Franz Schönhofer, John Noakes. 135–148.
63. Canberra; http://www.canberra.com/literature/931.asp Date of access: 15-09-2011

Annexure 1: Spectra obtained with the Quantulus for some nuclide specific reference standards

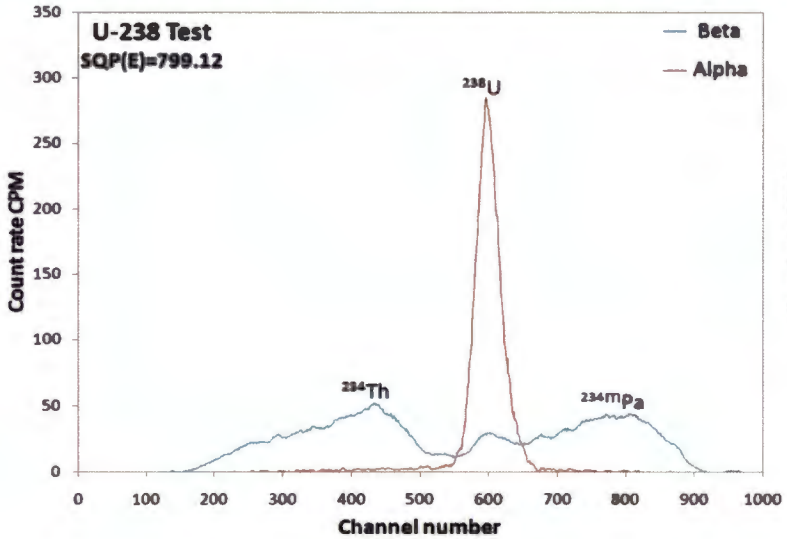

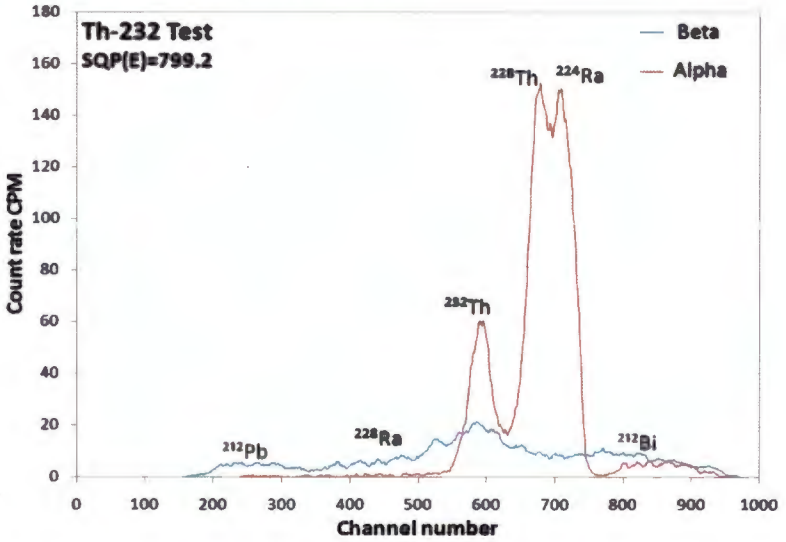

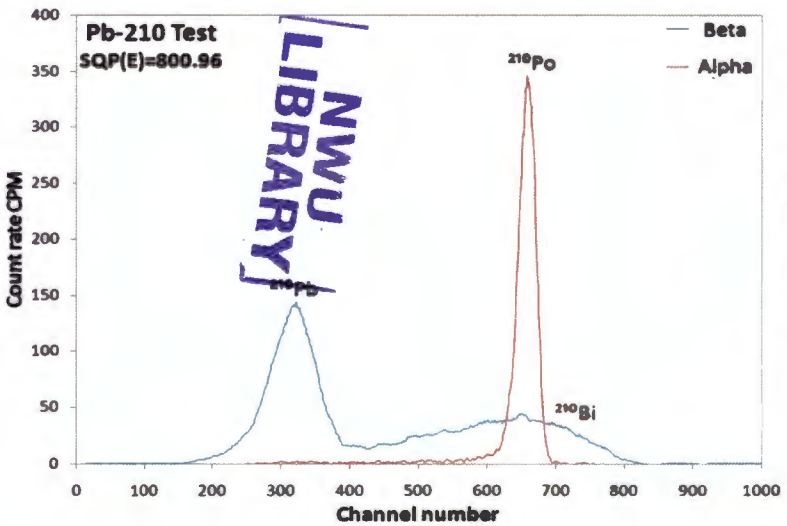

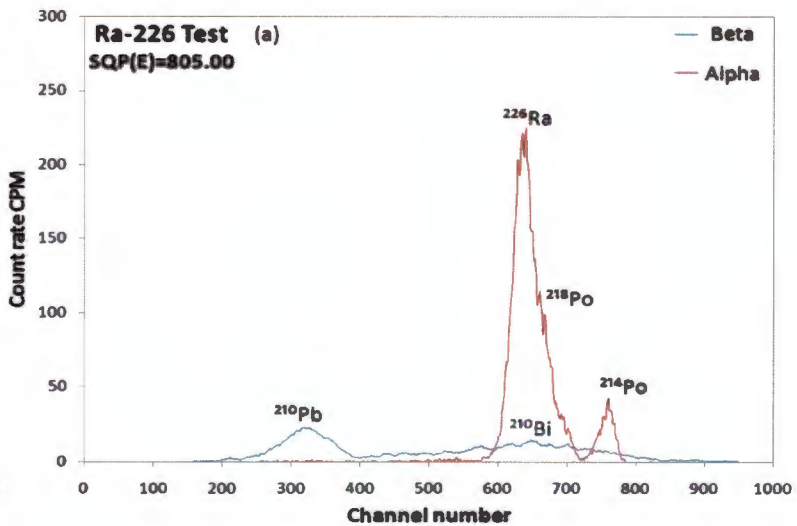

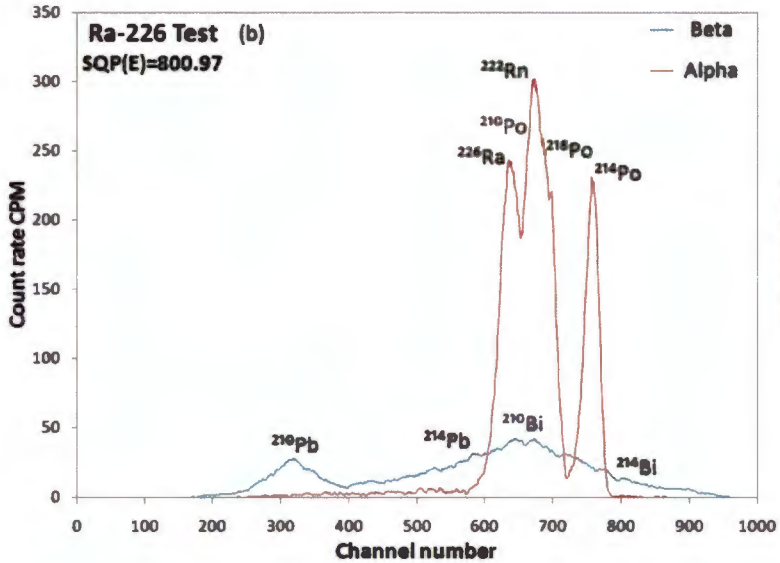
Ra-226 Test (b)
SQP(E)=800.97
Beta
Alpha
222Rn
210Po
218Po
214Po
226Ra
210Pb
214Pb
210Bi
214Bi
Count rate CPM
Channel number

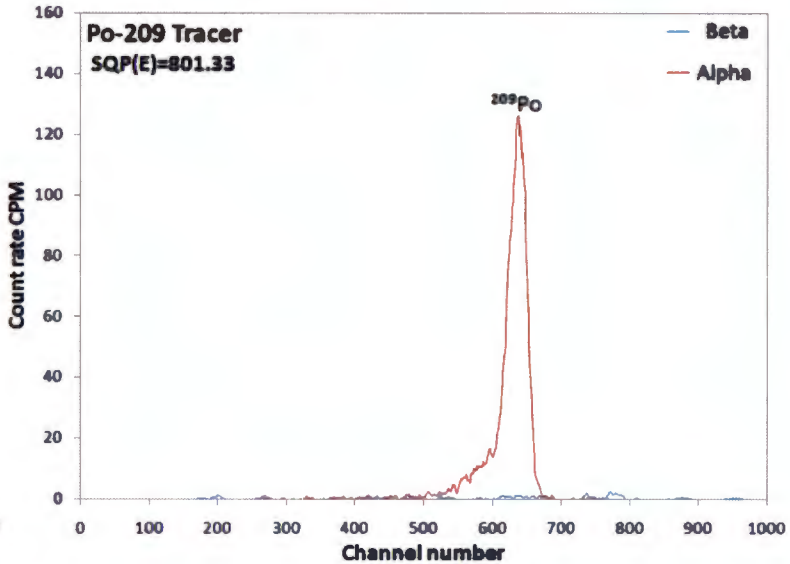
Po-209 Tracer
SQP(E)=801.33
Beta
Alpha
209Po
Count rate CPM
Channel number

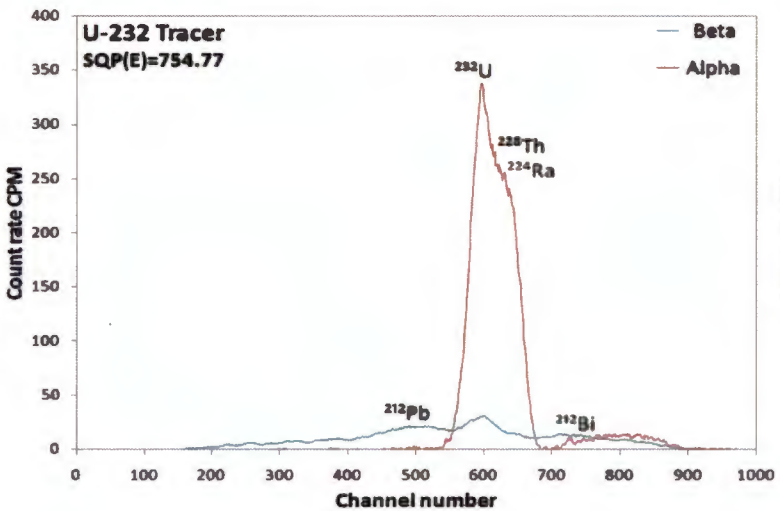
U-232 Tracer
SQP(E)=754.77
Beta
Alpha
232U
228Th
224Ra
212Pb
212Bi
Count rate CPM
Channel number

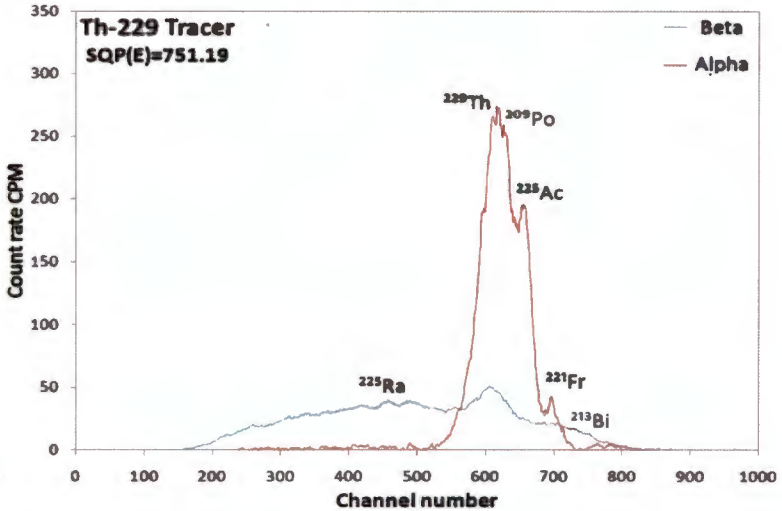
Th-229 Tracer
SQP(E)=751.19
Beta
Alpha
229Th
209Po
225Ac
225Ra
221Fr
213Bi
Count rate CPM
Channel number

Annexure 2: The gross α and β spectra of the Quantulus from the environmental water samples.

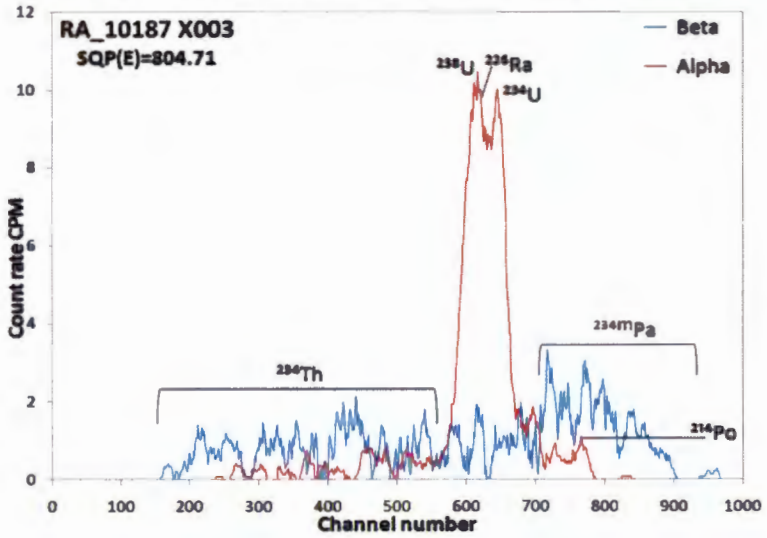

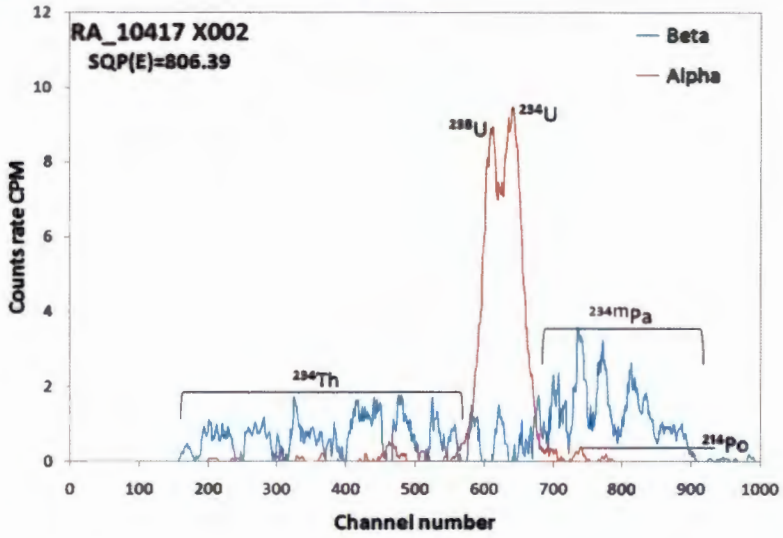

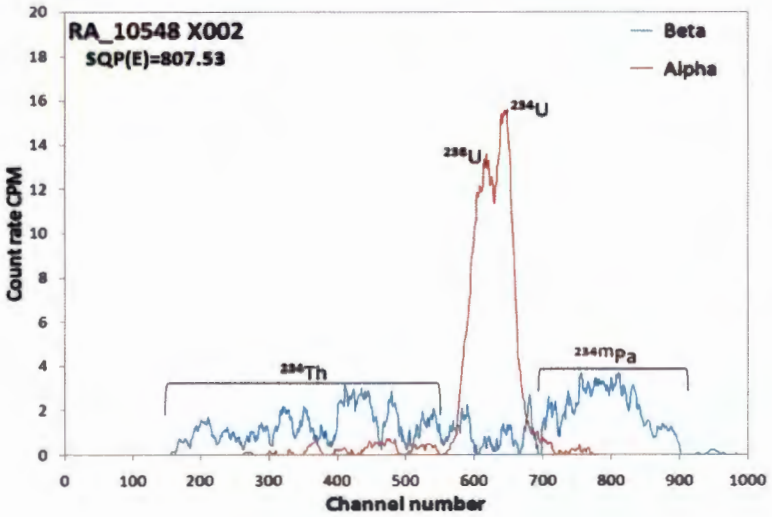

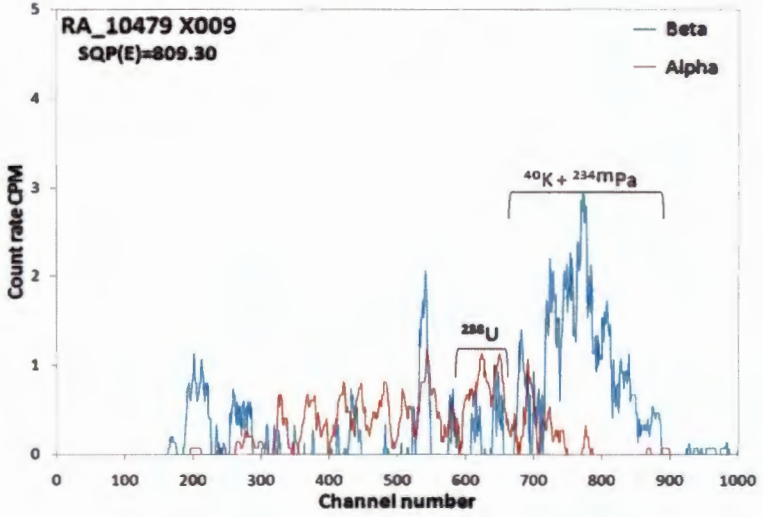

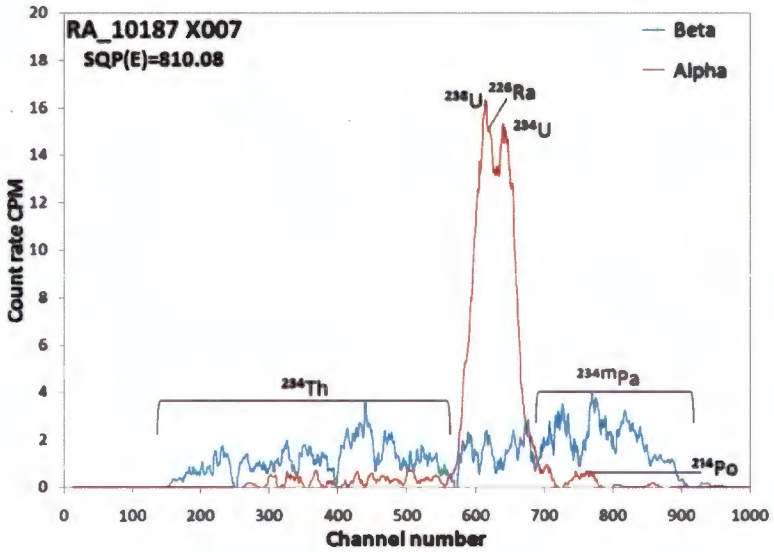
RA_10187 X007
SQP(E)=810.08
Beta
Alpha
238U
226Ra
234U
234Th
234mPa
214Po
Count rate CPM
Channel number

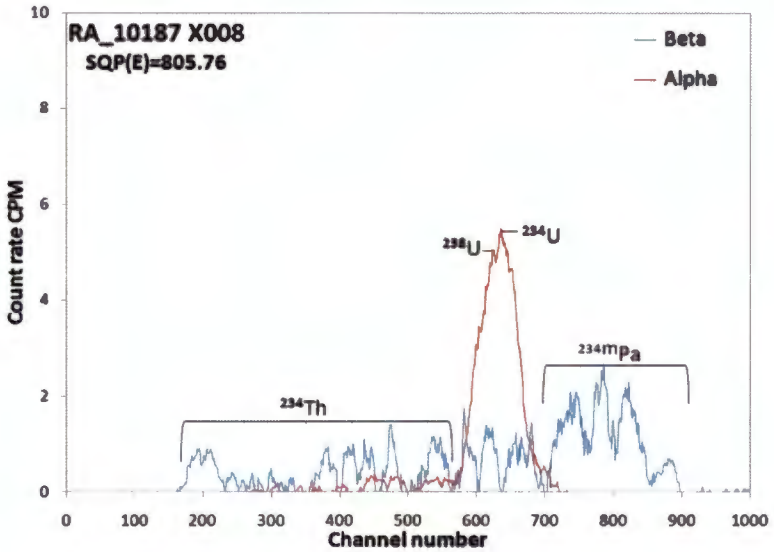
RA_10187 X008
SQP(E)=805.76
Beta
Alpha
238U
234U
234mPa
234Th
Count rate CPM
Channel number

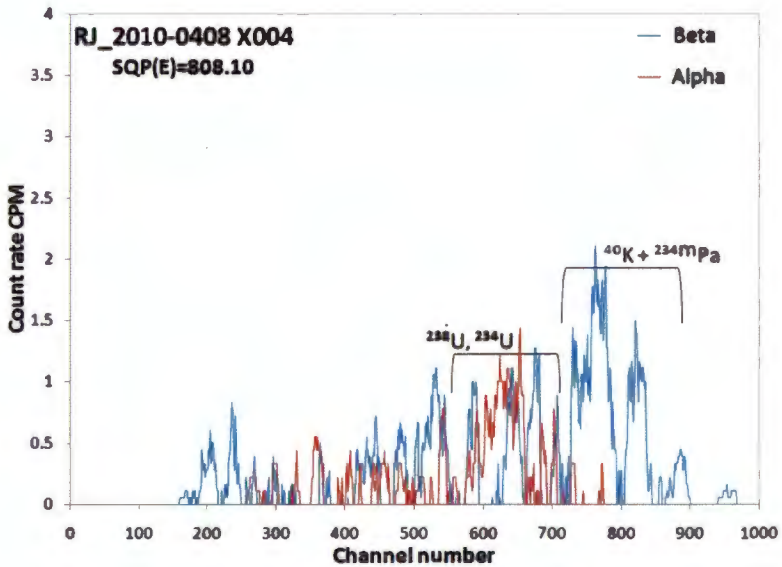
RJ_2010-0408 X004
SQP(E)=808.10
Beta
Alpha
40K + 234mPa
238U, 234U
Count rate CPM
Channel number

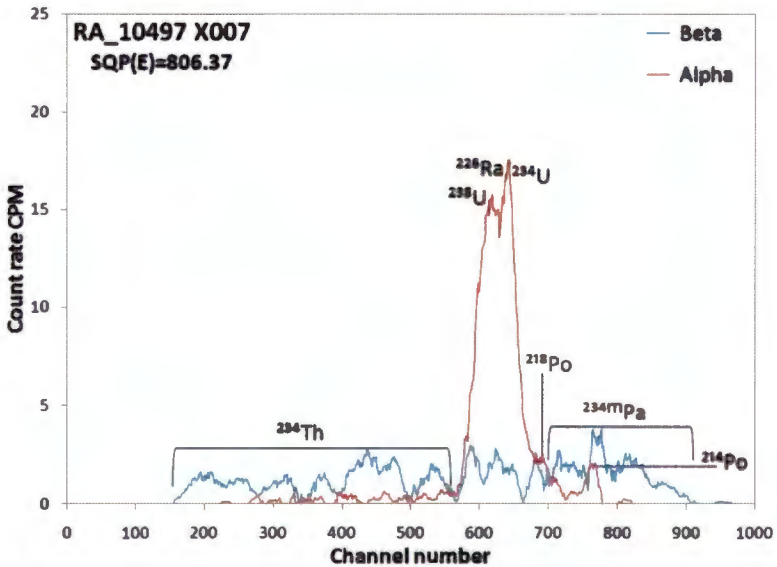
RA_10497 X007
SQP(E)=806.37
Beta
Alpha
226Ra
234U
238U
218Po
234mPa
234Th
214Po
Count rate CPM
Channel number

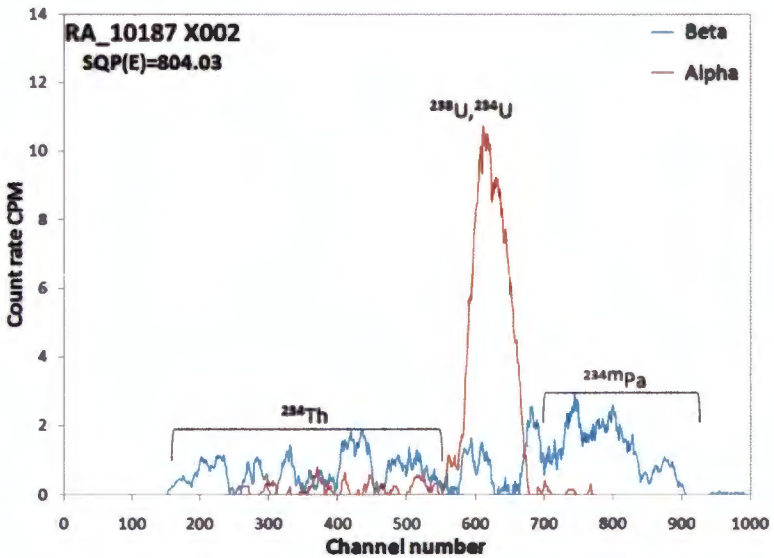
RA_10187 X002
SQP(E)=804.03
Beta
Alpha
Count rate CPM
Channel number
238U, 234U
234Th
234mPa

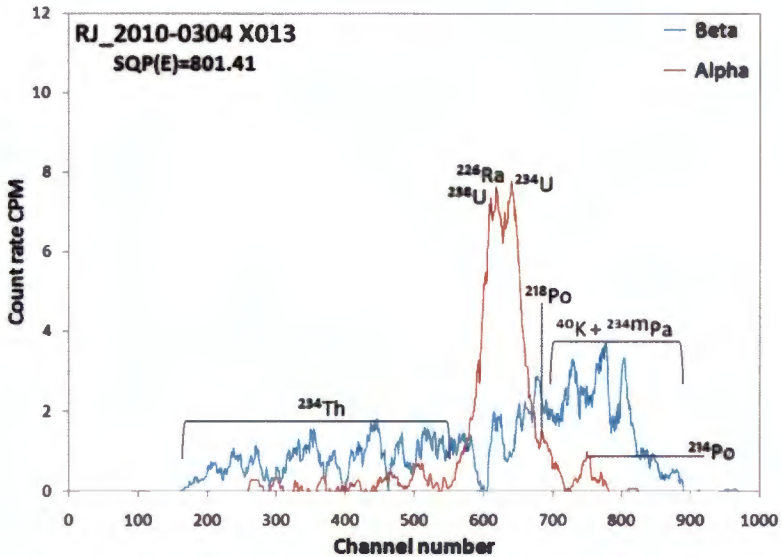
RJ_2010-0304 X013
SQP(E)=801.41
Beta
Alpha
Count rate CPM
Channel number
226Ra
238U
234U
218Po
40K + 234mPa
234Th
214Po

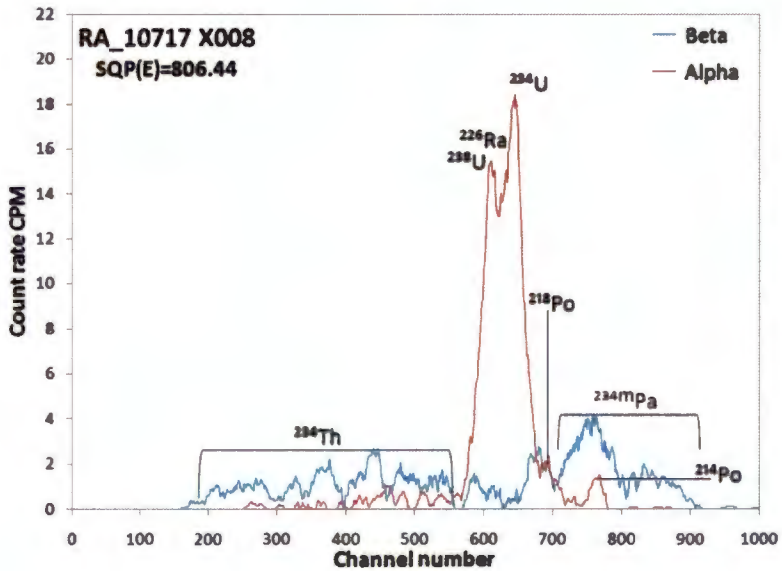
RA_10717 X008
SQP(E)=806.44
Beta
Alpha
Count rate CPM
Channel number
234U
226Ra
238U
218Po
234mPa
234Th
214Po

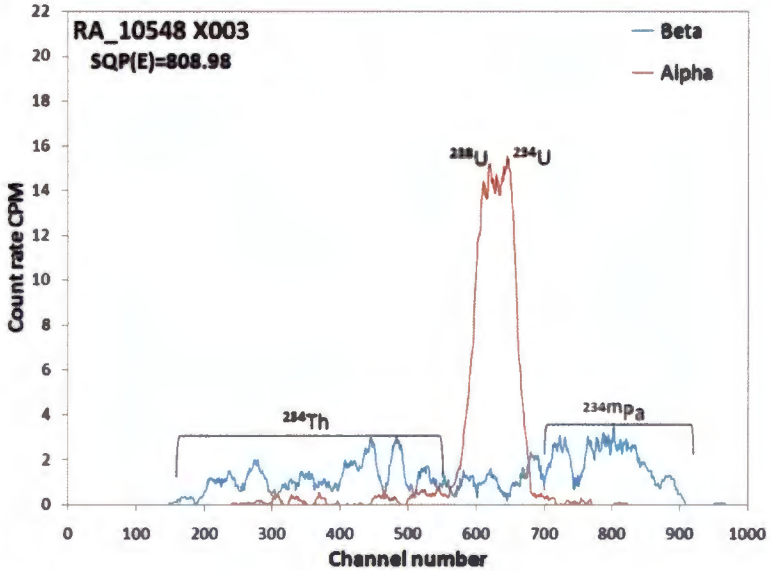
RA_10548 X003
SQP(E)=808.98
Beta
Alpha
Count rate CPM
Channel number
238U
234U
234Th
234mPa

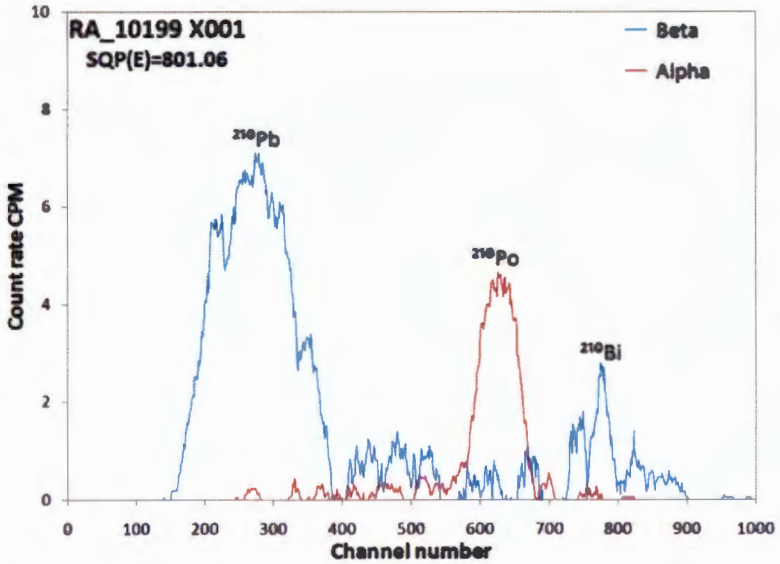
RA_10199 X001
SQP(E)=801.06
Beta
Alpha
210Pb
210Po
210Bi
Count rate CPM
Channel number

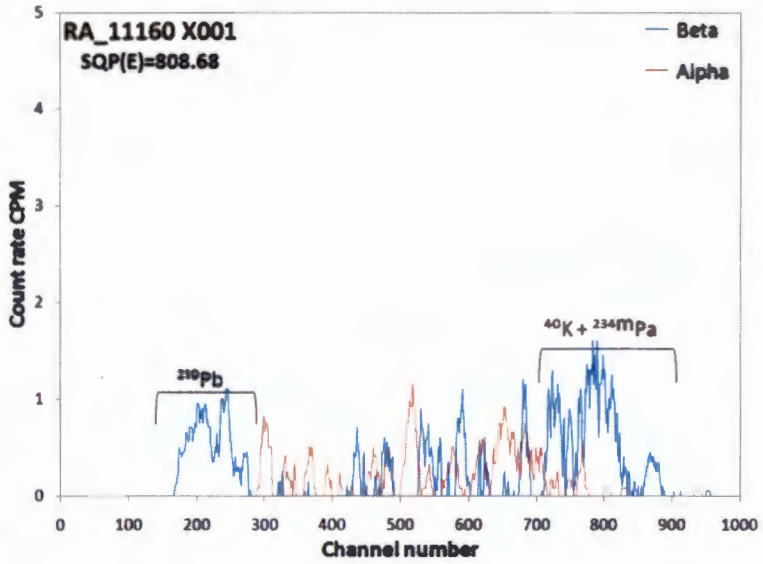
RA_11160 X001
SQP(E)=808.68
Beta
Alpha
210Pb
40K + 234mPa
Count rate CPM
Channel number

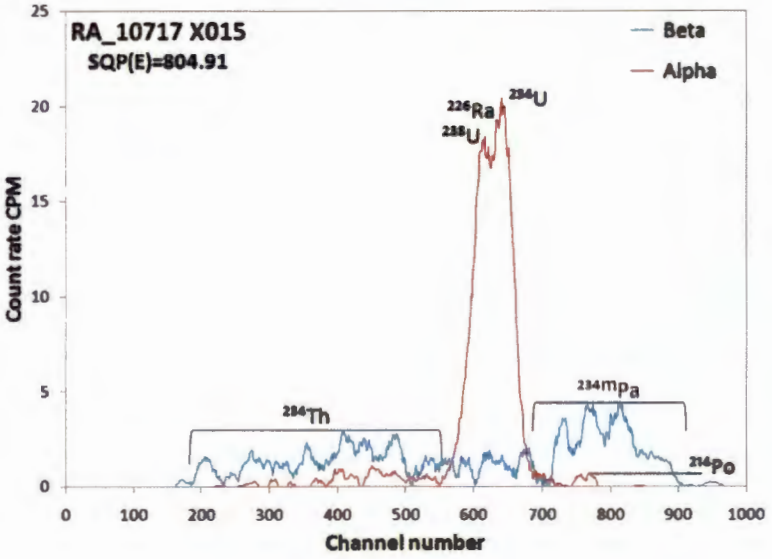
RA_10717 X015
SQP(E)=804.91
Beta
Alpha
226Ra
234U
238U
234Th
234mPa
214Po
Count rate CPM
Channel number

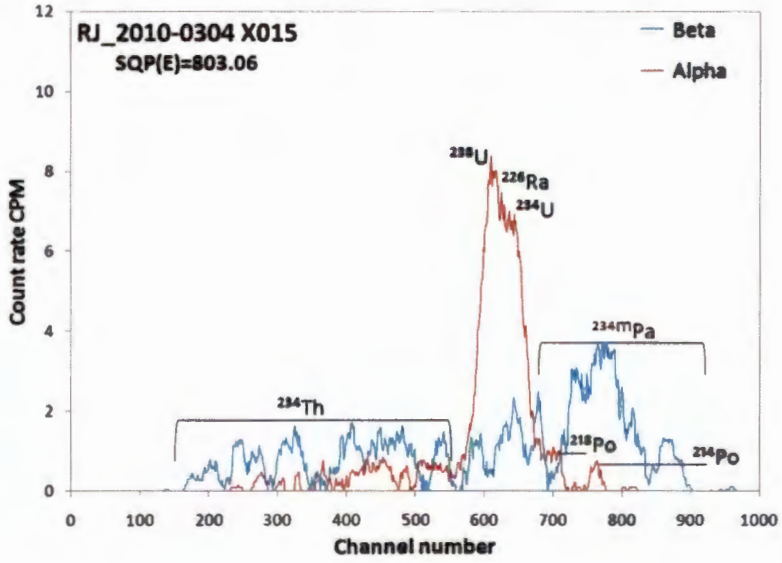
RJ_2010-0304 X015
SQP(E)=803.06
Beta
Alpha
238U
226Ra
234U
234mPa
234Th
218Po
214Po
Count rate CPM
Channel number

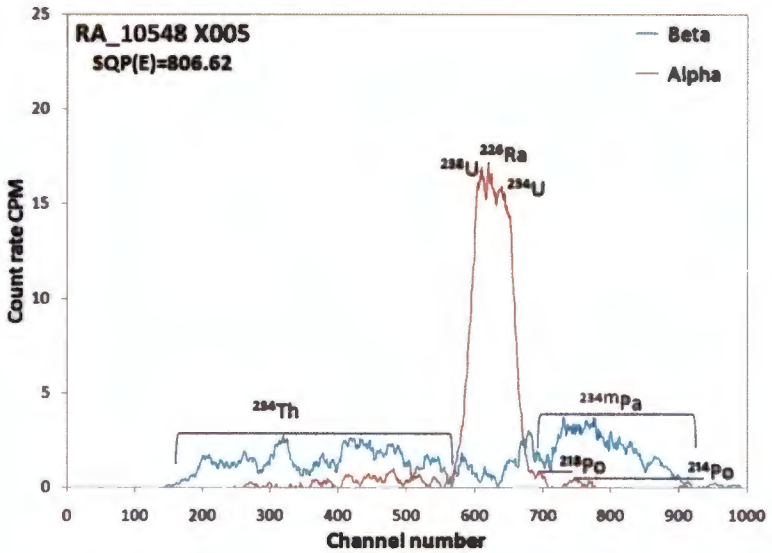
RA_10548 X005
SQP(E)=806.62
Beta
Alpha
Count rate CPM
Channel number
234Th
238U
226Ra
234U
234mPa
218Po
214Po

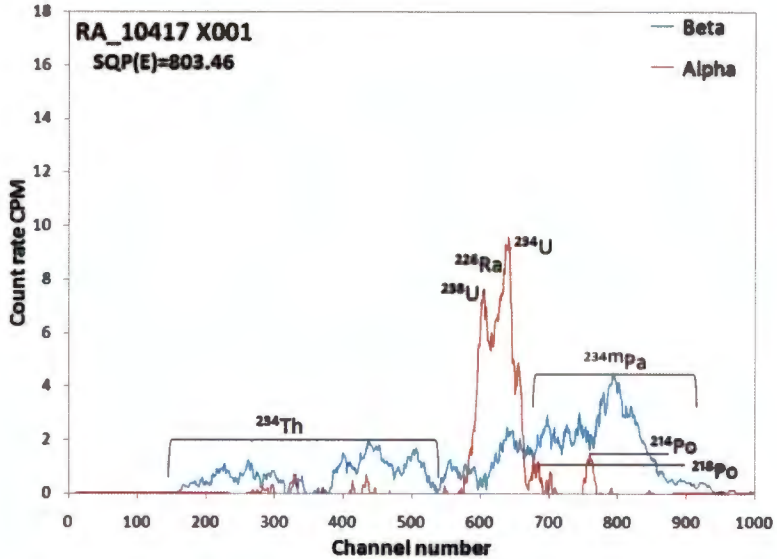
RA_10417 X001
SQP(E)=803.46
Beta
Alpha
Count rate CPM
Channel number
234Th
238U
226Ra
234U
234mPa
214Po
218Po

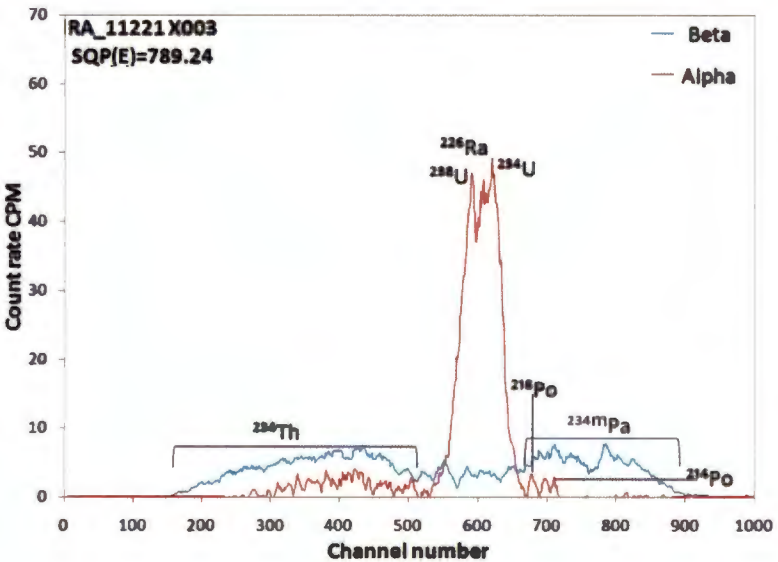
RA_11221 X003
SQP(E)=789.24
Beta
Alpha
Count rate CPM
Channel number
234Th
238U
226Ra
234U
218Po
234mPa
214Po

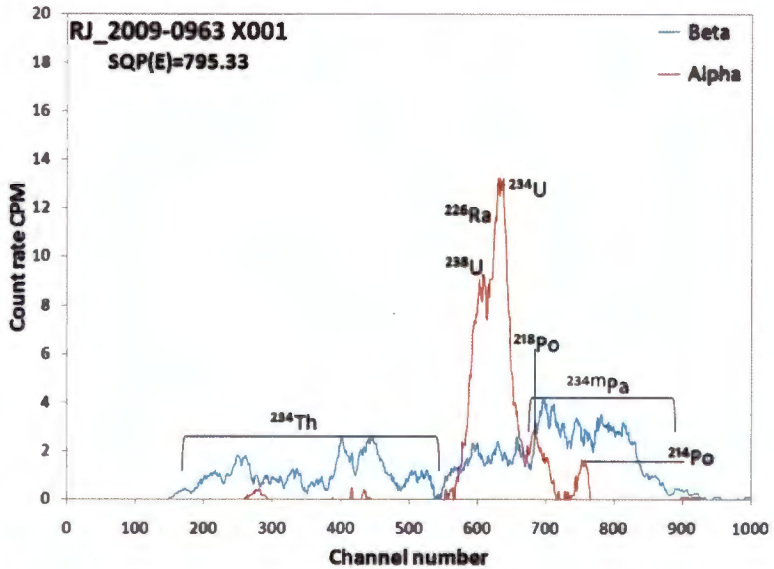
RJ_2009-0963 X001
SQP(E)=795.33
Beta
Alpha
Count rate CPM
Channel number
234Th
238U
226Ra
234U
218Po
234mPa
214Po

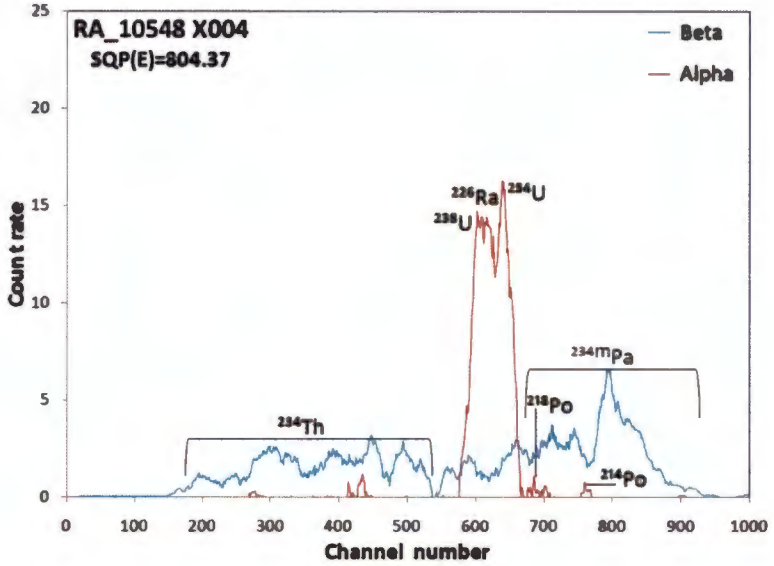
RA_10548 X004
SQP(E)=804.37
Beta
Alpha
Count rate
Channel number
234Th
226Ra
238U
234U
218Po
234mPa
214Po

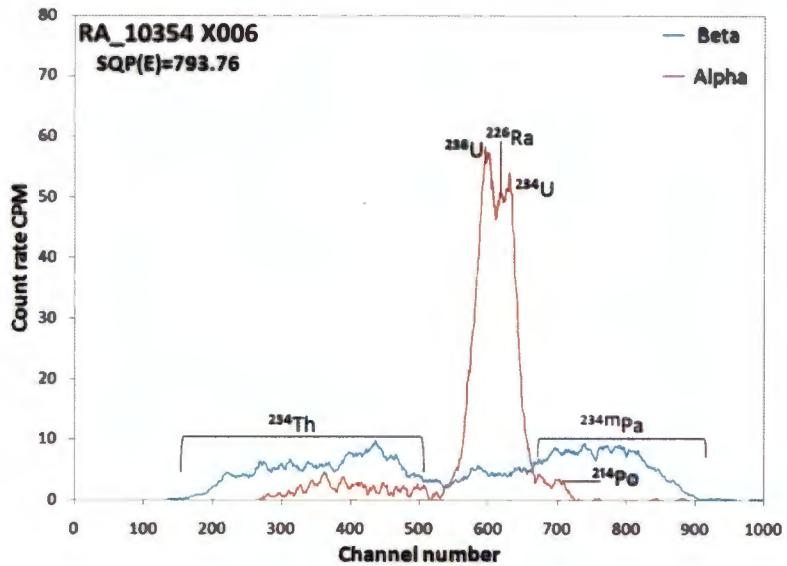
RA_10354 X006
SQP(E)=793.76
Beta
Alpha
Count rate CPM
Channel number
234Th
238U
226Ra
234U
234mPa
214Po

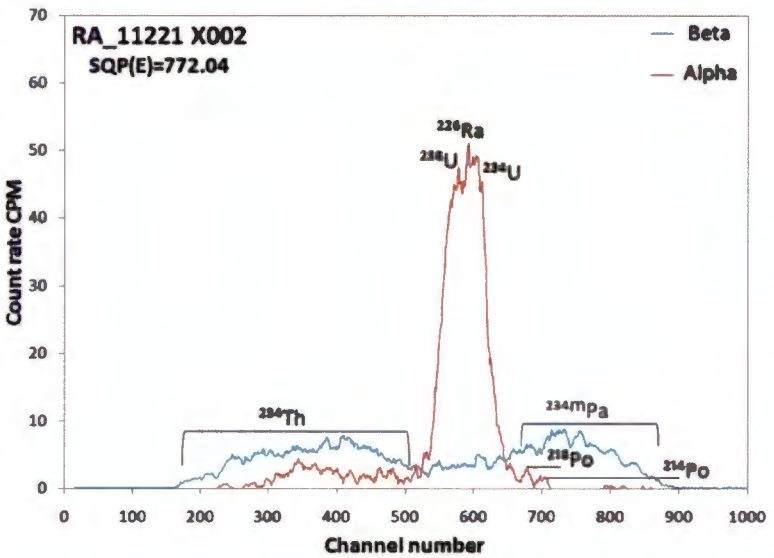
RA_11221 X002
SQP(E)=772.04
Beta
Alpha
Count rate CPM
Channel number
234Th
226Ra
238U
234U
234mPa
218Po
214Po

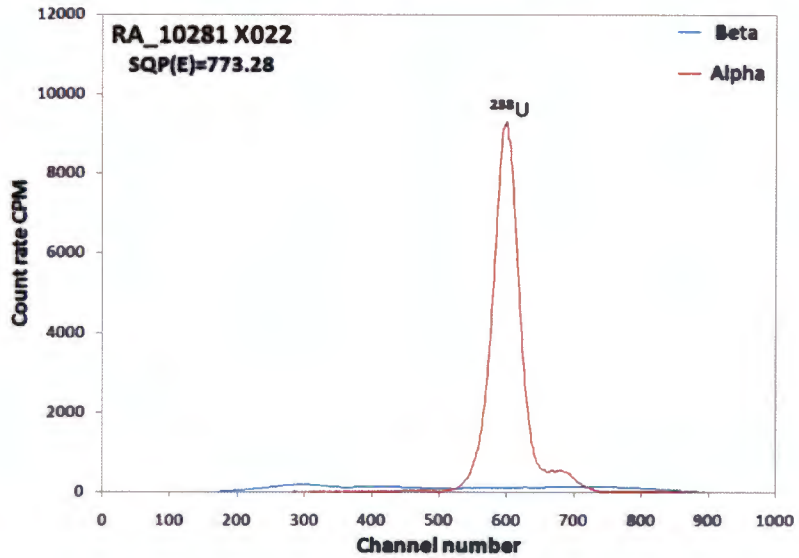
RA_10281 X022
SQP(E)=773.28
Beta
Alpha
Count rate CPM
Channel number
238U

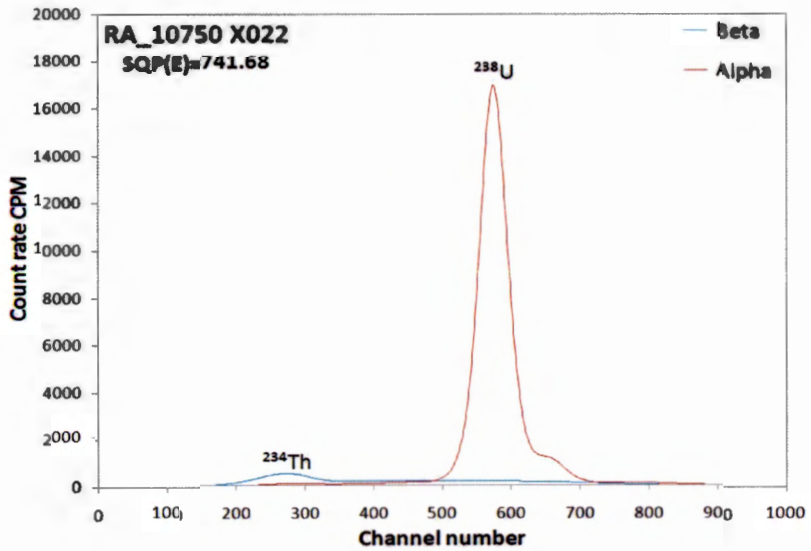
RA_10750 X022
SQP(E)=741.68
Beta
Alpha
238U
234Th
Count rate CPM
Channel number
20000
18000
16000
14000
12000
10000
8000
6000
4000
2000
0
0
100
200
300
400
500
600
700
800
900
1000

Annexure 3: Calculated results from nuclide specific analysis

mBq/l	RA_10187_X003		RA_10417_X002		RA_10548_X002		RA_10479_X009		RA_10187_X007		RA_10187_X008	
	α	β	α	β	α	B	α	β	α	β	α	β
U-238	3048		2783		5122		904		5694		1670	
Th-234		3048		2783		5122		904		5694		1670
Pa-234		3048		2783		5122		904		5694		1670
U-234	2791		2678		4743		873		5529		15245	
Th-230	113		13.5		7.94		10.4		8.53		6.12	
Ra-226	280		114		143		44.8		215		59.7	
Rn-222	280		114		143		44.8		215		59.7	
Po-218	280		114		143		44.8		215		59.7	
Pb-214		280		114		143		44.8		215		59.7
Bi-214		280		114		143		44.8		215		59.7
Po-214	280		114		143		44.8		215		59.7	
Pb-210		78		1.36		2.89		8.31		2.63		3.08
Bi-210		78		1.36		2.89		8.31		2.63		3.08
Po-210	9.20		1.36		2.89		8.31		2.63		3.08	
U-235	136		128		238		41.6		262		76.9	
Th-231		136		128		238		41.6		262		76.9
Pa-231	32.4		3.21		14.6		47.8		6.55		4.56	
Ac-227	32.4		3.21		14.6		47.8		6.55		4.56	
Th-227	32.4		3.21		14.6		47.8		6.55		4.56	
Ra-223	23.9		14.0		4.88		3.71		3.96		3.47	
Rn-219	23.9		14.0		4.88		3.71		3.96		3.47	
Po-215	23.9		14.0		4.88		3.71		3.96		3.47	
Pb-211		23.9		14.0		4.88		3.71		3.96		3.47
Bi-211	23.9		14.0		4.88		3.71		3.96		3.47	
Tl-207		23.9		14.0		4.88		3.71		3.96		3.47
Th-232	4.52		0.72		1.88		1.08		2.70		0.69	
Ra-228	4.52		0.72		1.88		1.08		2.70		0.69	
Ac-228	4.52		0.72		1.88		1.08		2.70		0.69	
Th-228	19.8		5.22		2.45		3.60		12.12		2.82	
Ra-224	4.85		1.69		2.35		3.13		2.47		2.40	
Rn-220	4.85		1.69		2.35		3.13		2.47		2.40	
Po-216	4.85		1.69		2.35		3.13		2.47		2.40	
Pb-212		4.85		1.69		2.35		3.13		2.47		2.40
Bi-212	4.85		1.69		2.35		3.13		2.47		2.40	
Po-212		4.85		1.69		2.35		3.13		2.47		2.40
Tl-208		4.85		1.69		2.35		3.13		2.47		2.40
Calculated	7463	7010	6139	5957	10766	10791	2194	1973	12419	12099	3562	3557
Measured	9456	8689	6401	7514	11550	12934	2182	2884	12935	13165	4073	5472

The nuclides printed in red are the ones that were measured by element specific separations followed by alpha spectrometry, while short-lived progeny is assumed to be in equilibrium with their respective longer-lived parents.

Annexure 3: Calculated results from nuclide specific analysis (continued)

mBq/l	RJ_2010-0405X004		RA_10497_X007		RA_10187_X002		RJ_2010-0304X013		RA_10717_X008		RA_10548_X003	
	α	β	α	β	α	B	A	β	α	β	α	β
U-238	293		4645		3500		2073		4678		5160	
Th-234		293		4645		3500		2073		4678		5160
Pa-234		293		4645		3500		2073		4678		5160
U-234	434		4712		3149		1405		4361		4755	
Th-230	53.2		35.0		23.6		124		41.7		52.6	
Ra-226	8.47		1078		25.1		433		829		168	
Rn-222	8.47		1078		25.1		433		829		168	
Po-218	8.47		1078		25.1		433		829		168	
Pb-214		8.47		1078		25.1		433		829		168
Bi-214		8.47		1078		25.1		433		829		168
Po-214	8.47		1078		25.1		433		829		168	
Pb-210		10.0		24.1		5.28		496		5.03		3.06
Bi-210		10.0		24.1		5.28		496		5.03		3.06
Po-210	10.0		2.53		1.02		496		5.03		3.06	
U-235	13.5		214		161		95.4		215		255	
Th-231		13.5		214		161		95.4		215		255
Pa-231	34.9		15.3		5.69		19.3		37.5		6.32	
Ac-227	34.9		15.3		5.69		19.3		37.5		6.32	
Th-227	34.9		15.3		5.69		19.3		37.5		6.32	
Ra-223	13.5		4.46		1.87		4.76		6.98		18.9	
Rn-219	13.5		4.46		1.87		4.76		6.98		18.9	
Po-215	13.5		4.46		1.87		4.76		6.98		18.9	
Pb-211		13.5		4.46		1.87		4.76		6.98		18.9
Bi-211	13.5		4.46		1.87		4.76		6.98		18.9	
Tl-207		13.5		4.46		1.87		4.76		6.98		18.9
Th-232	1.86		1.11		4.09		6.57		37.0		13.8	
Ra-228	1.86		1.11		4.09		6.57		37.0		13.8	
Ac-228	1.86		1.11		4.09		6.57		37.0		13.8	
Th-228	7.88		11.5		3.44		13.5		25.5		6.94	
Ra-224	3.74		7.51		3.14		4.30		2.89		6.02	
Rn-220	3.74		7.51		3.14		4.30		2.89		6.02	
Po-216	3.74		7.51		3.14		4.30		2.89		6.02	
Pb-212		3.74		7.51		3.14		4.30		2.89		6.02
Bi-212	3.74		7.51		3.14		4.30		2.89		6.02	
Po-212		3.74		7.51		3.14		4.30		2.89		6.02
Tl-208		3.74		7.51		3.14		4.30		2.89		6.02
Calculated	1025	675	14028	11739	6987	7234	6051	6120	12904	11261	11063	10972
Measured	844	2266	13706	12450	7587	7901	6496	9982	14071	11427	12278	12244

The nuclides printed in red are the ones that were measured by element specific separations followed by alpha spectrometry, while short-lived progeny is assumed to be in equilibrium with their respective longer-lived parents.

Annexure 3: Calculated results from nuclide specific analysis (continued)

mBq/l	RA_10199_X001		RA_11160_X001		RA_10717_X015		RJ_2010-0304X015		RA_10548_X005		RA_10417_X001	
	α	β	α	β	α	β	α	β	α	β	α	B
U-238	1589		91.3		6461		2459		6352		2735	
Th-234		1589		91.3		6461		2459		6352		2735
Pa-234		1589		91.3		6461		2459		6352		2735
U-234	1574		115		6041		1887		5738		2508	
Th-230	121		18.9		41.7		132		114		48.7	
Ra-226	4.83		1.29		306		452		146		436	
Rn-222	4.83		1.29		306		452		146		436	
Po-218	4.83		1.29		306		452		146		436	
Pb-214		4.83		1.29		306		452		146		436
Bi-214		4.83		1.29		306		452		146		436
Po-214	4.83		1.29		306		452		146		436	
Pb-210		11.1		3.10		7.92		313		3.93		4.25
Bi-210		11.1		3.10		7.92		313		3.93		4.25
Po-210	11.1		3.10		7.92		116		3.93		4.25	
U-235	73.2		4.20		296		113		292		126	
Th-231		73.2		4.20		296		113		292		126
Pa-231	4.27		13.6		15.2		12.2		18.4		11.5	
Ac-227	4.27		13.6		15.2		12.2		18.4		11.5	
Th-227	4.27		13.6		15.2		12.2		18.4		11.5	
Ra-223	17.5		0.51		4.49		2.96		20.0		15.8	
Rn-219	17.5		0.51		4.49		2.96		20.0		15.8	
Po-215	17.5		0.51		4.49		2.96		20.0		15.8	
Pb-211		17.5		0.51		4.49		2.96		20.0		15.8
Bi-211	17.5		0.51		4.49		2.96		20.0		15.8	
Tl-207		17.5		0.51		4.49		2.96		20.0		15.8
Th-232	12.4		1.77		3.01		8.58		10.6		2.06	
Ra-228	12.4		1.77		3.01		8.58		10.6		2.06	
Ac-228	12.4		1.77		3.01		8.58		10.6		2.06	
Th-228	10.2		4.65		6.24		14.2		3.99		4.38	
Ra-224	11.5		1.13		3.59		8.31		2.32		2.25	
Rn-220	11.5		1.13		3.59		8.31		2.32		2.25	
Po-216	11.5		1.13		3.59		8.31		2.32		2.25	
Pb-212		11.5		1.13		3.59		8.31		2.32		2.25
Bi-212	11.5		1.13		3.59		8.31		2.32		2.25	
Po-212		11.5		1.13		3.59		8.31		2.32		2.25
Tl-208		11.5		1.13		3.59		8.31		2.32		2.25
Calculated	3565	3353	296	200	14166	13866	6639	6592	13267	13344	7283	6515
Measured	3415	14493	1059	1532	15847	13783	7370	9587	13497	14241	9819	4948

The nuclides printed in red are the ones that were measured by element specific separations followed by alpha spectrometry, while short-lived progeny is assumed to be in equilibrium with their respective longer-lived parents.

Annexure 3: Calculated results from nuclide specific analysis (continued)

mBq/l	RA_11221_X003		RJ_2009-0963X001		RA_10548_X004		RA_10354_X006		RA_11221_X002		RA_10281_X022		RA_10750_X022	
	α	β	A	β	α	β	α	β	α	β	α	β	A	β
U-238	16200		2786		6026		17498		15000		173000		261000	
Th-234		16200		2786		6026		17498		15000		173000		261000
Pa-234		16200		2786		6026		17498		15000				
U-234	15200		3077		5422		16475		14400		163000		256000	
Th-230	196		23.4		8.50		369		336					
Ra-226	13.1		591		141		27.2		9.52					
Rn-222	13.1		591		141		27.2		9.52					
Po-218	13.1		591		141		27.2		9.52					
Pb-214		13.1		591		141		27.2		9.52				
Bi-214		13.1		591		141		27.2		9.52				
Po-214	13.1		591		141		27.2		9.52					
Pb-210		13.1		27.2		6.17		147		9.52				
Bi-210		13.1		27.2		6.17		147		9.52				
Po-210	13.1		1.22		1.18		147		9.52					
U-235	748		128		277		806		692		8460		11300	
Th-231		748		128		277		806		692		8460		11300
Pa-231	32.5		45.1		9.59		18.0		-18					
Ac-227	32.5		45.1		9.59		18.0		-18					
Th-227	32.5		45.1		9.59		18.0		-18					
Ra-223	3.01		3.48		13.2		9.99		1.59					
Rn-219	3.01		3.48		13.2		9.99		1.59					
Po-215	3.01		3.48		13.2		9.99		1.59					
Pb-211		3.01		3.48		13.2		9.99		1.59				
Bi-211	3.01		3.48		13.2		9.99		1.59					
Tl-207		3.01		3.48		13.2		9.99		1.59				
Th-232	451		1.72		1.85		1285		372					
Ra-228	451		1.72		1.85		1285		372					
Ac-228	451		1.72		1.85		1285		372					
Th-228	442		1.70		5.37		691		740					
Ra-224	15.3		2.88		5.82		294		18.2					
Rn-220	15.3		2.88		5.82		294		18.2					
Po-216	15.3		2.88		5.82		294		18.2					
Pb-212		15.3		2.88		5.82		294		18.2				
Bi-212	15.3		2.88		5.82		294		18.2					
Po-212		15.3		2.88		5.82		294		18.2				
Tl-208		15.3		2.88		5.82		294		18.2				
Calculated	34357	33252	8546	6952	12412	12667	41221	37053	32357	30788	344460	179460	528300	272300
Measured	44822	33394	13080	7442	14500	11651	54114	43985	38381	54128	5242079	1171626	9638210	7413934

The nuclides printed in red are the ones that were measured by element specific separations followed by alpha spectrometry, while short-lived progeny is assumed to be in equilibrium with their respective longer-lived parents.

Annexure 4: ^{226}Ra spectra used for the determination of the quench parameter related energy-to-channel calibration

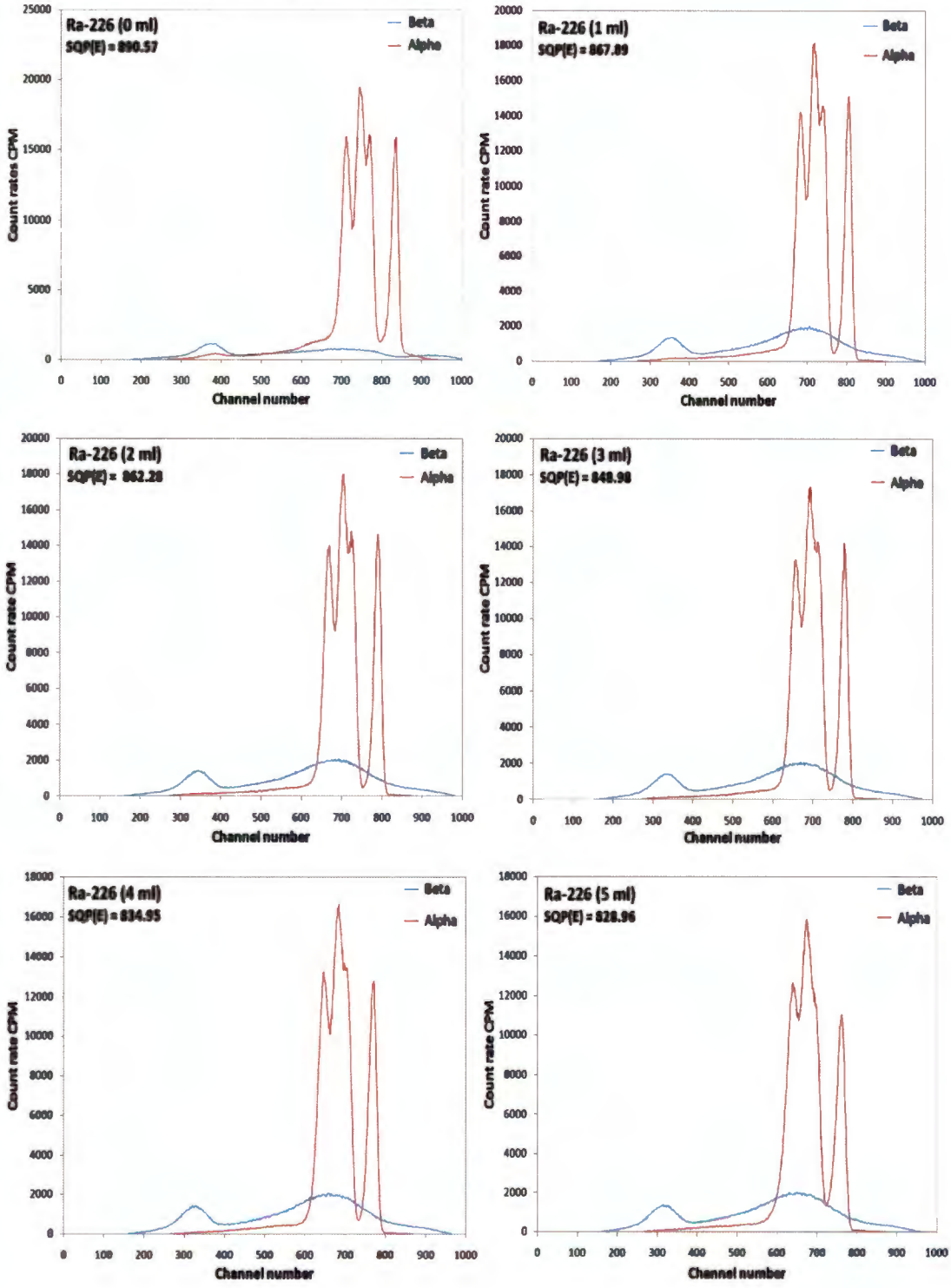

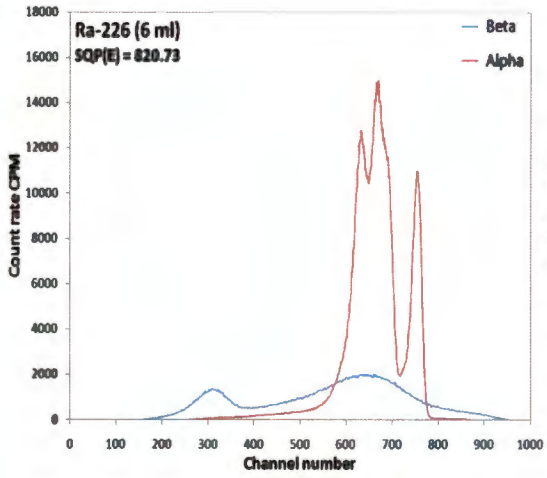
Ra-226 (6 ml)
SQP(E) = 820.73
Beta
Alpha
Count rate CPM
Channel number

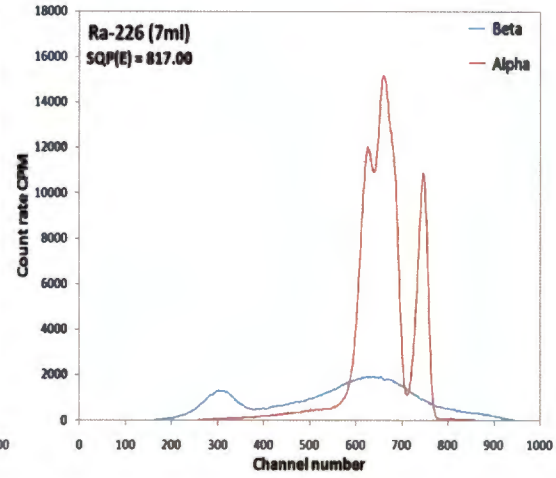
Ra-226 (7ml)
SQP(E) = 817.00
Beta
Alpha
Count rate CPM
Channel number

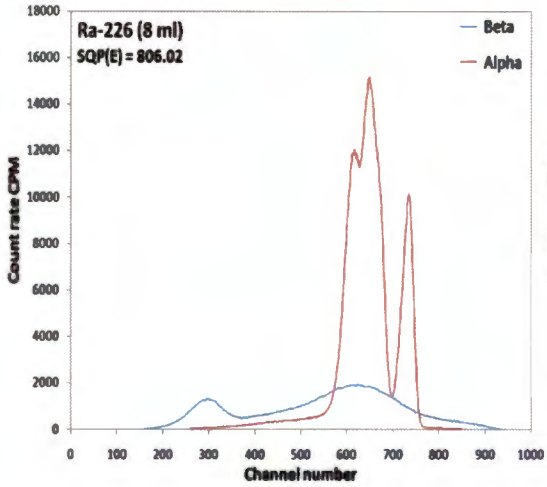
Ra-226 (8 ml)
SQP(E) = 806.02
Beta
Alpha
Count rate CPM
Channel number

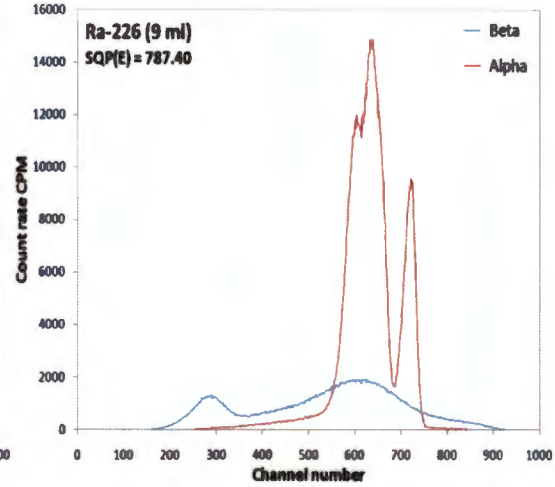
Ra-226 (9 ml)
SQP(E) = 787.40
Beta
Alpha
Count rate CPM
Channel number

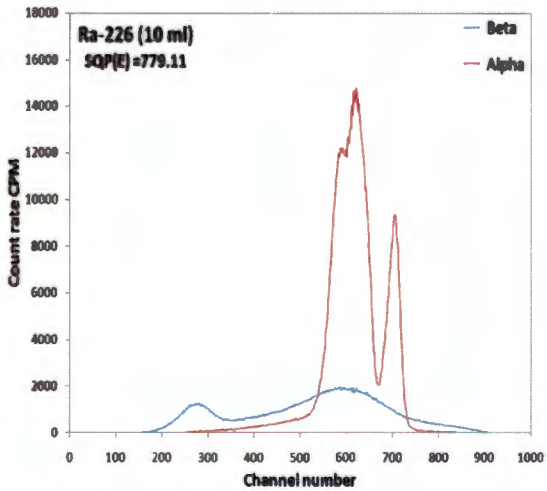
Ra-226 (10 ml)
SQP(E) =779.11
Beta
Alpha
Count rate CPM
Channel number

Annexure 5: The certified ^{226}Ra standard reference solution used for energy-to-channel number calibration

Amersham plc
The Grove Centre

Certificate of calibration of
radium-226 reference solution

UKAS CALIBRATION

ISSUED BY: Amersham plc
Radiation & Radioactivity
Calibration Laboratory
The Grove Centre
White Lion Road
Amersham
Buckinghamshire
HP7 9LL

ISSUED FOR: MSA Technology QSA GmbH
Attn.:
Gieselweg 1
D-38110 Braunschweig
Germany

Description
Principal radionuclide: Radium-226
Product code:
Solution number:

Measurement
Reference time: 1200 GMT on 4 March 2003
Radioactive concentration of radium-226: 92.59 kilobecquerels per gram of solution
which is equivalent to: 2.178 microcuries per gram of solution
Mass of solution: 5.0225 grams
Total activity of radium-226: 230.9 kilobecquerels
which is equivalent to: 6.206 microcuries

Method of measurement used
The activity of the solution was measured using a high pressure re-entrant ionisation chamber calibrated with a large number of absolutely standardised solutions.

Calibration date(s): 4 March 2003
The calibration date is provided for added information only, and must not be confused with the reference date. It is the reference date that must be used in all calculations relating to the values of activity.

Uncertainty
Expanded uncertainty on the radioactive concentration quoted above: ± 2.2%
Combined Type A uncertainty: ± 0.3%
Combined Type B uncertainty: ± 1.6%

Approved Signatory: P J Singleton
Date of issue: 5th March 2003

Amersham

Page 1 of 2 pages

This certificate is issued in accordance with the laboratory accreditation requirements of the United Kingdom Accreditation Service. It provides traceability of measurement to recognised national standards, and to units of measurement realised at the National Physical Laboratory or other recognised national standards laboratories. This certificate may not be reproduced other than in full, except with the prior written approval of the issuing laboratory.

Certificate of calibration of radium-226 reference solution

NPL 11987

UKAS ACCREDITED CALIBRATION LABORATORY No. 0146

Radionuclidic Purity The estimated activities of any radioactive impurities found by high-resolution gamma-ray spectrometry, or on any other examination of the solution, are listed below expressed as percentages of the activity of the principal radionuclide at the reference time.

None detected.

Chemical Composition Carrier free in 0.5M HCl

Half-life Recommended half-life 1600 ± 7 a (1 year = 3652.25 days)

Remarks This product meets the quality assurance requirements for achieving traceability to NIST as defined in ANSI N42.22-1995.

Nuclear data quoted on this certificate are taken from the Joint European File, Version 2.2.

At the reference date radium-226 was shown to be in radioactive equilibrium with its daughter nuclides down the decay chain to polonium-214 and thallium-210, the precursors of lead-210. The ionization chamber was calibrated using a standard supplied by the National Institute of Standards and Technology, Washington DC, USA.

The uncertainty associated with the mass of the solution as ± 0.002 % and is included in the expanded uncertainty

Expression of Uncertainties The reported expanded uncertainty is based on a standard uncertainty multiplied by a coverage factor $k = 2.00$, which for a t-distribution with $\nu_{eff} = \infty$ effective degrees of freedom corresponds to a coverage probability of approximately 95 %. The uncertainty evaluation has been carried out in accordance with UKAS requirements.

Unless indicated, all other uncertainties are expressed at the confidence level associated with one standard uncertainty.

The format used for the uncertainties in the values of radionuclidic purity is illustrated in the following examples.

6.2(21)	=	6.2 ± 2.1
6.54(2n)	=	6.54 ± 0.2n
6.543(21)	=	6.543 ± 0.021